

*Internal Note No. 68-FM-62*

*Bellcomm/R. L. Wagner*



NATIONAL AERONAUTICS AND SPACE ADMINISTRATION

MSC INTERNAL NOTE NO. 68-FM-62

March 13, 1968

*mi*  
Technical Library, Bellcomm, Inc.

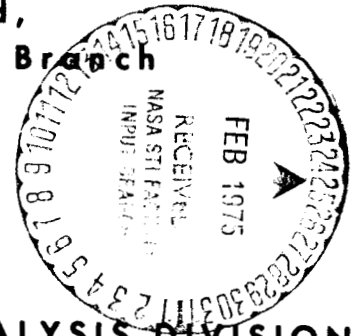
OCT 30 1968

**APOLLO 6  
(A-2 OR AS-502/CSM-020)  
SPACECRAFT OPERATIONAL  
TRAJECTORY  
VOLUME I - MISSION PROFILE**

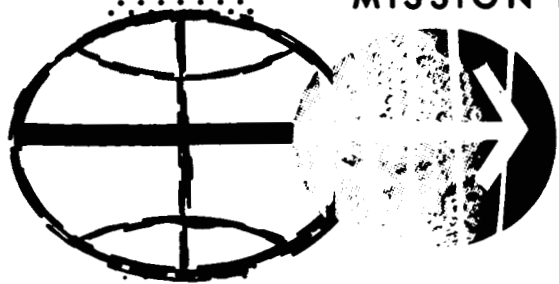
MAR 20 1968

APOLLO 6
A. P. BOYSEN, JR.
J. Z. MENARD
M & L
R. E. GRADY
L. M. ROSS
W. R. CLINE

**By William J. Bennett and Ronny H. Moore,  
Orbital Mission Analysis Branch,  
and Jon C. Harpold,  
Lunar Mission Analysis Branch**



MISSION PLANNING AND ANALYSIS DIVISION



**MANNED SPACECRAFT CENTER  
HOUSTON, TEXAS**

PROJECT APOLLO


APOLLO 6 (A-2 OR AS-502/CSM-020)  
SPACECRAFT OPERATIONAL TRAJECTORY  
VOLUME I - MISSION PROFILE


By William J. Bennett and Ronny H. Moore, Orbital Mission Analysis Branch,  
and Jon C. Harpold, Lunar Mission Analysis Branch

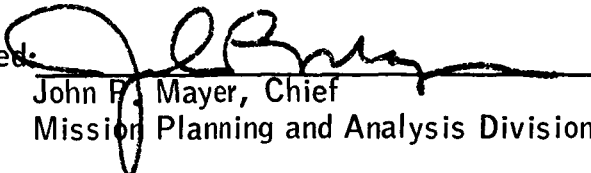
---

March 13, 1968

MISSION PLANNING AND ANALYSIS DIVISION  
NATIONAL AERONAUTICS AND SPACE ADMINISTRATION  
MANNED SPACECRAFT CENTER  
HOUSTON, TEXAS

Approved:   
\_\_\_\_\_  
Edgar C. Lineberry, Chief  
Orbital Mission Analysis Branch

Approved:   
\_\_\_\_\_  
M. P. Frank III, Chief  
Lunar Mission Analysis Branch

Approved:   
\_\_\_\_\_  
John P. Mayer, Chief  
Mission Planning and Analysis Division

## CONTENTS

Section		Page
1.0	INTRODUCTION AND SUMMARY. . . . .	1
1.1	1.1 Purpose. . . . .	1
	1.2 Scope. . . . .	1
	1.3 Summary of Spacecraft Operational Trajectory . .	2
2.0	SUMMARY OF INPUT DATA . . . . .	4
	2.1 Saturn V Launch Vehicle. . . . .	4
	2.2 Spacecraft (CSM-020) . . . . .	4
	2.3 MSFN Tracking Stations . . . . .	4
	2.4 Spacecraft and Attitude Reference Coordinate System. . . . .	4
	2.4.1 Spacecraft body coordinate system ( $X_B, Y_B, Z_B$ ). . . . .	5
	2.4.2 Launch site inertial attitude reference system ( $X_I, Y_I, Z_I$ ) . . . . .	5
	2.4.3 Earth-reference rotating attitude co- ordinate system ( $X_R, Y_R, Z_R$ ). . . . .	5
	2.4.4 Platform coordinate system ( $X_P, Y_P, Z_P$ ) .	5
	2.4.5 Navigation base coordinate system ( $X_{NB}, Y_{NB}, Z_{NB}$ ) . . . . .	5
	2.4.6 Relative vehicle coordinate system ( $X_{RV}, Y_{RV}, Z_{RV}$ ) . . . . .	6
	2.4.7 Spacecraft look angles ( $\phi, \theta$ ) . . . . .	6
2.5	Orbital Geometry and Trajectory Parameter Definitions. . . . .	6
	2.5.1 Orbital geometry. . . . .	6
	2.5.2 Trajectory parameters . . . . .	7

Section	Page
3.0 NOMINAL MISSION DESCRIPTION . . . . .	8
3.1 Prelaunch. . . . .	8
3.2 Saturn V Ascent to Orbit . . . . .	8
3.3 Earth Parking Orbit. . . . .	9
3.4 Second S-IVB Burn. . . . .	10
3.5 S-IVB/CSM Separation . . . . .	10
3.6 First SPS Burn . . . . .	11
3.7 Earth Intersecting Coast . . . . .	11
3.8 Second SPS Burn. . . . .	13
3.9 Preentry Sequence. . . . .	13
3.10 Atmospheric Entry . . . . .	14
4.0 MISSION PROFILES RESULTING FROM SPS ENGINE FAILURE. .	16
4.1 First SPS Burn; No Second SPS Burn . . . . .	16
4.2 Summary of Splash Points . . . . .	16
5.0 TRACKING AND COMMUNICATIONS DATA. . . . .	17
REFERENCES. . . . .	107

## FIGURES

Figure		Page
1-1	Mission summary . . . . .	34
2-1	Saturn V reference dimensions . . . . .	35
2-2	Command and service modules reference dimensions. . . .	36
2-3	Spacecraft body coordinate system . . . . .	37
2-4	Launch site inertial attitude reference coordinate system . . . . .	38
2-5	Earth-reference rotating attitude coordinate system . .	39
2-6	Platform coordinate system. . . . .	40
2-7	Navigation base coordinate system relative to spacecraft body coordinate system. . . . .	41
2-8	Relative vehicle coordinate system. . . . .	42
2-9	Spacecraft look angles. . . . .	43
2-10	Orbital geometry. . . . .	44
2-11	Trajectory parameters . . . . .	45
3-1	Ground track and daylight-darkness history. . . . .	46
3-2	Altitude-longitude history	
	(a) Mission profile. . . . .	47
	(b) Launch phase . . . . .	47
	(c) Entry phase. . . . .	47
3-3	Effect of sun lighting on launch time . . . . .	48
3-4	Saturn V ascent to parking orbit	
	(a) Altitude, latitude, and longitude. . . . .	49
	(b) Inertial velocity, flight-path angle and azimuth .	50
	(c) Relative velocity and flight-path angle. . . . .	51
	(d) Altitude, mach number, and dynamic pressure. . . .	52
	(e) Pitch angle of attack. . . . .	53
	(f) Inertial yaw, pitch and roll . . . . .	54

Figure	Page
3-5	Earth parking orbit
	(a) Altitude, latitude and longitude . . . . . 55
	(b) Inertial velocity, flight-path angle, and azimuth. . . . . 56
	(c) Inertial yaw, pitch, and roll. . . . . 57
3-6	Second S-IVB burn
	(a) Altitude, latitude, and longitude. . . . . 58
	(b) Inertial velocity, flight-path angle, and azimuth. . . . . 59
	(c) Inertial yaw, pitch, and roll. . . . . 60
3-7	CSM/S-IVB separation characteristics. . . . . 61
3-8	Time history of CSM/S-IVB relative velocity and separation distance . . . . . 62
3-9	Spacecraft attitude orientation requirements during earth intersecting coast. . . . . 63
3-10	Effect of launch delay on sun look angles
	(a) Primary solar soak attitude. . . . . 64
	(b) Secondary solar soak attitude. . . . . 65
3-11	First SPS burn
	(a) Altitude, latitude, and longitude. . . . . 66
	(b) Inertial velocity, flight-path angle, and azimuth. . . . . 67
	(c) Inertial yaw, pitch, and roll. . . . . 68
	(d) Relative yaw, pitch, and roll. . . . . 69
	(e) IMU gimbal angles. . . . . 70
	(f) Time of free fall to reentry, predicted velocity and flight-path angle at entry . . . . . 71
	(g) Instantaneous apogee and perigee altitude. . . . . 72
3-12	Earth intersecting coast
	(a) Altitude, latitude, and longitude. . . . . 73
	(b) Inertial velocity, azimuth, and flight-path angle. . . . . 74

Figure		Page
	Earth intersecting coast (concluded)	
	(c) Inertial yaw, pitch, and roll . . . . .	75
	(d) Relative yaw, pitch, and roll . . . . .	76
	(e) IMU gimbal angles . . . . .	77
3-13	Second SPS burn	
	(a) Altitude, latitude, and longitude . . . . .	78
	(b) Inertial velocity, flight-path angle, and azimuth . . . . .	79
	(c) Inertial yaw, pitch, and roll . . . . .	80
	(d) Relative yaw, pitch, and roll . . . . .	81
	(e) IMU gimbal angles . . . . .	82
	(f) Time of free fall to reentry, predicted velocity and flight-path angle at entry. . . . .	83
	(g) Instantaneous apogee and perigee altitudes. . . . .	84
3-14	CM/SM separation distance. . . . .	85
3-15	Preentry sequence	
	(a) Altitude, latitude, and longitude . . . . .	86
	(b) Inertial velocity, flight-path angle, and azimuth . . . . .	87
	(c) Inertial yaw, pitch, and roll . . . . .	88
	(d) Relative yaw, pitch, and roll . . . . .	89
	(e) IMU gimbal angles . . . . .	90
3-16	Spacecraft landing footprint . . . . .	91
3-17	Reentry altitude range profile . . . . .	92
3-18	Atmospheric entry	
	(a) Heat rate, heat load, and load factor . . . . .	93
	(b) Altitude, bank angle, and load factor . . . . .	94
	(c) Altitude, latitude, and longitude . . . . .	95
	(d) Inertial velocity, flight-path angle, and azimuth . . . . .	96
	(e) Relative velocity, flight-path angle, and azimuth . . . . .	97
	(f) Altitude, dynamic pressure, and mach number . . . . .	98
	(g) Bank angle and trim angle of attack . . . . .	99
	(h) IMU gimbal angles . . . . .	100

Figure		Page
3-19	Entry communications blackout . . . . .	101
4-1	Spacecraft landing footprint - no second SPS burn . . .	102
4-2	Summary of splash points . . . . .	103
5-1	Ground track and radar coverage	
	(a) First revolution . . . . .	104
	(b) Second revolution. . . . .	105
	(c) Third revolution . . . . .	106



## TABLES

Table	Page	
2-I	MSFN GROUND STATIONS AND CAPABILITIES	
	(a) Unified S-band stations . . . . .	18
	(b) C-band stations . . . . .	19
3-I	APOLLO 6 MISSION DISCRETE EVENTS SUMMARY	
	(a) Saturn V operations . . . . .	20
	(b) Spacecraft operations . . . . .	21
3-II	APOLLO 6 MISSION SPACECRAFT ATTITUDE SUMMARY . . . . .	22
3-III	SERVICE MODULE RCS PROPELLANT EXPENDITURES . . . . .	24
3-IV	SUMMARY OF S-IVB ATTITUDE MANEUVERS	
	(a) Earth parking orbit . . . . .	25
	(b) Post injection . . . . .	26
3-V	SPACECRAFT GUIDANCE TARGETING PARAMETERS . . . . .	27
3-VI	APOLLO 6 AERODYNAMIC COEFFICIENTS AT TRIM ANGLE OF ATTACK AS A FUNCTION OF MARCH NUMBER . . . . .	28
3-VII	APOLLO COMMAND MODULE PARACHUTE DESCENT EVENTS AND AERODYNAMICS . . . . .	29
4-I	SPLASH POINTS. . . . .	30
4-II	COMPARISON OF NOMINAL AND NO-SPS-BURN ENTRY. . . . .	30
5-I	RADAR TRACKING COVERAGE SUMMARY. . . . .	31

APOLLO 6 (A-2 OR AS-502/CSM-020)

SPACECRAFT OPERATIONAL TRAJECTORY

VOLUME I - MISSION PROFILE

By William J. Bennett, and Ronny H. Moore, OMAB

and Jon C. Harpold, LMAB

1.0 INTROUCTION AND SUMMARY

1.1 Purpose

This spacecraft operational trajectory defined in this document is designed for the unmanned Apollo 6 Mission (AS-502/CSM-020/LTA-2R). This document presents the spacecraft portion of a combined launch vehicle and spacecraft trajectory which is designed to satisfy the spacecraft mission objectives without violating any of the launch vehicle and spacecraft constraints or the mission guidelines. This report describes the complete mission profile and incorporates all trajectory design refinements and revisions issued since publication of the AS-502 Spacecraft Reference Trajectory (ref. 1).

1.2 Scope

This report is presented in four volumes. This volume, Volume I, summarizes the launch vehicle and spacecraft data used in developing a mission profile which achieves the mission requirements specified in reference 2. It contains the mission guidelines, input data for mission simulation, and trajectory analysis where applicable. Also included are graphical and tabular time histories of the spacecraft attitude, position, dynamics, entry heating, separation characteristics, and a summary of the Manned Space Flight Network coverage.

Only brief descriptions of the launch, earth parking orbits, and translunar injection phases of the mission are included in this document; more detailed descriptions are contained in the AS-502 Launch Vehicle Operational Trajectory (ref. 3).

Volume II of this report contains the spacecraft trajectory listing of the mission simulation and the spacecraft input data specifications. Also included are definitions of symbols and reference coordinate systems.

Volume III presents detailed tracking time history data of range, azimuth, elevation, range rate, and the two spacecraft-to-radar look angles for the ground stations available during this mission.

Volume IV presents an analysis of the consumables useage for the Apollo 6 Mission.

### 1.3 Summary of Spacecraft Operational Trajectory

The purpose of the Apollo 6 Mission is to demonstrate the structural compatibility of the launch vehicle and spacecraft and to verify the adequacy of the Block II heat shield when subjected to lunar-return entry conditions. This flight will be the second launch of a Saturn V vehicle and differs from the Apollo 4 Mission primarily because the second S-IVB burn is a typical translunar injection burn.

For mission simulation purposes, the launch is assumed to occur at 13:00 Greenwich mean time (G.m.t.) March 20, 1968 from pad A of complex 39 in the Merritt Island Launch Area and on a flight azimuth of  $72^{\circ}$  from true North.

The major events of the trajectory profile are illustrated in figure 1-1. For discussion purposes the profile has been divided into the following phases.

1. Saturn V ascent to orbit.
2. Earth parking orbit.
3. Second S-IVB burn.
4. S-IVB/CSM separation.
5. First SPS burn.
6. Earth intersecting coast.
7. Second SPS burn.
8. Preentry sequence.
9. Atmospheric entry.

The Saturn V boost to earth parking orbit consists of nominal burns of the S-IC and S-II stages and a partial burn of the S-IVB stage. Thrust termination occurs in a near 100-n. mi. circular parking orbit. The vehicle remains in this orbit for approximately two revolutions while vehicle subsystem checkout is accomplished. No major propulsion systems are used during the two revolutions in earth parking orbit but the orbit is continually perturbed by low-level thrusting due to  $LH_2$  venting and the ullage-engine burns that occur during the initial and final seconds of the parking orbit. Boost from parking orbit occurs during the second revolution shortly after signal acquisition by the Cape Kennedy tracking station. The second S-IVB burn is an optimum burn which injects the vehicle onto a conic typical of the translunar conics used for lunar landing missions. However, the launch vehicle is not targeted to attain terminal conditions near the moon.

After second S-IVB cutoff, the S-IVB orients the spacecraft to the S-IVB/CSM separation attitude. This orientation is completed 180 seconds after the start of S-IVB time base 7 and is followed immediately by the CSM/S-IVB separation sequence. The sequence consists of 10 seconds of CSM RCS +X translation and a coast for 90 seconds to obtain the attitude and adequate separation distance for the first SPS ignition.

First SPS ignition occurs 280 seconds after the start of S-IVB time base 7. At completion of the first SPS burn, which is nominally performed in a retrograde attitude, the spacecraft is in an orbit characterized by an apogee altitude of 11 989 n. mi. and an inertial flight-path angle at entry of  $-6^\circ$ . This earth intersecting orbit insures CM recovery if the SPS fails to reignite for the second burn.

Approximately 6 hours after the first SPS burn is completed and following a G&N position and velocity update from the Carnarvon ground station, the SPS is reignited. This burn accelerates the spacecraft so that an inertial velocity of 36 500 fps and an inertial flight-path angle of  $-6.5^\circ$  are achieved at entry interface (400 000 ft). Coverage of this burn is provided by the Guam tracking station. At SPS cutoff, approximately 4 minutes of coast remain before the spacecraft reaches entry. During this time the CSM orients to the desired CM/SM separation attitude, separation occurs, and the CM orients to the required attitude.

Atmospheric entry occurs at approximately 9 hours 29.5 minutes after lift-off at  $154.96^\circ$  E longitude and  $31.87^\circ$  N latitude. As a result of the entry conditions, a maximum heating rate of  $372$  (B.t.u./ft<sup>2</sup>)/sec and a total heat load of  $37\ 615$  B.t.u./ft<sup>2</sup> are achieved. The maximum load factor encountered during reentry is  $5.74$  g. The spacecraft flies a nominal under-shoot entry trajectory over a 2500-n. mi. range to a CM splash point target of  $157.138^\circ$  W longitude and  $27.354^\circ$  N geodetic latitude.

## 2.0 SUMMARY OF INPUT DATA

The input data summarized in this section have been compiled from references 3 through 8 and include the pertinent MSFN station specifications and a quantitative description of the spacecraft. The detailed data specifications of the spacecraft can be found in Volume II of this report. These data form the basis for the spacecraft operational trajectory for the Apollo 6 Mission.

### 2.1 Saturn V Launch Vehicle

The Saturn V launch vehicle, illustrated in figure 2-1, is comprised of the S-IC, S-II, and S-IVB stages. It will place the CSM/S-IVB into parking orbit. Data for this vehicle were based on the AS-502 Launch Vehicle Operational Trajectory (ref. 3). The conditions at translunar injection, taken from the launch vehicle trajectory listing, were used as the initial conditions for the spacecraft trajectory profile.

### 2.2 Spacecraft (CSM-020)

The data necessary to describe the spacecraft were obtained from references 4 through 8 and are summarized in Volume II of this report. Spacecraft reference dimensions are presented in figure 2-2.

### 2.3 MSFN Tracking Stations

The locations for MSFN tracking stations used for this simulation of the Apollo 6 Mission were obtained from reference 7 and are summarized in table 2-I. Locations of the two Apollo tracking ships available for support of this mission are also included in these tables. The insertion ship, the Redstone, has been located east of Bermuda Island to provide extended coverage following insertion into earth parking orbit. The entry ship, the Watertown, has been located in the Pacific Ocean, east of Guam to provide radar coverage during the ballistic skip and final phases of the CM entry trajectory.

### 2.4 Spacecraft and Attitude Reference Coordinate Systems

The spacecraft attitude is measured by the pitch, yaw, and roll angles required to rotate from a reference coordinate system to the current spacecraft orientation. The reference coordinate systems used in the generating this profile are illustrated in figures 2-3 through 2-8.

2.4.1 Spacecraft body coordinate system ( $X_B, Y_B, Z_B$ ).- This right-handed, orthogonal coordinate system (fig. 2-3) has its origin at the current vehicle position. The  $+X_B$  axis extends through the apex of the CSM. The  $+Z_B$  axis is normal to  $X_B$  and extends in the direction of the foot end of the astronaut's couches. The  $+Y_B$  axis completes the right-handed coordinate system.

2.4.2 Launch site inertial attitude reference system ( $X_I, Y_I, Z_I$ ).- This inertial right-handed, orthogonal coordinate system (fig. 2-4) coincides with the launch site at the instant of lift-off. The  $+X_I$  axis extends down range in the direction of the launch azimuth and lies in the local horizontal plane. The  $+Z_I$  axis extends upward along the reference ellipsoid normal passing through the launch site. The  $+Y_I$  axis completes the right-handed coordinate system.

2.4.3 Earth-reference rotating attitude coordinate system ( $X_R, Y_R, Z_R$ ).- This right-handed, orthogonal coordinate system (fig. 2-5) coincides with the current subvehicle point. The  $+Z_R$  axis extends downward along the reference ellipsoid normal passing through the subvehicle point. The  $+X_R$  axis extends north along the local meridian and is normal to  $Z_R$ . The  $+Y_R$  axis completes the right-handed system.

2.4.4 Platform coordinate system ( $X_P, Y_P, Z_P$ ).- This right-handed, orthogonal coordinate system (fig. 2-6) coincides with the launch site at the instant of lift-off. The  $+X_P$  axis extends upward along the reference ellipsoid normal passing through the launch site. The  $+Z_P$  axis extends down range in the direction of the flight azimuth and lies in the local horizontal plane. The  $+Y_P$  axis completes the right-handed system. This system does not rotate with the earth but moves with the earth with respect to inertial space.

2.4.5 Navigation base coordinate system ( $X_{NB}, Y_{NB}, Z_{NB}$ ).- The origin of this right-handed, orthogonal coordinate system (fig. 2-7) coincides with the origin of the spacecraft body coordinate system at all times. The  $+X_{NB}$  axis makes a  $33^\circ$  angle with the  $+X_B$ , has a  $+X_{NB}$  component lying along the  $-Z_B$  axis, and lies in the  $X_B-Z_B$  plane. The  $+Z_{NB}$  axis makes a  $33^\circ$  angle with the  $+Z_B$  axis, has a  $+Z_{NB}$  component lying along the  $+X_B$  axis,

and lies in the  $X_B-Z_B$  plane. The  $+Y_{NB}$  axis completes the right-handed coordinate system and coincides with the  $+Y_B$  axis.

2.4.6 Relative vehicle coordinate system ( $X_{RV}, Y_{RV}, Z_{RV}$ ).- This left-handed, orthogonal coordinate system (fig. 2-8) is centered at the current vehicle position. The  $+X_{RV}$  axis extends in the direction of and is colinear with the  $+X_B$  axis. The  $Y_{RV}$  axis lies in the local horizontal plane, is normal to  $X_{RV}$ , and is positive in the direction of yaw right. The  $+Z_{RV}$  axis completes the left-handed coordinate system.

2.4.7 Spacecraft look angles ( $\phi, \theta$ ).- The spacecraft orientation with respect to the sun or to the radar vector is illustrated in figure 2-9 and is defined by the following two angles.

1. Theta                      The angle between the spacecraft roll axis ( $+X_B$  axis) and the spacecraft-to-sun or spacecraft-to-radar vector.
2. Phi                         The angle between the spacecraft negative yaw axis ( $-Z_B$  axis) and the spacecraft-to-sun (or radar) vector projected on the roll plane ( $Y_B-Z_B$  plane).  
From the rear of the spacecraft, this angle is measured positive clockwise from the negative yaw axis.

## 2.5 Orbital Geometry and Trajectory Parameter Definitions

The parameters which describe the geometry of the orbital plane in inertial space and the vehicle state in the orbit are presented in this section. The parameters are illustrated in figure 2-10 and 2-11 and are discussed in the following paragraphs.

2.5.1 Orbital geometry.- The size of the orbit can be described by either the semimajor axis or the semilatus rectum of the ellipse. The shape of the ellipse is characterized by the orbital eccentricity. The semilatus rectum and the orbital eccentricity are used as the targeting criteria in the guidance equations for the SPS burns. The semilatus rectum is denoted in figure 2-10 as the distance from the center of the earth (focus) to the ellipse measured at right angles to the major axis.

The orientation of the trajectory plane in inertial space can be described by the following orbital parameters.

1. Longitude of the ascending node - The angle between the vernal equinox and the ascending node of the ellipse measured in the plane of the equator.

2. Orbital inclination - The angle between the trajectory plane and the equatorial plane of the earth.

The position of the spacecraft in orbit can be described by the two following parameters.

1. Argument of perigee - The angle measured in the trajectory plane from the ascending node to the perigee point of the ellipse.

2. True anomaly - The angle between the perigee point and the current position of the spacecraft on the ellipse.

2.5.2 Trajectory parameters. - The vehicle state in orbit is usually described by specifying a radius vector, latitude, longitude, a velocity vector, the flight-path angle, and the azimuth which are referenced to a given coordinate system. These parameters are illustrated in figure 2-11.



### 3.0 NOMINAL MISSION DESCRIPTION

A description of the Apollo 6 Mission simulation and the results of pertinent trajectory analysis are presented in this section. The ascent-to-orbit, the earth parking orbit, and the second S-IVB burn phases of this mission simulation are based upon the MSFC listing of the AS-502 Launch Vehicle Operational Trajectory (ref. 3). The SPS burn phases utilize the cross-product steering guidance philosophy of reference 9 for thrust vector control, and the reentry phase uses the entry guidance logic also from reference 9.

The earth ground track and the altitude-longitude history for the nominal mission profile are presented in figures 3-1 and 3-2, respectively. Earth shadow data (daylight and darkness) are also illustrated in figure 3-1. A discrete events summary is presented in table 3-1. The spacecraft attitude summary is presented in table 3-II and the SM RCS propellant expenditures are summarized in table 3-III.

#### 3.1 Prelaunch

For this mission simulation, launch is planned to occur March 20, 1968. The lighting requirements at the launch site limit the lift-off to occur no earlier than 11:46 G.m.t. (6:46 e.s.t.). Similarly, since 1.5 hours of daylight should remain after landing in the primary recovery area, the launch can occur no later than 17:24 G.m.t. (12:24 e.s.t.).

Another factor which restricts the launch window is the solar requirement for heat-shield cold soak. The requirement as presently defined limits lift-off to occur no earlier than 13:20 G.m.t. (8:20 e.s.t.) and no later than 18:54 G.m.t. (13:54 e.s.t.) for the assumed launch date. These constraints and the resulting solar attitude orientation are discussed in more detail in section 3.7 of this report. The effects of sun lighting and solar requirements for heat-shield cold soak on the launch time are illustrated in figure 3-3.

#### 3.2 Saturn V Ascent to Orbit

Launch of Apollo 6 Mission is planned to occur from pad A of launch complex 39 of the Merritt Island launch area. The geodetic coordinates of the launch site are  $28^{\circ}36'30.32''$  N latitude and  $80^{\circ}36'14.88''$  W longitude. For the trajectory simulation, launch was assumed to occur at 13:00 G.m.t. (08:00 e.s.t.) on March 20, 1968. It should be noted the actual lift-off time will be consistent with solar orientation requirements given in reference 10.

The launch profile of this mission utilizes a  $72^\circ$  flight azimuth from true north and includes the thrusting phases of the S-IC, S-II, and S-IVB stages. A summary of the trajectory events during the phase is included in table 3-I.

MSFN coverage of the ascent-to-orbit phase is provided by the Cape Kennedy, Grand Bahama, Bermuda, and insertion ship tracking stations. The tracking data for this phase and the two revolutions in the earth parking orbit are consistent with reference 3.

Time histories of the trajectory characteristics during the ascent-to-orbit phase are presented in figure 3-4.

### 3.3 Earth Parking Orbit

At first S-IVB engine cutoff, which occurs 10 minutes 52 seconds after lift-off, the spacecraft is inserted into a 100-n. mi. circular parking orbit having an inclination of  $32.561^\circ$  and a period of approximately 88 minutes. The state vector at insertion can be described as follows:

Altitude, ft . . . . .	628 270.000
Geodetic latitude, deg N . . . . .	32.639
Longitude, deg W . . . . .	55.088
Inertial velocity, fps . . . . .	25 569.913
Inertial flight-path angle, deg. . . . .	+0.001
Inertial azimuth, deg. . . . .	87.407

The vehicle remains in earth parking orbit for approximately two revolutions while subsystems checkout is made. The nominal S-IVB/CSM attitude maneuvers during this period are presented in table 3-IV(a). No major thrusting occurs during the parking orbit; however, the orbit is continuously perturbed by low-level thrusting due to  $LH_2$  venting. Also, the ullage engine burns during the initial and final seconds of the parking orbit perturb the orbit.

At approximately 1 hour 34 minutes after lift-off, the S-IVB orients the spacecraft to an attitude such that the -Z axis of the spacecraft will be along the local vertical. The S-IVB holds this attitude until approximately 3 hours 8 minutes into the mission when the S-IVB begins orientation for the second S-IVB ignition. During this period, the camera mounted in the hatch window will photograph the earth.

The S-IVB preignition sequence is initiated after the spacecraft passes over the western coast of the United States on the second parking orbit revolution. During this sequence, the launch vehicle maneuvers at an assumed 1-deg/sec rate to align to the predetermined attitude for the

second S-IVB burn. This event occurs approximately 3 hours 6 minutes after lift-off or about 4.1 minutes prior to second S-IVB ignition.

The trajectory characteristics during earth parking orbit phase are presented in figure 3-5.

### 3.4 Second S-IVB Burn

Second S-IVB engine ignition occurs on the second parking orbit revolution, 3 hours 10 minutes after lift-off as the spacecraft approaches Cape Kennedy. The boost to translunar injection lasts for 327.34 seconds, and the injection occurs at an altitude of 186.7 n. mi., an inertial velocity of 35 539 fps, and an inertial flight-path angle of 7.383°.

Figure 3-6 presents the trajectory characteristics during the second S-IVB burn. Injection occurs at 3 hours 15 minutes 47 seconds after lift-off, which is 10 seconds after  $t_{B7}$ .

### 3.5 S-IVB/CSM Separation

At 20 seconds after launch vehicle  $t_{B7}$ , the S-IVB orients the spacecraft to the S-IVB/CSM separation attitude. The IMU gimbal angles for separation are

Inner, deg . . . . .	61.04
Middle, deg. . . . .	-1.40
Outer, deg . . . . .	-0.60

One hundred and sixty seconds have been allowed for the S-IVB to orient the CSM to the separation attitude. At  $t_{B7} + 180$  seconds, the CM mission control programmer (MCP) sends the discrete separation start sequence. Upon receipt of this signal, the SM RCS jets are turned on for +X translation. After 1.7 seconds of thrusting, physical separation occurs. The RCS jets continue thrusting for another 8.3 seconds, then the CSM coasts for 90 seconds to attain separation distance prior to first SPS ignition. During this coast period the CSM performs a prethrust alignment to place the spacecraft in the proper attitude for the first SPS burn. This attitude is defined by the IMU gimbal angles as follows:

Inner, deg . . . . .	64.59
Middle, deg. . . . .	-1.40
Outer, deg . . . . .	-.60

The spacecraft characteristics from CSM/S-IVB separation to first SPS ignition are illustrated in figures 3-7 and 3-8.

### 3.6 First SPS Burn

The first SPS ignition occurs 280 seconds after launch vehicle  $t_{B7}$ , which corresponds to 3 hours 20 minutes 16.94 seconds after lift-off. The spacecraft pitch attitude at ignition is approximately  $173.1^\circ$  from the inertial velocity vector or  $25.8^\circ$  below the local horizontal. The burn lasts for 254 seconds during which the attitude changes with respect to the velocity vector by only  $6.4^\circ$ .

This burn is targeted using the cross-product steering logic of reference 9 to a coplanar ellipse having a semilatus rectum of 34 340 227 ft and an eccentricity of 0.63429326. This ellipse has an apogee altitude of 11 989 n. mi. and a perigee altitude of 18 n. mi. If the second SPS ignition does not occur, the inertial velocity and flight-path angle at reentry will be 32 813.4 fps and  $-6^\circ$ , respectively.

Figures 3-11(a) through 3-11(e) present the spacecraft trajectory characteristics during the first SPS burn. Figure 3-11(f) presents the time of free fall ( $t_{ff}$ ) to the entry interface as a function of burn time. Also presented on this figure are the instantaneous predicted values of the inertial velocity and flight-path angle at entry. Figure 3-11(g) presents a time history of the instantaneous apogee and perigee altitudes during the first SPS burn.

### 3.7 Earth Intersecting Coast

At first SPS engine cutoff, 3 hours 24 minutes 32 seconds after lift-off, the SPS injected the spacecraft into an orbit characterized by a semimajor axis of 34 339 859 ft, an eccentricity of 0.6342907, and an inclination of  $32.49^\circ$ . It should be noted that the spacecraft does not achieve the exact target ellipse of the first SPS burn. However, this is within the tolerances of the guidance cutoff logic. The state vector at injection into the coast ellipse can be described as follows:

Altitude, ft . . . . .	6 229 926
Geodetic latitude, deg N . . . . .	9.253
Longitude, deg W . . . . .	24.214
Inertial velocity, fps . . . . .	28 139
Inertial flight-path angle, deg. . . . .	24.504
Inertial azimuth, deg. . . . .	121.299

Immediately following SPS engine cutoff, the CSM initiates an attitude reorientation maneuver to place the spacecraft into the desired attitude for cold soak. The proposed attitude for cold soaking CSM-020 is defined in figure 3-9. To achieve this attitude the spacecraft -X axis is

oriented toward the sun placing the CM in shadow. Although the aforementioned attitude is optimum, the acceptable operational limits have been defined so that the sun-to-spacecraft vector may vary from the -X axis within a  $30^\circ$  half-angle cone about that axis.

These constraints are defined in terms of sun look angles, phi and theta. Theta is measured from the +X axis of the spacecraft to the sun-to-spacecraft vector. Phi is the angle between the spacecraft -Z axis and the projection of the sun-to-spacecraft vector onto the Y-Z plane, measured positive clockwise. Therefore, considering only the solar requirement, an acceptable attitude for CSM-020 would be one for which the theta angle varies between  $150^\circ$  to  $180^\circ$  and the phi angle varies from  $0^\circ$  to  $360^\circ$ . The phi angle is varied in order to obtain satisfactory communications throughout the cold soak. However, this must be performed with due consideration of the gimbal lock limit of the IMU which is  $60^\circ$  for the middle gimbal angle.

The primary attitude defined within the above constraints is given in terms of IMU gimbal angles (ref. 11 and 12) as follows:

Inner, deg . . . . .	111.83
Middle, deg. . . . .	-28.16
Outer, deg . . . . .	119.14

Figure 3-10(a) shows that the primary attitude is within the defined tolerances for the assumed launch between 8:20 and 11:45 e.s.t. on March 20, 1968. A secondary attitude which can be loaded into the computer when a launch time beyond 10:00 becomes imminent is within the defined tolerances from 10:00 to 02:00 e.s.t. as shown in figure 3-10(b) is shown in terms of IMU gimbal angles as follows:

Inner, deg . . . . .	139.79
Middle, deg. . . . .	-41.46
Outer, deg . . . . .	173.75

A recent change to the solar requirements has required a reevaluation of the primary cold soak attitude. These changes and their effect on the primary cold soak gimbal angles will be finalized shortly. The secondary attitude will remain unchanged. Following SPS engine cutoff, the AGC begins calculating the  $t_{ff}$  to entry interface.

The coast phase is then set to end 25 minutes before the free-flight trajectory intersects 400 000 ft.

Approximately 6 hours 22 minutes after first SPS cutoff, the spacecraft reaches apogee altitude and starts its descent. At the end of the coast phase, the spacecraft position and velocity and  $t_{ff}$  to entry will be updated in the AGC by the Carnarvon ground station in preparation for the

second SPS burn. Approximately 2 minutes after the update has been received, the AGC initiates a reorientation maneuver from the cold soak attitude to the ignition attitude for the second SPS burn. The spacecraft holds this attitude until SPS ignition occurs.

When the  $t_{ff}$  to entry falls below 631 seconds ( $t_{ff \text{ min}}$ ), the AGC schedules the second SPS ignition to occur within 2 minutes. The spacecraft coasts in an attitude-hold mode until the  $t_{ff} = 540$  seconds. The CSM RCS jets are then turned on for a 30-second ullage maneuver. Immediately following the ullage, the second SPS ignition occurs.

The spacecraft position and velocity during the earth intersecting coast phase are presented in figures 3-12(a) through (b). The time histories of the IMU gimbal angles during this phase are presented in figure 3-12(e).

### 3.8 Second SPS Burn

The nominal mission plan calls for the second S-IVB burn to accelerate the spacecraft so that at entry the velocity is 36 500 fps and the flight-path angle is  $-6.5^\circ$ . These conditions are accomplished by targeting the spacecraft to coplanar orbit characterized by a semilatus rectum of 42 418 422 ft and an eccentricity of 1.0164386. The cross-product steering logic of reference 9 is again used for thrust vector control. The duration of this burn is approximately 188 seconds.

The spacecraft pitch attitude at SPS ignition is approximately  $25^\circ$  below the inertial velocity vector or  $46^\circ$  down from the local horizontal. At nominal SPS engine cutoff, the spacecraft pitch attitude is  $17^\circ$  below the velocity vector.

Figure 3-13 presents the spacecraft position, attitude, and dynamic characteristics throughout the SPS burn. Figure 3-13(e) presents the IMU gimbal angle histories. Figure 3-13(f) presents the time of free fall to entry interface.

### 3.9 Preentry Sequence

At SPS second cutoff approximately 4 minutes remain before reentry. During this time, the CM/SM separation and preentry attitude reorientation maneuvers are performed.

When  $t_{ff} = 200$  seconds, the CSM initiates the reorientation maneuver to the desired attitude for CM/SM separation (+X axis up in the trajectory plane of motion  $60^\circ$  above the inertial velocity vector). This attitude is

held constant until  $t_{ff} = 85$  seconds, at which time physical CM/SM separation occurs. The separation maneuver is performed by firing four SM-RCS thrusters to provide  $-X$  translation. Translation continues until RCS propellant is depleted.

Approximately 5 seconds after CM/SM separation the guidance and navigation system will begin reorienting the CM to the predetermined attitude for atmospheric entry. This attitude is such that the angle of attack is  $157^\circ$  with the lift vector up. The preentry sequence is illustrated in figure 3-15.

### 3.10 Atmospheric Entry

Approximately 9 hours 29 minutes 23.59 seconds after lift-off, the CM enters the atmosphere at  $31.867^\circ$  N latitude and  $154.963^\circ$  E longitude. Reentry occurs at 400 000 ft; the inertial velocity is 36 500 fps and the inertial flight-path angle is  $6.5^\circ$  below the local horizontal (ref. 14).

Figure 3-16 shows a plot of the CM maneuver footprint and the nominal ground track on a map of the reentry area. The nominal touchdown target location is 2500 n. mi. down range from the reentry interface position, and the ground coordinates of the target are  $157.179^\circ$  W longitude and  $27.326^\circ$  N geodetic latitude. This target location was selected in order to maximize the total heat load under the constraints imposed by the reentry guidance system parameters and operation. The increased heat load resulting from this target will provide a more stringent test for the heat shield than that obtained from Mission A-1, Apollo 4.

The nominal flight time from lift-off to drogue deployment at 23 500-ft altitude is 9 hours 43 minutes 34 seconds. Figure 3-17, which shows altitude as a function of range from reentry interface, denotes the phase of the guidance system exercised. The load factor at the center of gravity, which reaches a maximum of  $5.74$  g at 9 hours 30 minutes 46 seconds after lift-off, is shown as a function of time in figure 3-18(a). The time histories of total heat load and total heating rate are also shown. The radiant heating rates were calculated from updated radiant heating tables (ref. 13) which give about one half the values that the tables used for A-1/CSM 017 Mission would have given (ref. 1). The maximum total heating rate is  $372$  (B.t.u./ft<sup>2</sup>)/sec at 9 hours 30 minutes 30 seconds after lift-off, and the total heat load is  $37\ 615$  B.t.u./ft<sup>2</sup>. Figure 3-18(b) shows time histories of altitude, load factor, and bank angle commanded by the guidance system. While performing the guidance commands during the reentry, the RCS system used 49.2 lb of fuel. This fuel consumption does not include any data before 400 000 ft, which is approximated at 10 lb.

The time histories of position, inertial and relative velocities and flight-path angles are presented in figures 3-18(c) through (e). Figure 3-18(f) shows the altitude, dynamic pressure, and Mach number as a function of time, and figure 3-18(g) gives the time histories of bank angle and trim angle of attack. Table 3-VI gives the Apollo 6 aerodynamic coefficients at trim angle of attack as a function of Mach number. Figure 3-18(h) presents a time history of the IMU gimbal angles during reentry.

In figure 3-19, altitude is plotted in relation to relative velocity, and the boundaries for S-band and C-band communication blackout are shown. Altitudes below the boundaries are areas of communications blackout.

The drogue parachute deployment sequence starts at 9 hours 43 minutes 35 seconds after lift-off at an altitude of 23 500 ft. The two drogue parachutes are deployed 2 seconds later. At an altitude of 10 200 ft, 9 hours 44 minutes 24 seconds after lift-off, the low altitude baroswitch closes, and the drogue parachutes are disconnected. The three main parachutes are deployed 1 second after the baroswitch closes. Table 3-VII presents the Apollo command module parachute descent events and aerodynamics. The CM, suspended on the main parachutes, reaches splashdown 9 hours 49 minutes 45 seconds after lift-off.



#### 4.0 MISSION PROFILES RESULTING FROM SPS ENGINE FAILURE

The second S-IVB burn of the Apollo 6 Mission is an optimum burn which injects the vehicle onto a conic typical of the translunar conics used for lunar landing missions. For the launch date assumed in this report, the vehicle will not attain terminal conditions near the moon. However, if the SPS fails to ignite for the first burn the spacecraft is committed to the trajectory of the S-IVB. Assuming an 8:00 e.s.t. launch on March 20, 1968, this trajectory is characterized by an apogee altitude of approximately 275 920 n. mi. and a perigee altitude of 1616 n. mi. However, if the SPS fails during the second SPS burn, the trajectory is designed to insure CM recovery. A summary of the events for a second SPS ignition failure is presented in the following paragraphs and will be discussed in detail in the alternate mission plan.

##### 4.1 First SPS Burn; No Second SPS Burn

The first SPS burn is targeted to a 11 989-n. mi. apogee coast ellipse which insures CM recovery if second SPS ignition does not occur. In this case the CM enters the atmosphere approximately 9 hours 31 minutes from lift-off with an inertial velocity of 32 813.4 fps and an inertial flight-path angle of  $-6.^{\circ}$ . Reentry occurs at  $32.28^{\circ}$  N geodetic latitude and  $159.07^{\circ}$  E longitude.

For this case, the spacecraft will fly as far down range as possible in an attempt to achieve the nominal splash point. The maximum entry heating rate achieved from this profile is 202 (B.t.u./ft<sup>2</sup>)/sec and the maximum load factor encountered during reentry is 5.18 g.

The CM splash for the no-second-SPS-burn trajectory occurs at approximately 9 hours 51 minutes after lift-off at  $28.14^{\circ}$  N geodetic latitude and  $159.75^{\circ}$  W longitude. The landing footprint is illustrated in figure 4-1.

##### 4.2 Summary of Splash Points

The splash points for the spent SM stage and the CM are summarized in table 4-I and illustrated in figure 4-2. A comparison of the nominal mission and no-second-SPS-burn entry and splash characteristics is presented in table 4-II.

## 5.0 TRACKING AND COMMUNICATIONS DATA

The spacecraft visibility periods for the ground stations listed in table 2-I are presented in table 5-I. The ground tracking coverage during the ascent to orbit, the second S-IVB burn, the SPS burns, and the preentry sequence is shown in figure 5-1. Spacecraft visibility is defined for tracking elevation angles greater than  $5^{\circ}$ .

Volume III presents detailed tracking time histories of range, azimuth, elevation, range rate, and two spacecraft-to-radar look angles for each of the ground stations and tracking ships available for operation on this mission. These data include the ascent-to-orbit and the earth parking orbit phases, as well as the earth-intersecting coast and reentry phases.

TABLE 2-1.- MSFN GROUND STATIONS AND CAPABILITIES  
(a) Unified S-band stations

Radar station	Call letters	Tracking		Telemetry	Voice	Command	Location <sup>a</sup>		
		Low speed	High speed				Geodetic latitude, deg (b)	Longitude, deg	Altitude, feet
Merritt Island	MIL	Yes	Yes	Yes	Yes	Yes	28.508272	279.30658	32.8
Grand Bahama Island	GBM	Yes	Yes	Yes	Yes	Yes	26.654722	281.84750	45.9
Bermuda Island	BDA	Yes	Yes	Yes	Yes	Yes	32.351286	295.34182	68.9
Grand Canary Island	CYI	Yes	Yes	Yes	Yes	Yes	27.764536	344.36519	567.6
Ascension Island	ACN	Yes	Yes	Yes	Yes	Yes	- 7.955056	345.67242	1843.8
Guam	GWM	Yes	Yes	Yes	Yes	Yes	13.309244	144.73441	416.7
Hawaii	HAW	Yes	No	Yes	Yes	Yes	22.124897	200.33501	3773.0
Goldstone, California	GDS	Yes	Yes	Yes	Yes	Yes	35.341694	243.12671	3166.0
Guaymas, Mexico	GYM	Yes	Yes	Yes	Yes	Yes	27.963206	249.27915	62.3
Texas	TEX	Yes	Yes	Yes	Yes	Yes	27.653750	262.62153	32.8
Madrid, Spain	MAD	Yes	Yes	Yes	Yes	Yes	40.455358	355.83261	2706.7
Canberra, Australia	CNB	Yes	Yes	Yes	Yes	Yes	-35.584739	148.97658	3766.4
Camaron, Australia	CRO	Yes	Yes	Yes	Yes	Yes	-24.907592	113.72425	190.3
Insertion Ship	RED	Yes	Yes	Yes	Yes	Yes	30.000000	310.00000	32.8

<sup>a</sup>Referenced to Fischer ellipsoid of 1960.

<sup>b</sup>Minus coordinate indicates south latitude.

TABLE 2-1.- MSFN GROUND STATIONS AND CAPABILITIES - Concluded

Radar station	Call letters	Tracking		Telemetry	Voice	Command	Location <sup>a</sup>		
		Low speed	High speed				Geodetic latitude, deg (b)	Longitude, deg	Altitude, feet
		Yes	Yes						
Merritt Island	MLA	Yes	Yes	No	No	No	28.424862	279.33560	39.4
Patrick AFB, Florida	PAT	Yes	Yes	No	No	No	28.226553	279.40071	49.2
Grand Bahama Island	GBI	Yes	Yes	Yes	Yes	Yes	26.636350	281.73229	39.4
Bermuda Island	BDA	Yes	Yes	Yes	Yes	Yes	32.348103	295.34620	59.1
Bermuda Island	BDQ	Yes	Yes	No	No	No	32.347964	295.34630	62.3
Antigua Island	ANT	Yes	Yes	Yes	Yes	Yes	17.144031	298.20714	190.3
Grand Canary Island	CYI	Yes	No	Yes	Yes	Yes	27.763206	344.36519	551.2
Ascension Island	ASC	Yes	Yes	No	Yes	No	- 7.972761	345.59831	469.2
Hawaii	HAW	Yes	Yes	Yes	Yes	Yes	22.122092	200.33462	3740.2
Pt. Arguello, California	CAL	Yes	Yes	No	Yes	No	34.582903	239.43885	2119.4
White Sands, New Mexico	WHS	Yes	Yes	No	No	No	32.358222	253.63044	4042.0
Tanarive	TAN	Yes	No	No	Yes	No	-19.000797	47.31505	4337.3
Carnarvon, Australia	CRO	Yes	Yes	Yes	Yes	Yes	-24.897403	113.71608	203.4
Insertion Ship	RED	Yes	Yes	No	No	No	30.000000	310.00000	32.8
Entry Ship	WTN	Yes	Yes	Yes	Yes	Yes	32.000000	184.00000	62.3

<sup>a</sup>Referenced to Fischer ellipsoid of 1960.<sup>b</sup>Minus coordinate indicates south latitude.

TABLE 3-1. - APOLLO 6 MISSION DISCRETE EVENTS SUMMARY

(a) Saturn V operations

Event	Time from lift-off, hr:min:sec	Revolution number	Geodetic latitude, deg	Longitude, deg	Altitude, ft	Inertial velocity, fps	Inertial flight-path angle, deg	Inertial azimuth, deg
Guidance reference release	-0:00:16.70	1	28.608	-80.604	197	1 340.674	0.000	90.000
Lift-off	0:00:00.00	1	28.608	-80.604	197	1 340.674	0.000	90.000
Maximum dynamic pressure	0:01:19.00	1	28.627	-80.535	44 293	2 814.329	28.165	81.725
S-IC engine cutoff (timebase 3)	0:02:28.38	1	28.836	-79.778	194 430	9 084.694	19.524	75.489
S-IC/S-II separation	0:02:29.15	1	28.840	-79.761	196 772	9 114.038	19.408	75.485
S-II ignition	0:02:30.88	1	28.850	-79.724	201 982	9 103.195	19.125	75.504
Jettison launch escape tower	0:03:04.78	1	29.055	-78.956	292 864	9 661.785	14.322	75.688
S-II engine cutoff (timebase 4)	0:08:38.60	1	31.759	-65.283	619 872	22 594.630	0.733	81.683
S-II/S-IVB separation	0:08:39.48	1	31.767	-65.226	620 133	22 610.176	0.724	81.715
S-IVB ignition	0:08:43.10	1	31.798	-64.988	621 159	22 610.747	0.664	81.848
S-IVB cutoff	0:10:52.07	1	32.605	-55.852	628 229	25 560.818	-0.001	86.974
Parking orbit insertion	0:11:02.07	1	32.639	-55.088	628 270	25 569.913	0.001	87.407
S-IVB reignition	3:10:09.40	2	32.468	-87.991	670 356	25 554.615	-0.017	94.367
Second S-IVB cutoff	3:15:36.74	3	27.107	-60.239	1 059 929	35 557.026	6.929	108.850
Timebase 7	3:15:36.94	3	27.101	-60.221	1 060 781	35 566.018	6.938	108.859
Translunar injection	3:15:46.74	3	26.805	-59.308	1 103 924	35 539.005	7.383	109.289

TABLE 3-1.- APOLLO 6 MISSION DISCRETE EVENTS SUMMARY - Concluded

(b) Spacecraft operations

Event	Time from lift-off, hr:min:sec	Revolution number	Geodetic latitude, deg	Longitude, deg	Altitude, ft	Inertial velocity, fps	Inertial flight-path angle, deg	Inertial azimuth, deg
Translunar injection	3:15:46.74	3	26.805	-59.308	1 103 924	35 539.005	7.383	109.289
S-IVB/CSM separation	3:18:38.64	3	21.013	-44.829	2 291 920	34 625.335	14.810	115.462
First SPS ignition	3:20:16.94	3	17.482	-37.855	3 260 446	33 912.735	18.663	117.891
First SPS cutoff	3:24:30.94	3	9.273	-24.243	6 221 917	28 151.262	24.495	121.294
Apogee	6:21:52.50	3	-32.224	44.731	72 847 244	7 415.190	-0.000	85.348
+X translation	9:21:43.84	3	20.602	116.889	4 545 281	29 336.372	-21.458	64.231
Second SPS ignition	9:22:13.84	3	21.409	118.568	4 227 353	29 583.373	-20.797	64.876
Second SPS cutoff	9:25:22.33	3	26.626	131.525	2 211 843	35 039.649	-17.553	70.471
CM/SM separation	9:27:53.98	3	30.366	145.507	888 789	36 090.975	-10.814	77.451
Entry	9:29:23.59	3	31.867	154.963	400 000	36 499.859	-6.501	82.523
Drogue chute deployment	9:43:33.99	3	27.351	-157.140	23 349	1 511.099	-14.842	84.239
Main chute deployment	9:44:23.19	3	23.354	-157.138	10 114	1 375.737	-9.402	90.018
CM splash	9:49:45.20	3	27.354	-157.138	0	1 356.500	-1.202	90.004

TABLE 3-II.- APOLLO 6 MISSION SPACECRAFT ATTITUDE SUMMARY

	Time from lift-off, hr:min:sec	Inertial			Earth relative			IMU gimbal angles		
		Pitch, deg	Yaw, deg	Roll, deg	Pitch, deg	Yaw, deg	Roll, deg	Inner, deg	Middle, deg	Outer, deg
Trans lunar injection	3:15:46.74	53.68	0.62	0.00	7.67	108.20	-1.23	-176.68	-0.52	179.66
Begin orientation to CSM/S-IVB separation attitude	3:15:56.94	53.68	0.62	0.00	8.60	108.64	-1.25	-176.68	-0.52	179.66
End orientation to S-IVB/CSM separation	3:18:01.06	241.97	0.85	178.73	-11.30	-65.09	-0.22	61.04	-1.40	-0.60
S-IVB/CSM separation	3:18:38.64	241.97	0.85	178.73	-14.45	-63.95	-0.24	61.04	-1.40	-0.60
Begin orientation to first SPS ign attitude	3:18:51.94	241.97	0.85	178.73	-15.55	-63.57	-0.25	61.04	-1.40	-0.60
End orientation to first SPS ignition attitude	3:18:52.83	238.42	0.85	178.73	-19.17	-63.61	-0.28	64.59	-1.40	-0.60
First SPS ignition	3:20:16.94	238.42	0.85	178.73	-25.82	-61.55	-0.33	64.59	-1.40	-0.60
First SPS cutoff	3:24:30.94	242.92	0.42	178.77	-37.77	-58.51	-0.11	60.07	-1.02	-0.81
Begin orientation for solar soak	3:24:36.63	242.92	0.42	178.77	-38.06	-58.47	-0.11	60.07	-1.02	-0.81
End orientation for solar soak	3:25:37.52	130.81	54.60	317.83	-15.99	64.95	-20.57	111.94	-28.16	119.14
Apogee	6:21:52.50	130.81	54.60	317.83	36.18	0.10	-125.43	111.94	-28.16	119.14
Begin orientation for second SPS burn	9:07:46.10	130.81	54.60	317.83	6.00	-68.49	144.69	111.94	-28.16	119.14

TABLE 3-II. - APOLLO 6 MISSION SPACECRAFT ATTITUDE SUMMARY - Concluded

	Time from lift-off, hr:min:sec	Inertial			Earth relative			IMU gimbal angles		
		Pitch, deg	Yaw, deg	Roll, deg	Pitch, deg	Yaw, deg	Roll, deg	Inner, deg	Middle, deg	Outer deg
End orientation for second SPS burn	9:08:45.22	26.18	-1.10	180.78	-82.55	58.22	179.34	-83.18	1.35	0.05
+X translation	9:21:43.84	26.18	-1.10	180.78	-47.42	64.25	179.97	-83.18	1.35	0.05
Second SPS ignition	9:22:13.84	26.18	-1.10	180.78	-45.55	64.89	179.98	-83.18	1.35	0.05
Second SPS cutoff	9:25:22.33	28.35	-0.70	180.79	-34.17	70.04	-179.76	-85.35	1.02	0.28
Begin orientation for CM/SM separation	9:25:59.02	28.35	-0.70	180.79	-31.05	71.55	-179.77	-85.35	1.02	0.28
End orientation for CM/SM separation	9:26:16.81	318.37	-1.05	179.29	40.46	72.68	179.99	-15.37	0.50	-1.17
CM/SM separation	9:27:53.98	318.37	-1.05	179.29	49.22	77.42	-180.00	-15.37	0.50	-1.17
Begin orientation for entry	9:27:58.98	318.37	-1.05	179.29	49.46	77.69	-180.00	-15.37	0.50	-1.17
End orientation for entry	9:28:22.69	225.32	0.51	179.14	35.04	-101.32	-0.03	77.68	-0.90	-0.45
Entry	9:29:23.59	225.32	0.51	179.14	29.19	-97.78	-0.00	77.68	-0.90	-0.45



TABLE 3-III.- SERVICE MODULE RCS PROPELLANT EXPENDITURES

Maneuver	RCS propellant expenditure, lb
CSM/S-IVB separation (10 sec of +X translation)	14.4
Attitude orientation to first SPS burn attitude	3.8
SPS cutoff damping	1.0
Attitude orientation to solar soak attitude	8.9
Attitude hold mode (0.2-degree deadband)	128.3
Attitude orientation to second SPS burn attitude	8.9
30-second RCS ullage prior to second SPS ignition	43.2
SPS cutoff damping	1.0
Attitude orientation for CM/SM separation	8.9
CM/SM separation	<sup>a</sup> 561.6
Total	<u>780.0</u>

NOTE: Propellant expenditure data was used in this simulation for weight bookkeeping. Volume IV of the report should be consulted for the official breakdown of RCS propellant consumption.

<sup>a</sup> CM/SM separation burn ends with RCS propellant depletion.

TABLE 3-IV.- SUMMARY OF S-IVB ATTITUDE MANEUVERS

(a) Earth parking orbits

Maneuver	Time from lift-off, hr:min:sec (a)
Maintain commanded cutoff inertial attitude	0:10:45.9 ( $t_{B5} + 0$ sec)
Initiate maneuver to align S-IVB/CSM +X axis with local horizontal (CSM forward, +Z <sub>B</sub> up) and maintain orbital rate	0:11:00.9 ( $t_{B5} + 15$ sec)
Roll 180° down and maintain orbital rate	0:12:15.9 ( $t_{B5} + 90$ sec)
Initiate 20° pitch down maneuver and maintain orbital rate	0:51:45.9 ( $t_{B5} + 2460$ sec)
Initiate 20° pitch up maneuver to the local horizontal and maintain orbital rate	1:28:45.9 ( $t_{B5} + 4680$ sec)
Initiate 180° roll maneuver to place +Z <sub>B</sub> down. Maintain +X axis along local horizontal until the beginning of the restart sequence	1:34:45.9 ( $t_{B5} + 5040$ sec)

<sup>a</sup> $t_{B5}$  is orbital insertion cutoff command

TABLE 3-IV. - SUMMARY OF S-IVB ATTITUDE MANEUVERS - Concluded

(b) Post injection

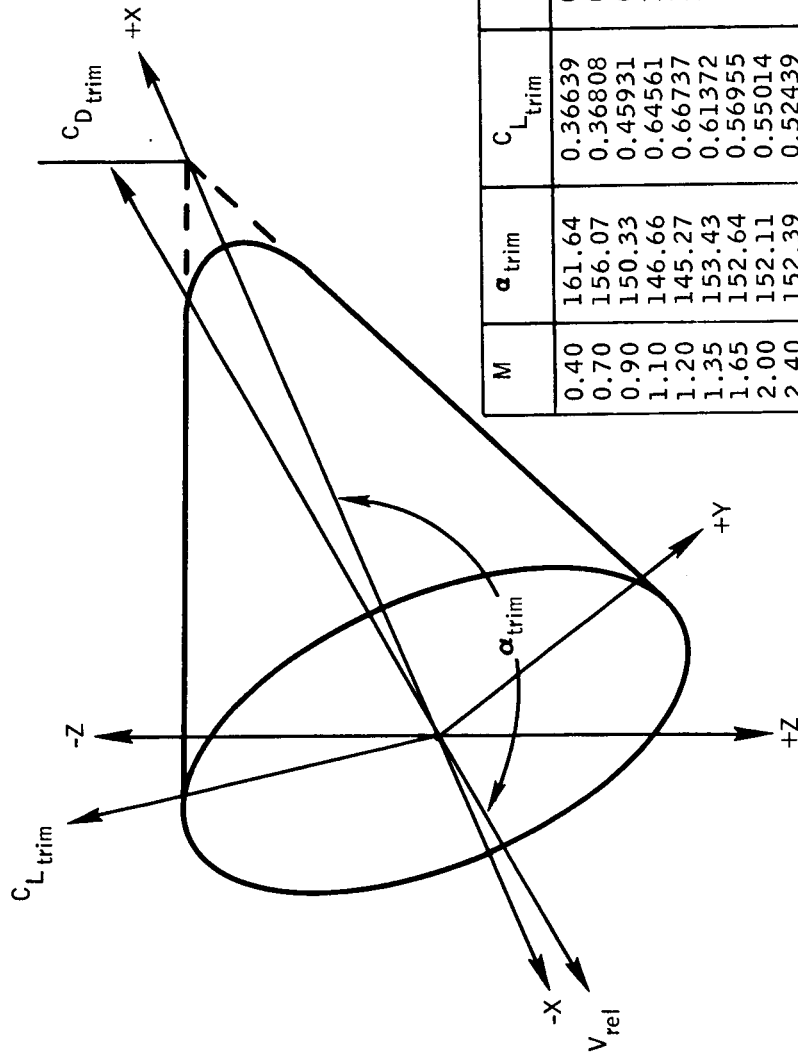
Maneuver	Maneuver mode	Initiation time of maneuver from lift-off, hr:min:sec (a)	Terminal time of maneuver from lift-off, hr:min:sec
Maintain second S-IVB commanded cutoff inertial attitude	Programmed	3:15:36.94 ( $t_{B7} + 0$ sec)	3:15:56.94
Orient to CSM/S-IVB separation attitude at 1.44 deg/sec in each axis Separation attitude: Inertial yaw = 0.849° Inertial pitch = 241.967° Inertial roll = 178.732°	Programmed	3:15:56.94 ( $t_{B7} + 20$ sec)	3:18:01.06
Maintain CSM/S-IVB separation attitude	Programmed	3:18:01.06	3:18:36.94
IU sends separation start sequence discrete to the CSM	Programmed	3:15:36.94 ( $t_{B7} + 180$ sec)	
CSM/S-IVB separation	Programmed	3:18:38.64 ( $t_{B7} + 181.7$ sec)	
First SPS ignition	Programmed	3:20:16.94 ( $t_{B7} + 280$ sec)	
Orient to post-separation inertial attitude Post-separation attitude: Inertial yaw = 0° Inertial pitch = -164° Inertial roll = 2°	Programmed	3:25:36.94 ( $t_{B7} + 600$ sec)	3:35:36.94
Hold post-separation attitude	Programmed	3:35:36.94	5:15:36.94
Orient to align S-IVB/IU/SLA +X axis with local horizontal SLA forward	Ground command with programmed backup	5:15:36.94 ( $t_{B7} + 7200$ sec)	

<sup>a</sup> $t_{B7}$  - Launch vehicle time sequence

TABLE 3-V.- SPACECRAFT GUIDANCE TARGETING PARAMETERS

Event	Desired orbit eccentricity, e	Desired semilatus rectum, p, feet	Bias on time-to-go calculation, sec	Guidance scaling constant	Resulting trajectory characteristics
First SPS burn	0.63429326	34 340 227	0.389	0.50	Apogee altitude = 11 989 n. mi. Inertial flight-path angle at 400 000 feet = -6.0°
Second SPS burn	1.0164386	42 418 422	0.389	0.50	Inertial velocity at 400 000 feet = 36 500 fps Inertial flight-path angle at 400 000 feet = -6.5°

TABLE 3-VI.- APOLLO 6 AERODYNAMIC COEFFICIENTS AT TRIM ANGLE OF ATTACK  
AS A FUNCTION OF MACH NUMBER



M	$\alpha_{trim}$	$C_{L_{trim}}$	$C_{D_{trim}}$	$L/D_{trim}$
0.40	161.64	0.36639	0.87887	0.41689
0.70	156.07	0.36808	0.94610	0.38905
0.90	150.33	0.45931	0.99520	0.46152
1.10	146.66	0.64561	1.07238	0.60204
1.20	145.27	0.66737	1.04722	0.63728
1.35	153.43	0.61372	1.27534	0.48122
1.65	152.64	0.56955	1.28498	0.44324
2.00	152.11	0.55014	1.27225	0.43242
2.40	152.39	0.52439	1.26508	0.41451
3.00	152.91	0.50320	1.22086	0.41217
4.00	153.56	0.47077	1.17335	0.40122
6.00	157.53	0.42246	1.24948	0.33811

TABLE 3-VII. - APOLLO COMMAND MODULE PARACHUTE DESCENT EVENTS AND AERODYNAMICS

Event	Altitude, ft	Time, sec	$C_D S$ per chute, ft <sup>2</sup>
High altitude baroswitch closed (actuate ELS)	23 500	0.0	0.0
Deploy drogue chutes <sup>a</sup>		2.0	0.0
Drogue line stretch		2.7	0.0
Drogue chute reefed inflation		2.8	40.0
Drogue chute disreef		10.8	40.0
Drogue chutes full open		11.0	68.0
Low altitude baroswitch closed	10 200	0.0	0.0
Deploy main chutes <sup>b</sup>		1.0	0.0
Main line stretch		2.0	0.0
Main chute reefed inflation		3.5	300.0
Begin main chute disreef		10.0	300.0
Mains full open		13.0	4000.0

<sup>a</sup>There are two drogue parachutes.

<sup>b</sup>There are three main parachutes.

TABLE 4-I.- SPLASH POINTS

Vehicle	Time of impact from lift-off, hr:min:sec	Impact latitude, deg	Impact longitude, deg
Service module Nominal	9:34:19.0	32.6	166.2
Command module No second SPS burn	9:51:23.9	28.14	-159.75
Nominal	9:49:45.2	27.35	-157.14

TABLE 4-II.- COMPARISON OF NOMINAL AND NO-SECOND-SPS-BURN ENTRY

Parameter	Nominal	No second SPS burn
G.e.t. at entry, hr:min:sec	9:29:23.6	9:30:48.7
Geodetic latitude at entry, deg	31.867	32.28
Longitude at entry, deg	154.963	159.07
Inertial velocity at entry, fps	36 499.9	32 813.4
Inertial flight-path angle at entry, deg	-6.501	-6.01
Inertial azimuth at entry, deg	82.52	84.89
Maximum load factor, g, nd	5.74	5.18
Maximum heat rate, Btu/ft <sup>2</sup> /sec	372.0	202.0
Total heat load, Btu/ft <sup>2</sup>	37 615.0	26 537.0
Geodetic latitude at splash, deg	27.35	28.14
Longitude at splash, deg	-157.14	-159.75
Time from entry to splash, hr:min:sec	00:20:25.6	00:20:35.2
Ground range from entry, n. mi.	2500	2295

TABLE 5-1.- RADAR TRACKING COVERAGE SUMMARY  
(Coverage from 5° to 5° elevation)

Station	AOS, hr:min:sec	LOS, hr:min:sec	Elapsed time, hr:min:sec	Maximum elevation, deg	Acquisition range, n. mi.	Minimum range, n. mi.	Rev. no.
MIL S	0:00:28	0:07:11	0:06:43	37.5	8	8	1
MLA C	0:00:33	0:07:11	0:06:38	35.2	11	11	1
PAT C	0:00:46	0:07:11	0:06:25	30.2	22	22	1
GBI C	0:01:56	0:07:40	0:05:44	20.3	162	152	1
GBM S	0:01:57	0:07:42	0:05:45	20.6	166	154	1
BDA C	0:05:35	0:11:28	0:05:53	85.1	610	108	1
BDQ C	0:05:35	0:11:28	0:05:53	85.1	610	108	1
BDA S	0:05:35	0:11:28	0:05:53	85.2	610	108	1
RED CS	0:09:41	0:14:33	0:04:52	31.3	604	192	1
CYI S	0:17:23	0:22:22	0:04:59	71.0	615	108	1
CYI C	0:17:23	0:22:22	0:04:59	71.0	615	108	1
TAN C	0:38:15	0:40:55	0:02:40	7.5	590	496	1
CRO S	0:53:22	0:56:39	0:03:17	9.1	610	467	1
CRO C	0:53:20	0:56:41	0:03:21	9.5	604	457	1
CNB S	1:00:35	1:04:20	0:03:45	11.1	595	416	1
GYM S	1:29:11	1:34:17	0:05:06	47.8	619	143	1
WHS C	1:30:43	1:35:21	0:04:38	20.1	621	281	1
TEX S	1:32:07	1:37:09	0:05:02	36.5	608	176	1
MIL S	1:36:03	1:40:50	0:04:26	22.7	633	257	1
MLA C	1:36:05	1:40:50	0:04:45	22.3	636	262	1

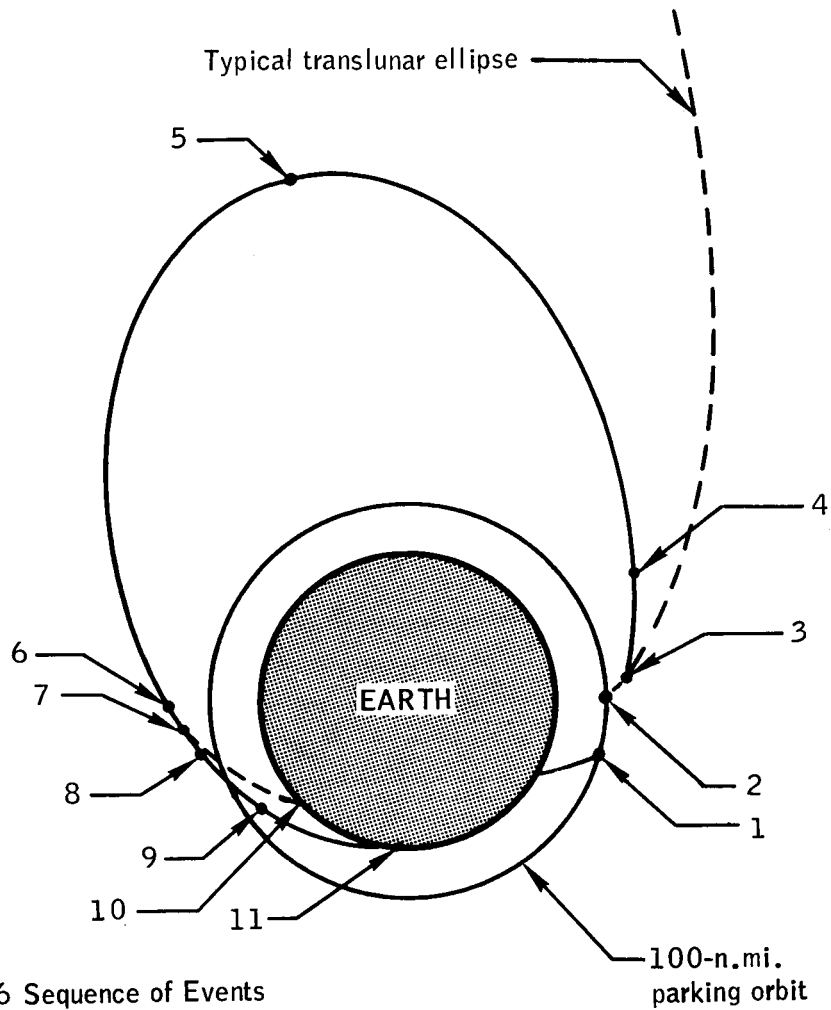


TABLE 5-1.- RADAR TRACKING COVERAGE SUMMARY - Continued  
(Coverage from 5° to 5° elevation)

Station	AOS, hr:min:sec	LOS, hr:min:sec	Elapsed time, hr:min:sec	Maximum elevation, deg	Acquisition range, n. mi.	Minimum range, n. mi.	Rev. no.
PAT C	1:36:08	1:40:49	0:04:41	21.1	608	273	1
GBI C	1:36:53	1:41:04	0:04:11	14.0	626	368	1
GBM S	1:36:54	1:41:07	0:04:13	13.9	630	367	1
BDA C	1:39:28	1:44:37	0:05:09	73.6	537	107	2
BDQ C	1:39:28	1:44:37	0:05:09	73.6	537	107	2
BDA S	1:39:28	1:44:37	0:05:09	73.5	537	107	2
RED CS	1:42:46	1:47:51	0:05:05	79.4	602	108	2
CYI S	1:51:39	1:53:51	0:02:12	6.5	608	546	2
CYI C	1:51:39	1:53:52	0:02:13	6.5	608	546	2
TAN C	2:10:09	2:15:06	0:04:57	34.1	603	182	2
CRO S	2:26:30	2:30:40	0:04:10	13.4	621	384	2
CRO C	2:26:28	2:30:41	0:04:13	13.8	615	376	2
HAW C	2:51:57	2:55:38	0:03:41	10.5	603	445	2
HAW S	2:51:57	2:55:38	0:03:41	10.5	603	445	2
CAL C	3:00:51	3:05:34	0:04:43	20.3	629	288	2
GDS S	3:01:40	3:06:23	0:04:43	20.1	625	289	2
GYM S	3:02:34	3:07:28	0:04:54	24.9	643	246	2
WHS C	3:03:31	3:08:45	0:05:14	84.2	632	111	2
TEX S	3:05:47	3:10:22	0:04:35	17.7	619	319	2
MIL S	3:09:23	3:14:15	0:04:52	28.9	643	218	2

TABLE 5-1.- RADAR TRACKING COVERAGE SUMMARY - Concluded  
(Coverage from 5° to 5° elevation)

Station	AOS, hr:min:sec	LOS, hr:min:sec	Elapsed time, hr:min:sec	Maximum elevation, deg	Acquisition range, n. mi.	Minimum range, n. mi.	Rev. no.
MLA C	3:09:25	3:14:15	0:04:50	28.3	636	222	2
PAT C	3:09:28	3:14:16	0:04:48	26.8	618	232	2
GBI C	3:10:11	3:14:47	0:04:36	19.9	626	298	2
GBM S	3:10:12	3:14:49	0:04:37	20.1	627	296	2
BDA C	3:12:32	3:18:40	0:06:08	30.6	640	263	3
BDQ C	3:12:32	3:18:40	0:06:08	30.6	640	263	3
BDA S	3:12:32	3:18:40	0:06:08	30.6	640	263	3
ANT C	3:14:37	3:22:21	0:07:44	14.4	729	615	3
RED CS	3:14:57	3:27:12	0:12:15	31.5	772	453	3
CYI S	3:19:46	4:13:41	0:45:54	27.6	1 597	1516	3
CYI C	3:19:46	4:13:41	0:45:54	27.6	1 592	1516	3
ASC C	3:21:40	8:05:41	4:44:01	67.1	2 013	1632	3
ACN S	3:21:40	8:05:41	4:44:01	67.6	2 015	1632	3
MADS	3:25:21	3:49:41	0:24:20	8.7	2 701	2701	3
TAN C	3:24:52	9:09:32	4:28:11	77.9	4 472	4472	3
CRO C	4:47:41	9:16:42	4:29:01	24.6	11 878	3012	3
CRO S	4:47:41	9:16:42	4:29:01	24.6	11 878	3013	3
GWM S	9:18:32	9:26:39	0:08:07	9.3	2 689	1048	3
WTN C	9:33:40	9:36:36	0:02:54	54.6	330	56	3



Apollo 6 Sequence of Events

100-n.mi.  
parking orbit

1. Insertion to a 100-nautical mile circular parking orbit for two revolutions.
2. Injection onto a 72-hour lunar transfer ellipse.
3. S-IVB/CSM separation and first SPS burn.
4. First SPS cutoff and earth intersecting coast.
5. 12 000-nautical mile apogee.
6. Second SPS ignition.
7. SPS engine cutoff.
8. SM/CM separation.
9. Atmosphere entry.
10. No second SPS burn splash.
11. Nominal splash.

Figure 1-1.- Mission summary.

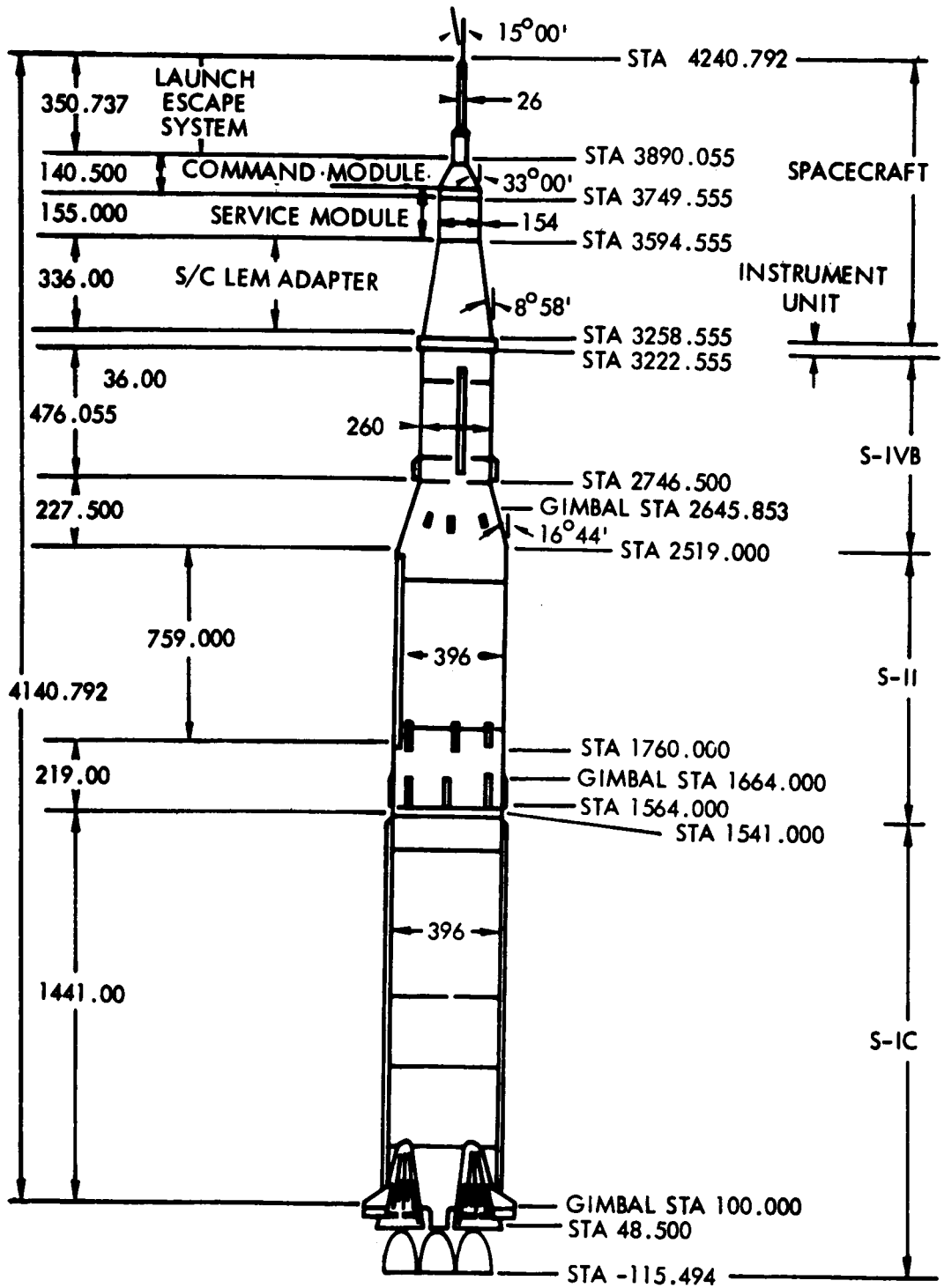
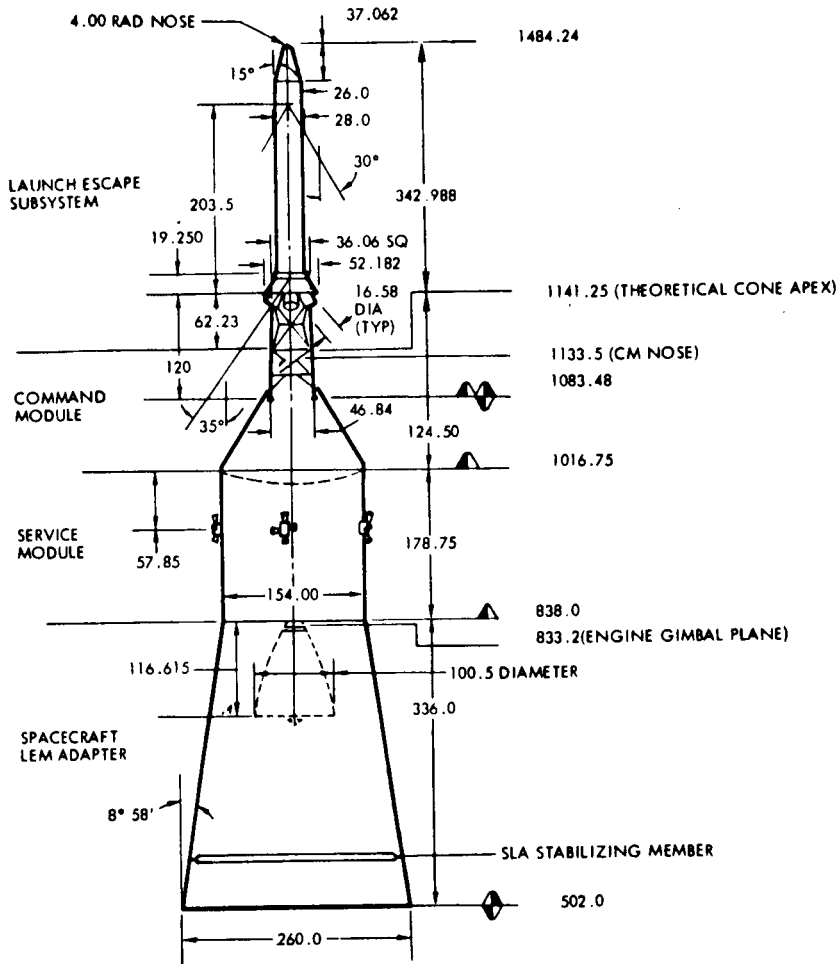


Figure 2-1.- Saturn V reference dimensions.



- Notes:  Separation Plane  
 Field Splice

All linear dimensions are in inches.

Figure 2-2.- Command and service modules reference dimensions.

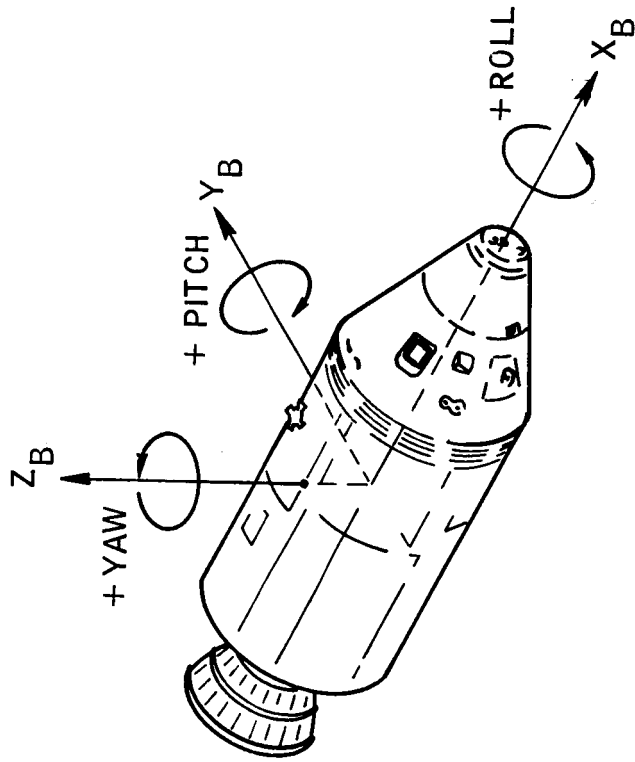


Figure 2-3.- Spacecraft body coordinate system.

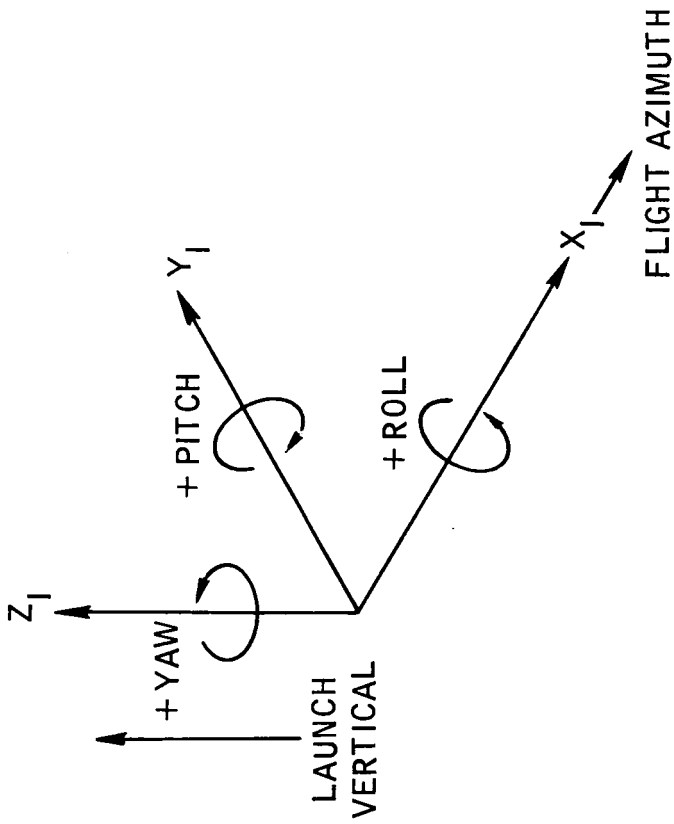


Figure 2-4.- Launch site inertial attitude reference coordinate system.

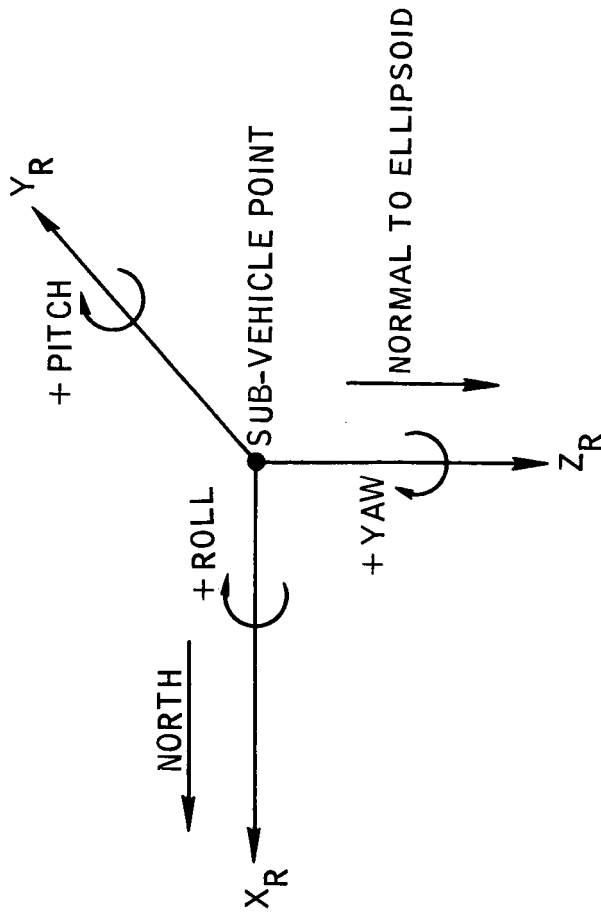


Figure 2-5.- Earth reference rotating attitude coordinate system.



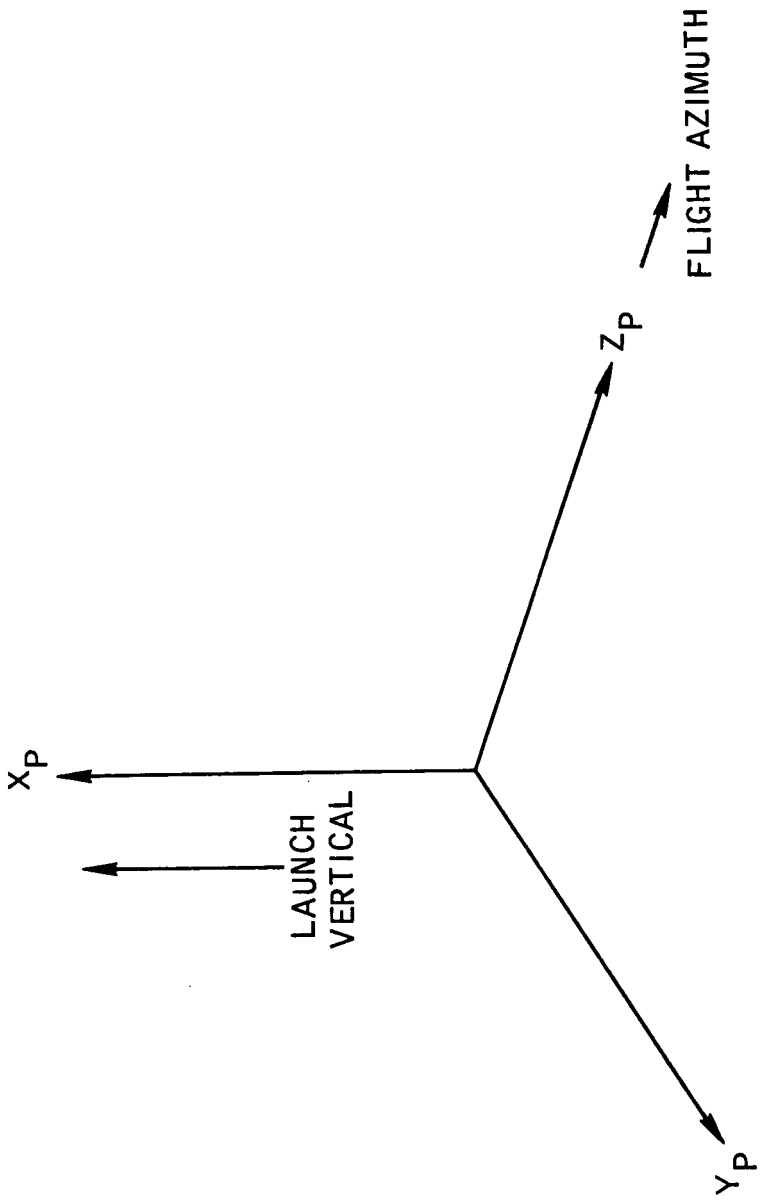


Figure 2-6.- Platform coordinate system.

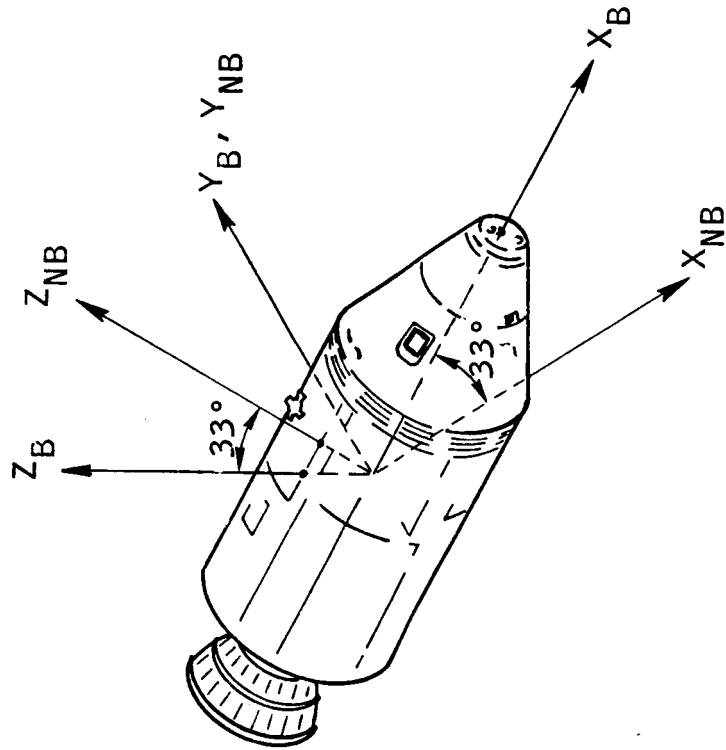


Figure 2-7.- Navigation base coordinate system relative to spacecraft body coordinate system.

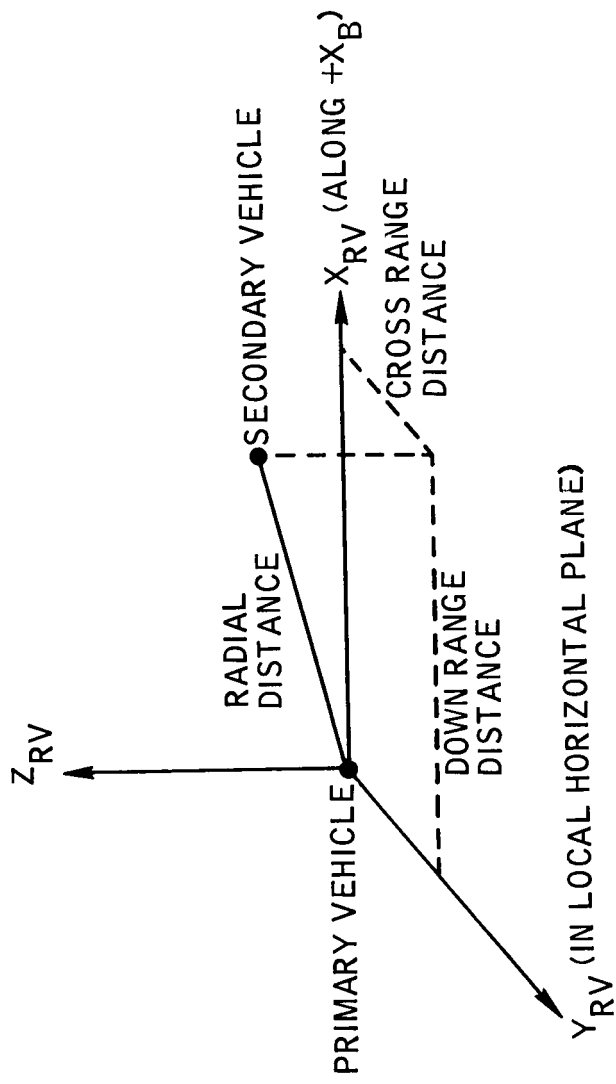


Figure 2-8.- Relative vehicle coordinate system.

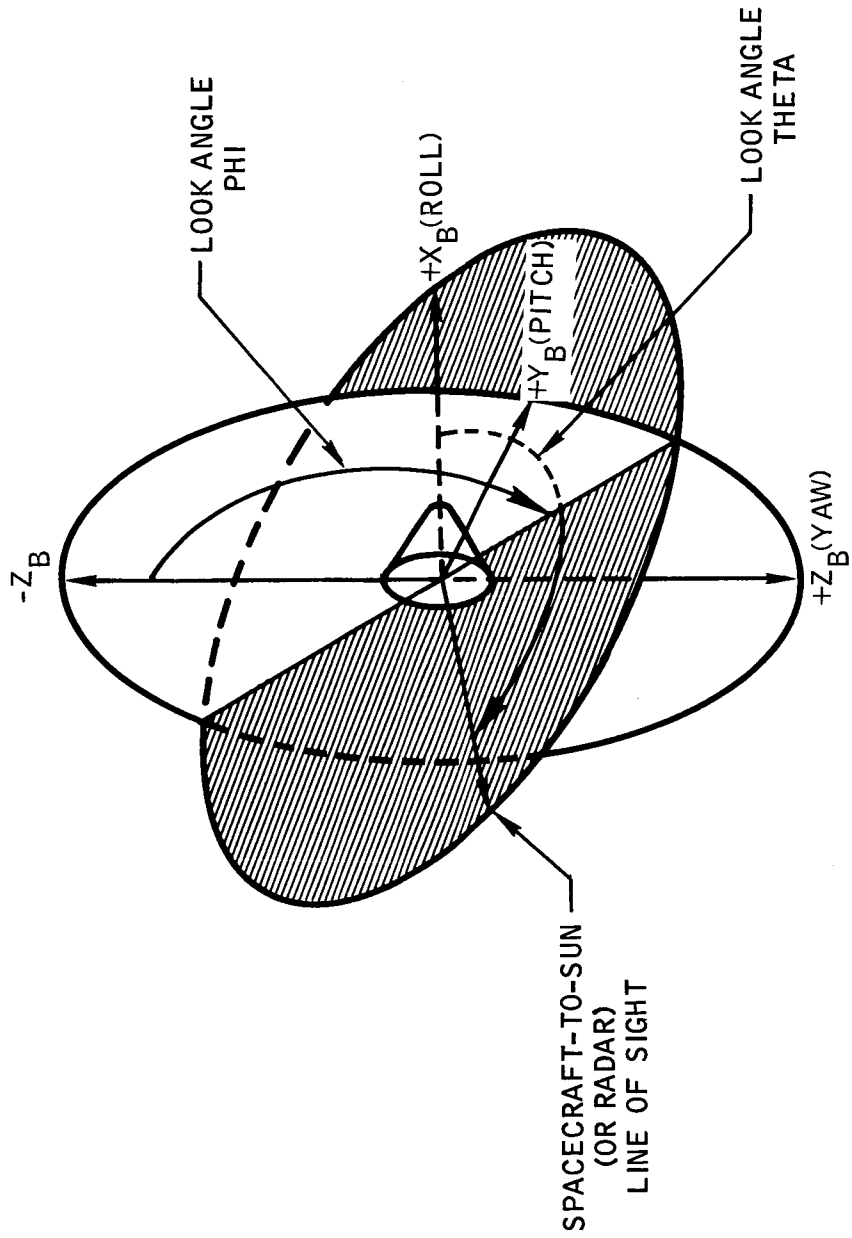


Figure 2-9.- Spacecraft look angles.

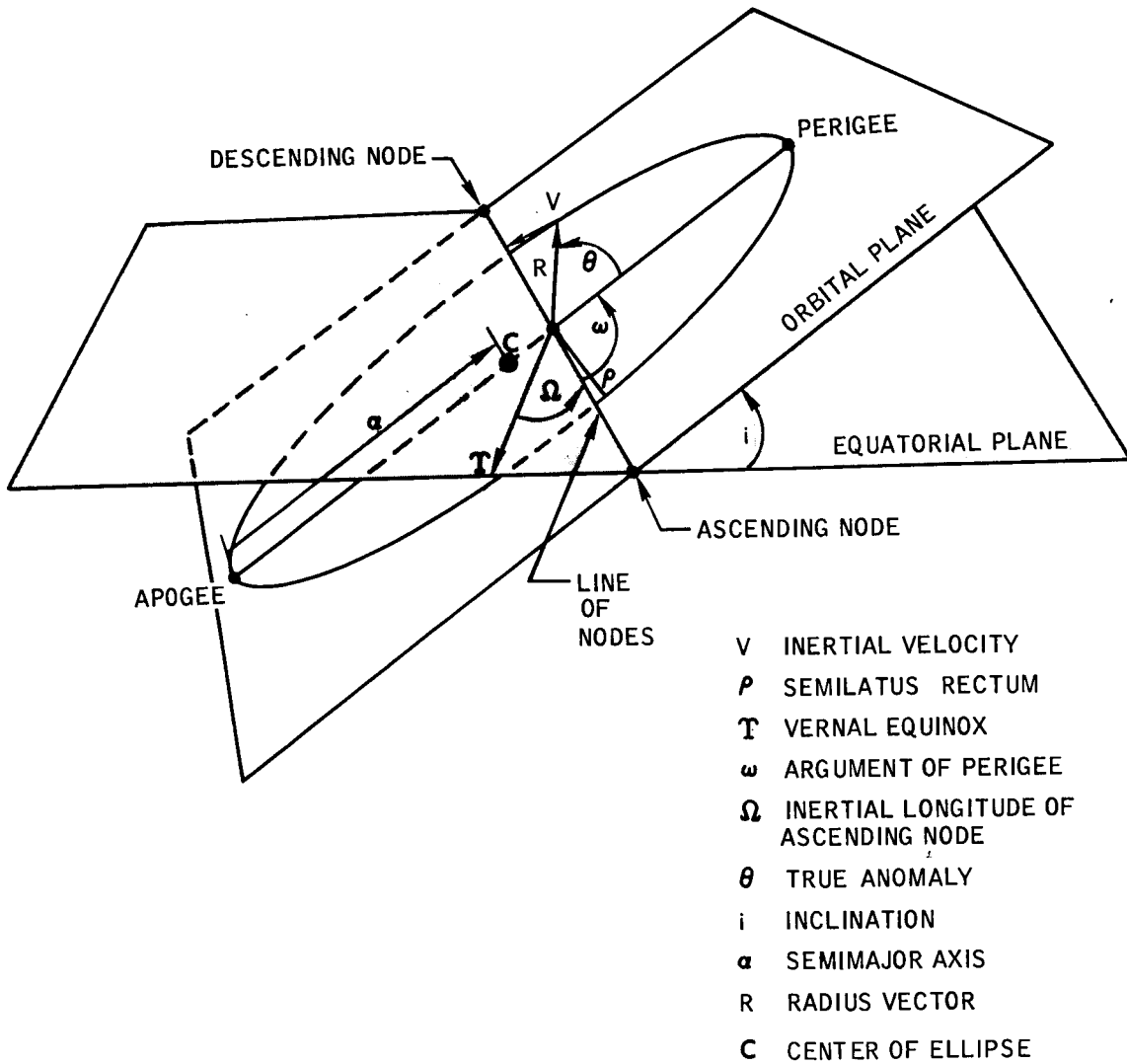


Figure 2-10.- Orbital geometry.

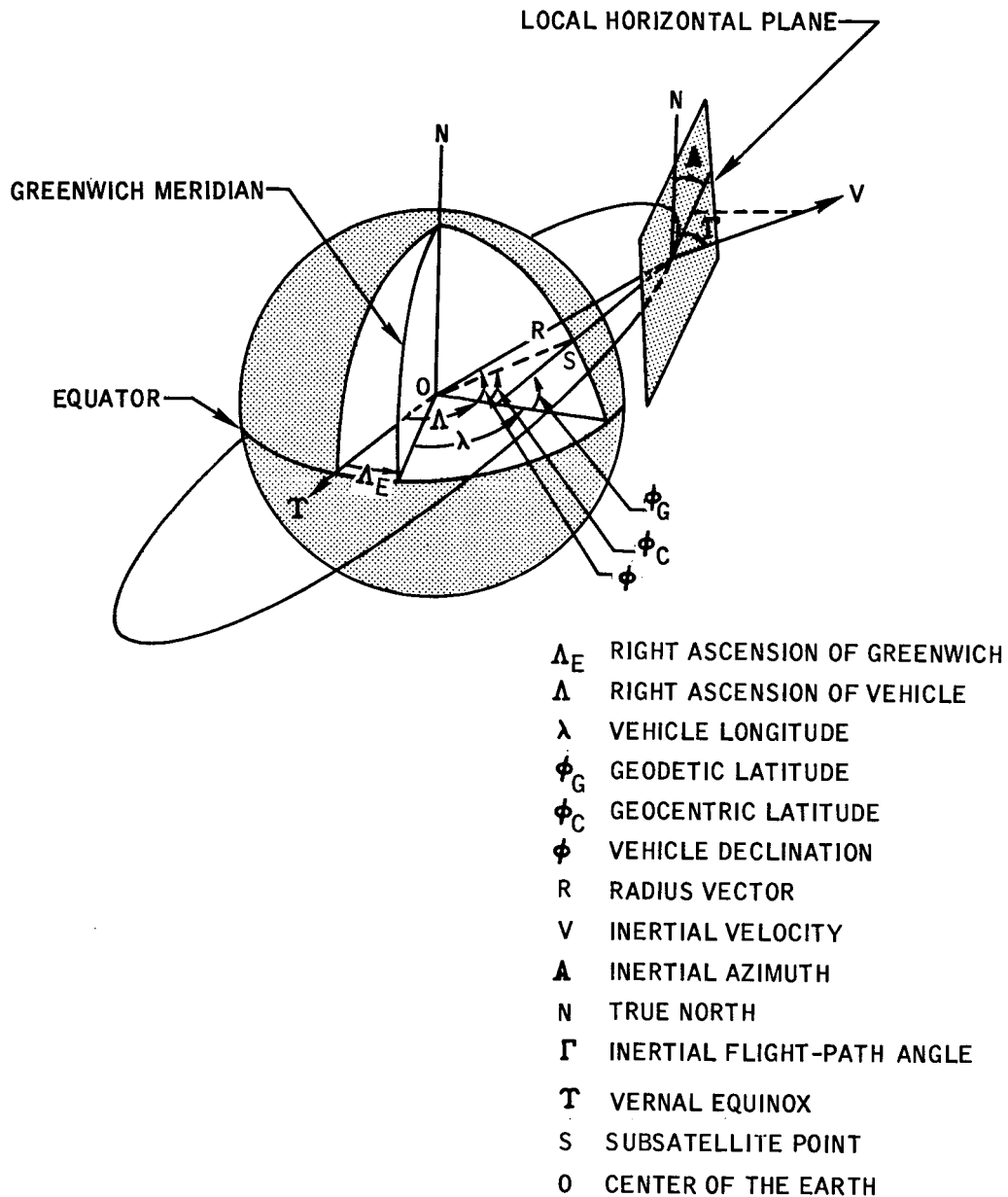


Figure 2-11.- Trajectory parameters.

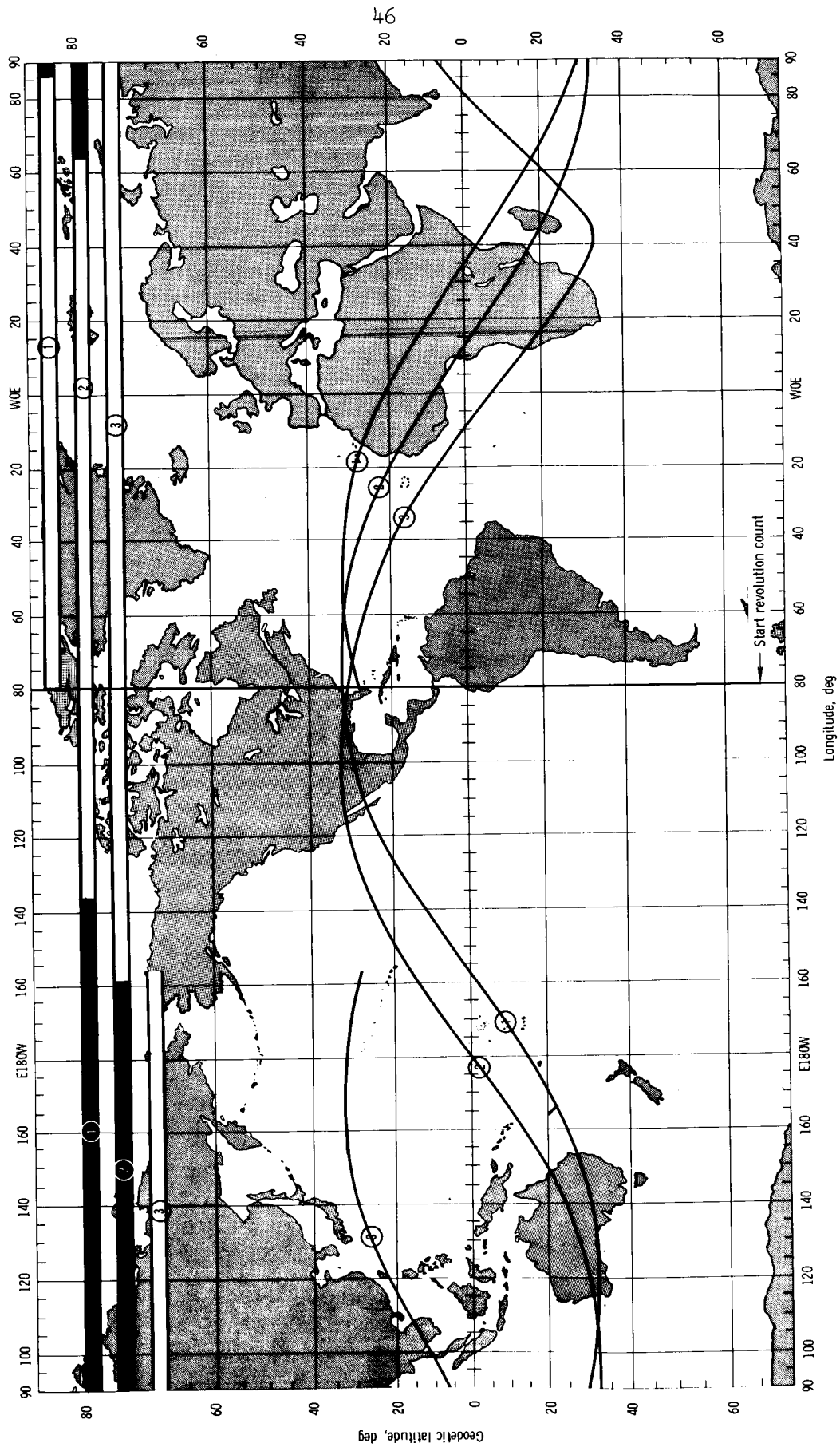
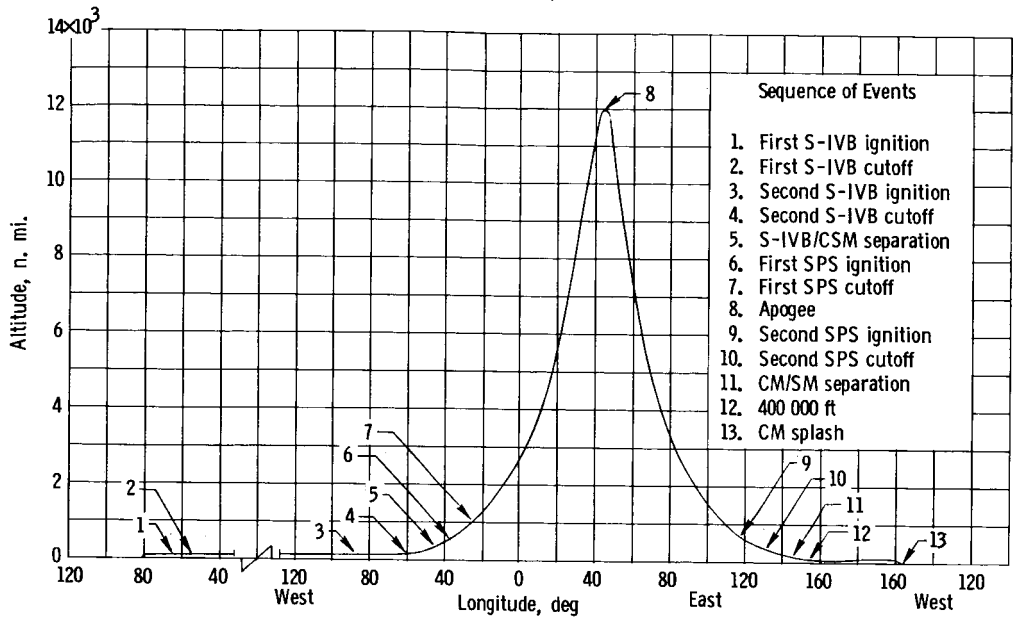
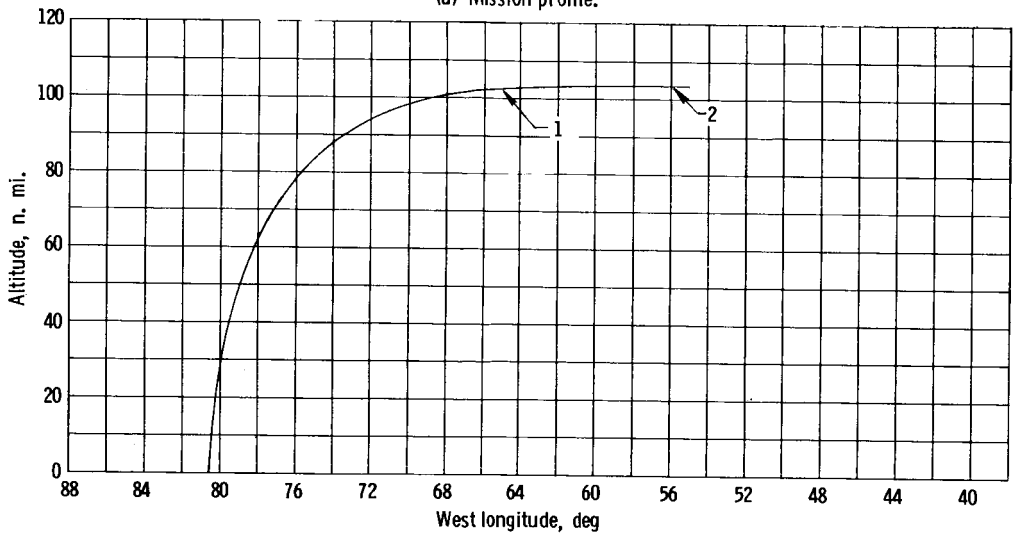


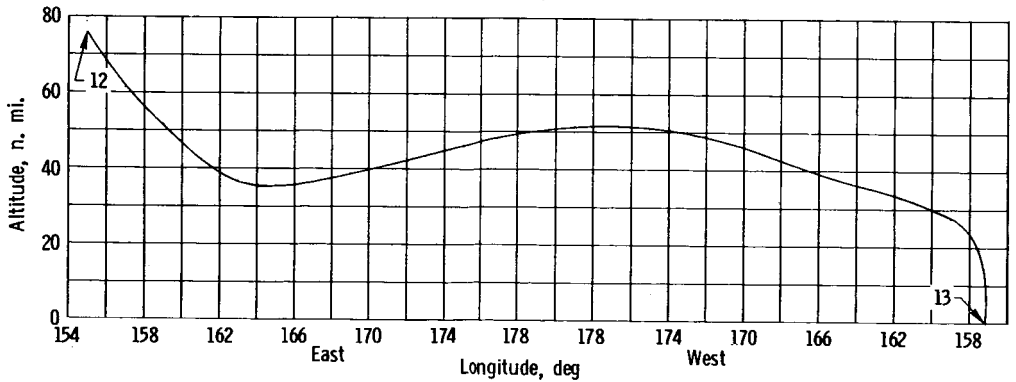
Figure 3-1. - Ground track and daylight-darkness history.



(a) Mission profile.



(b) Launch phase.



(c) Entry phase.

Figure 3-2. - Altitude-longitude history.



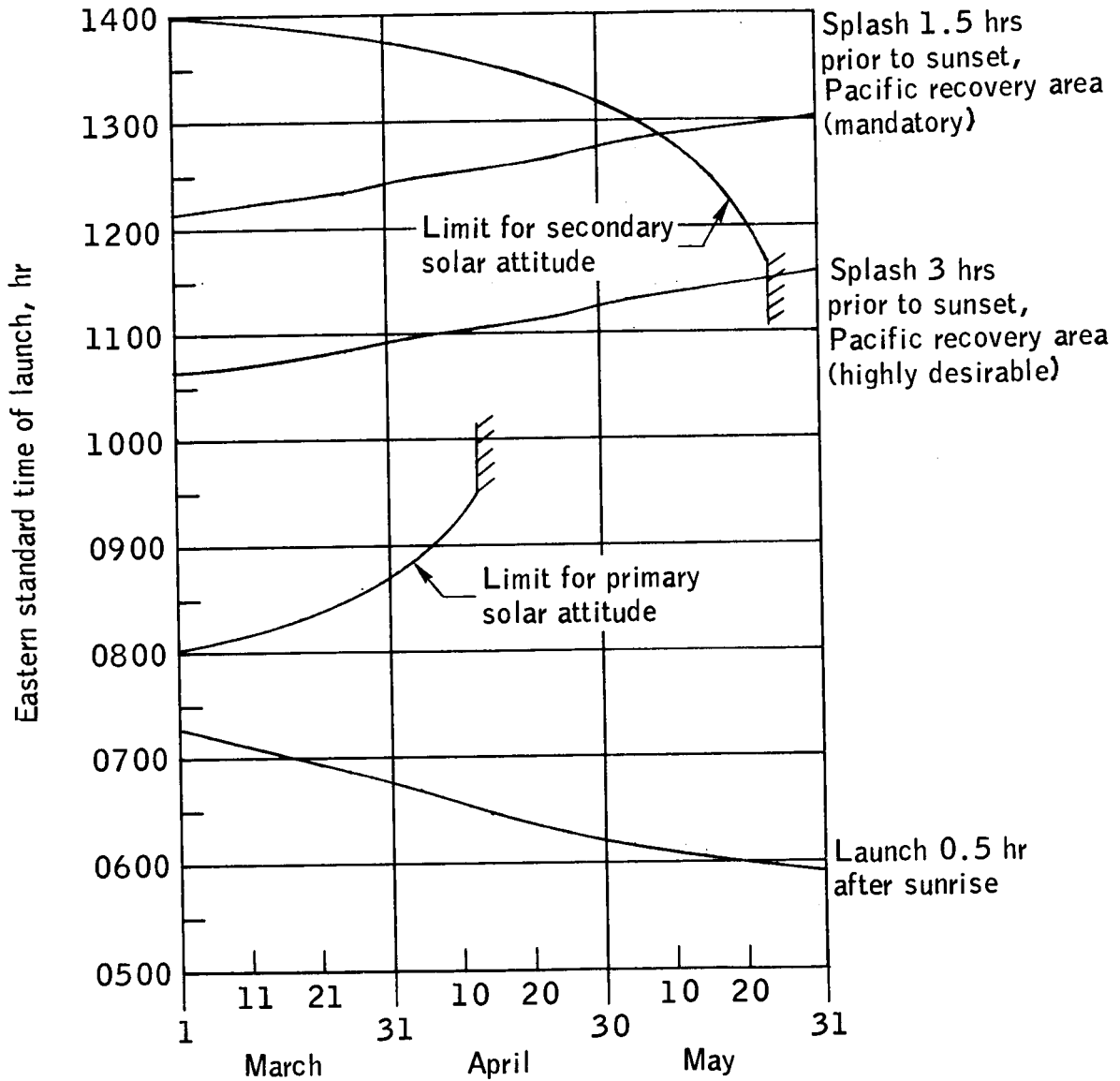
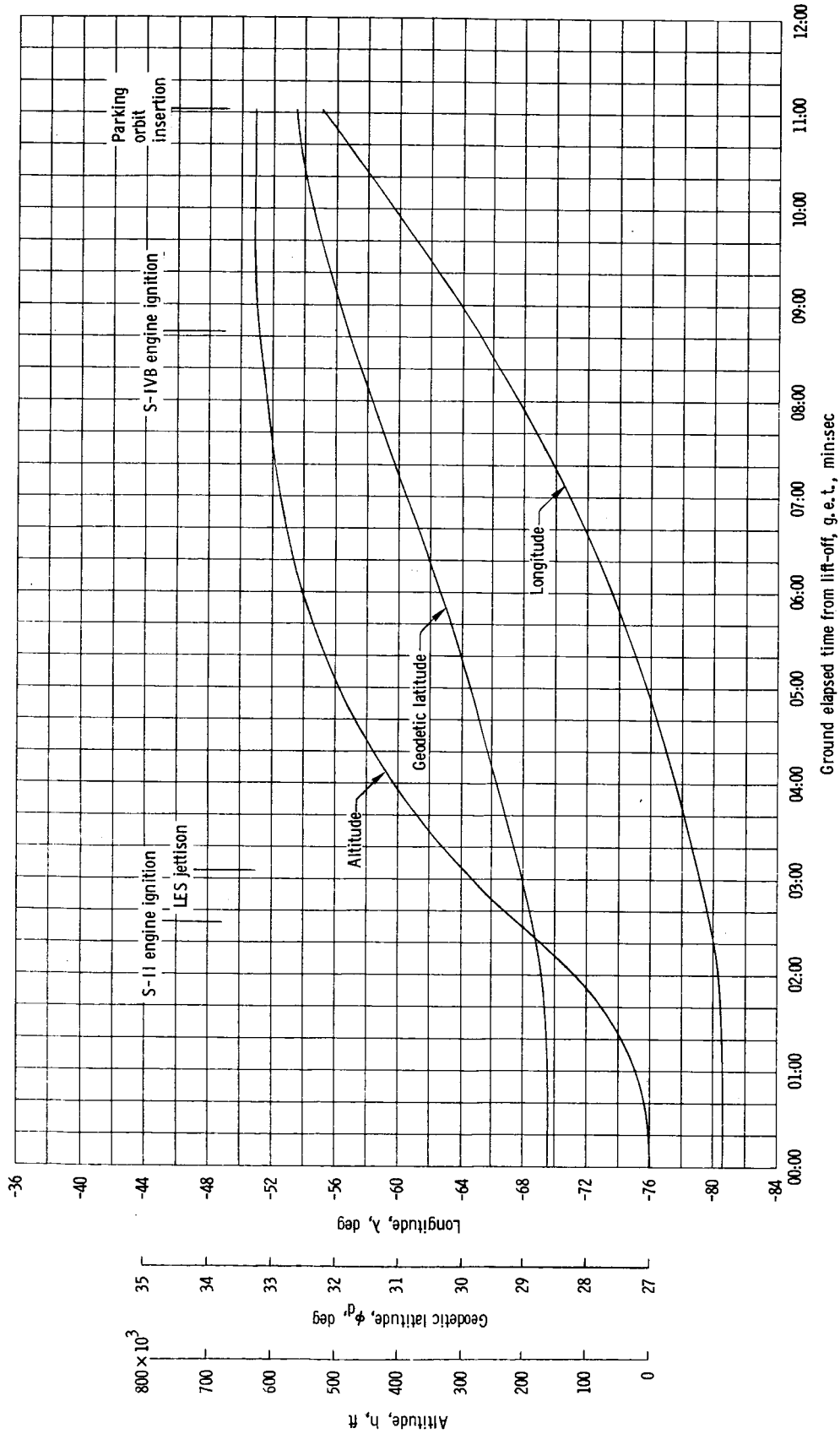
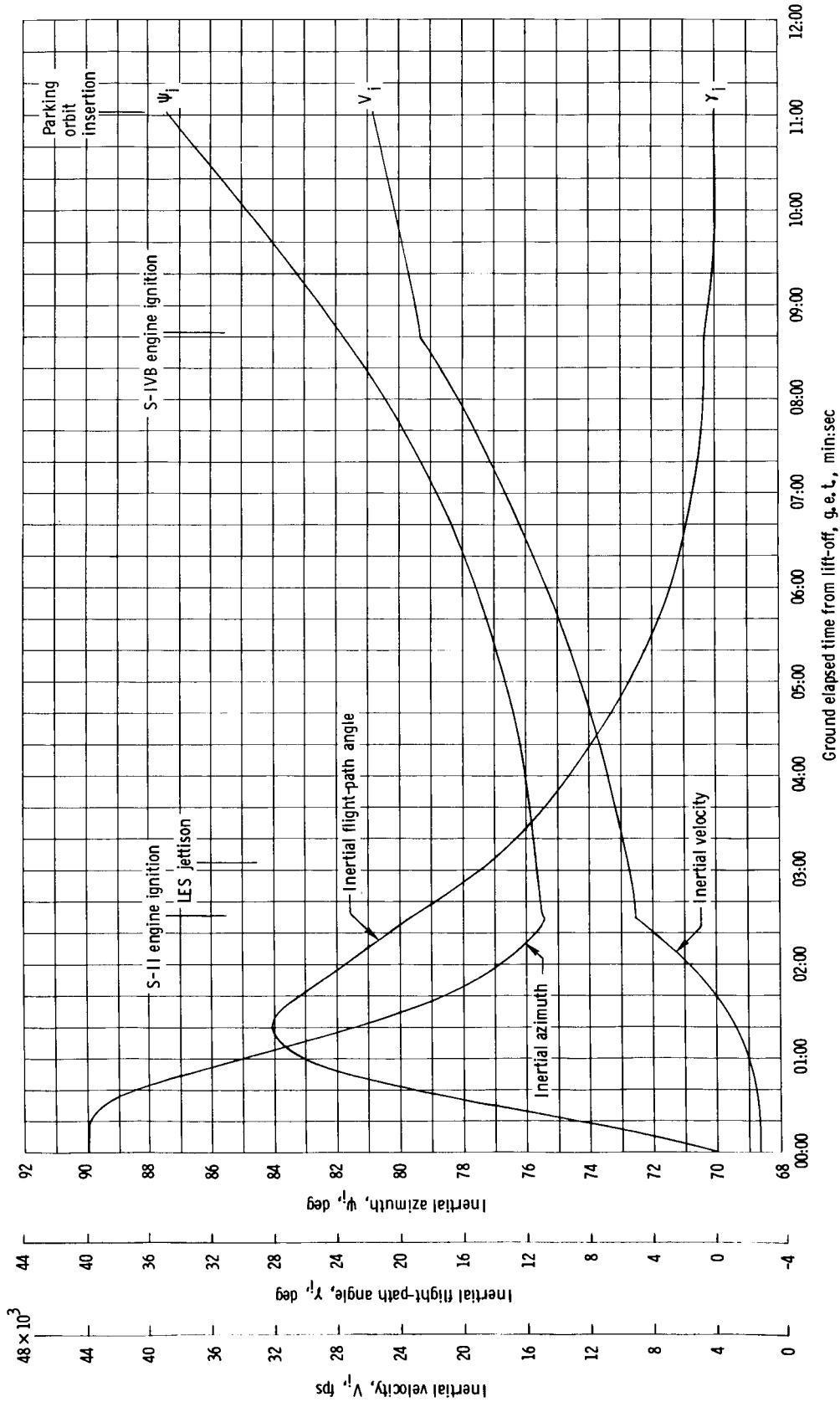


Figure 3-3.- Effect of sun lighting on launch time.



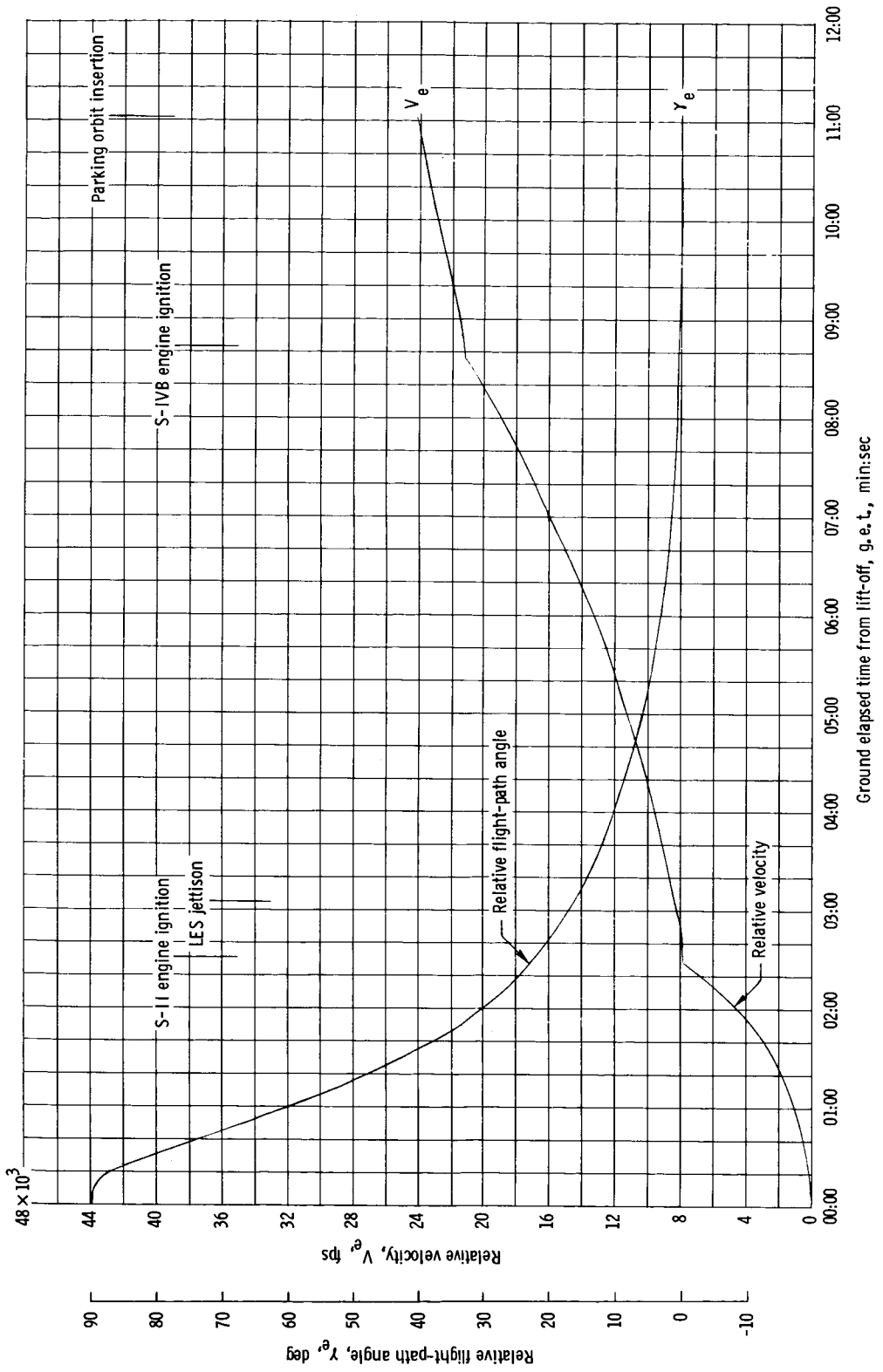
(a) Altitude, latitude, and longitude.

Figure 3-4. - Saturn V ascent to parking orbit.



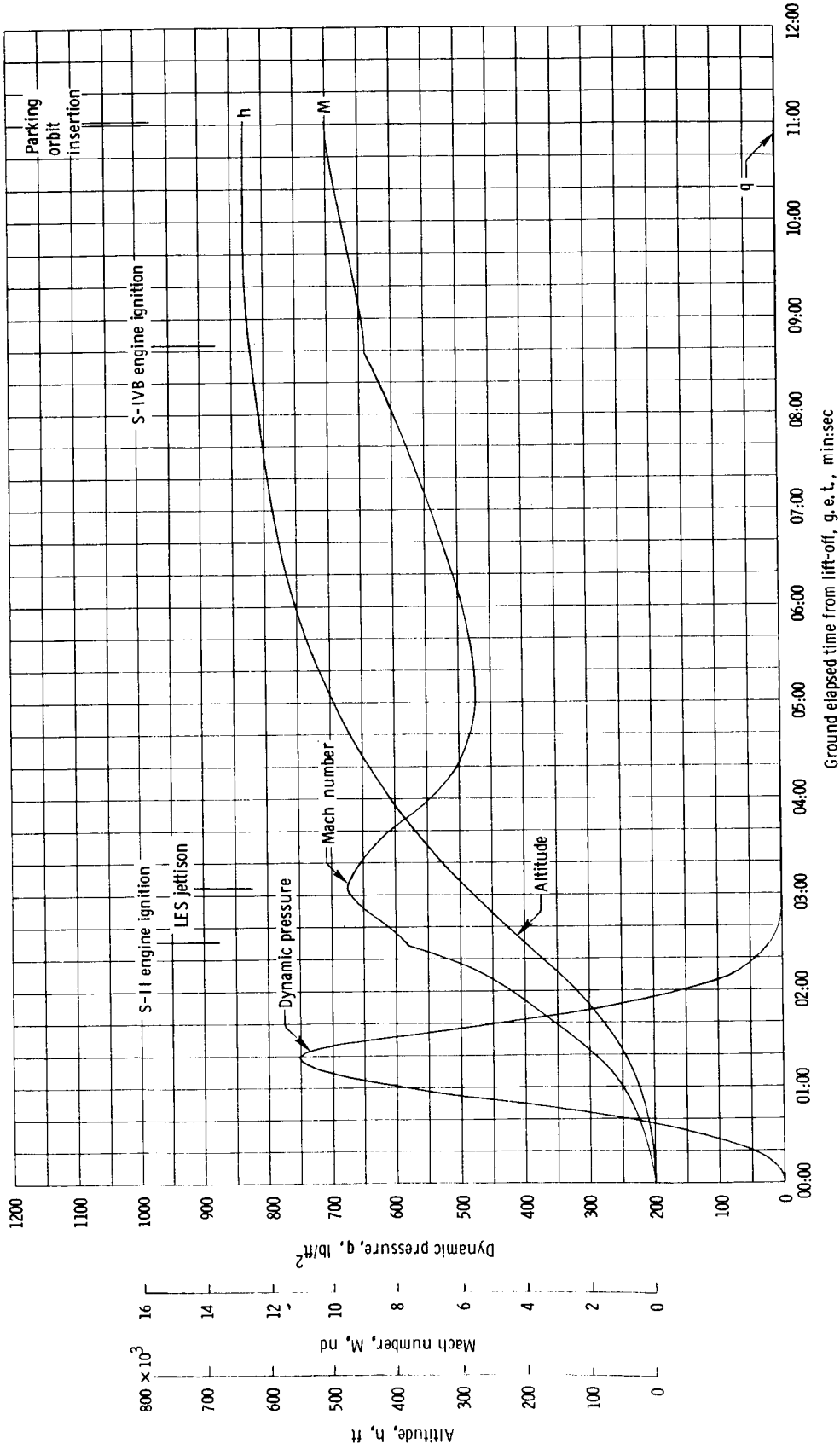
(b) Inertial velocity, flight-path angle and azimuth.

Figure 3-4. - Continued.



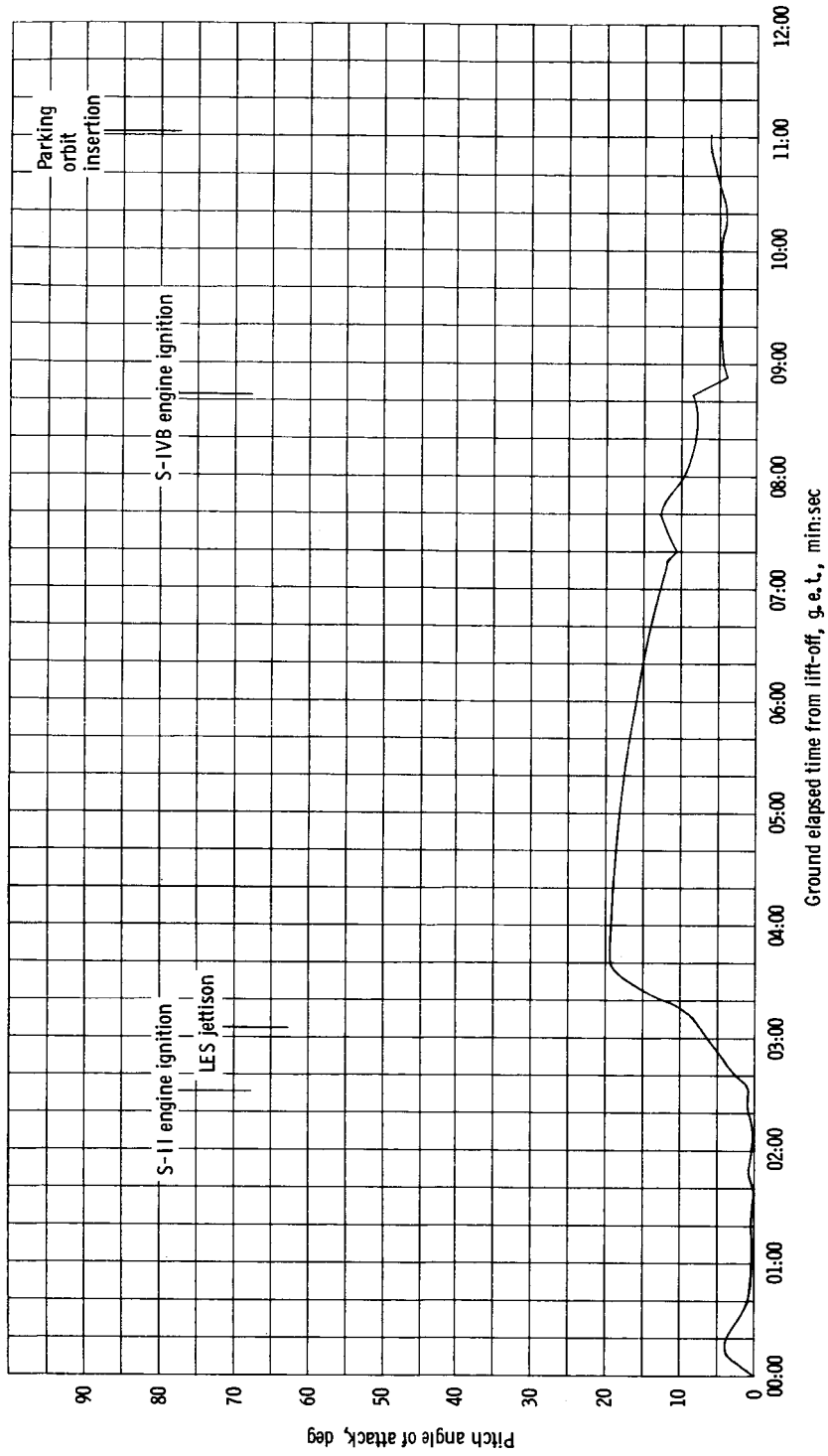
(c) Relative velocity and flight-path angle.

Figure 3-4. - Continued.



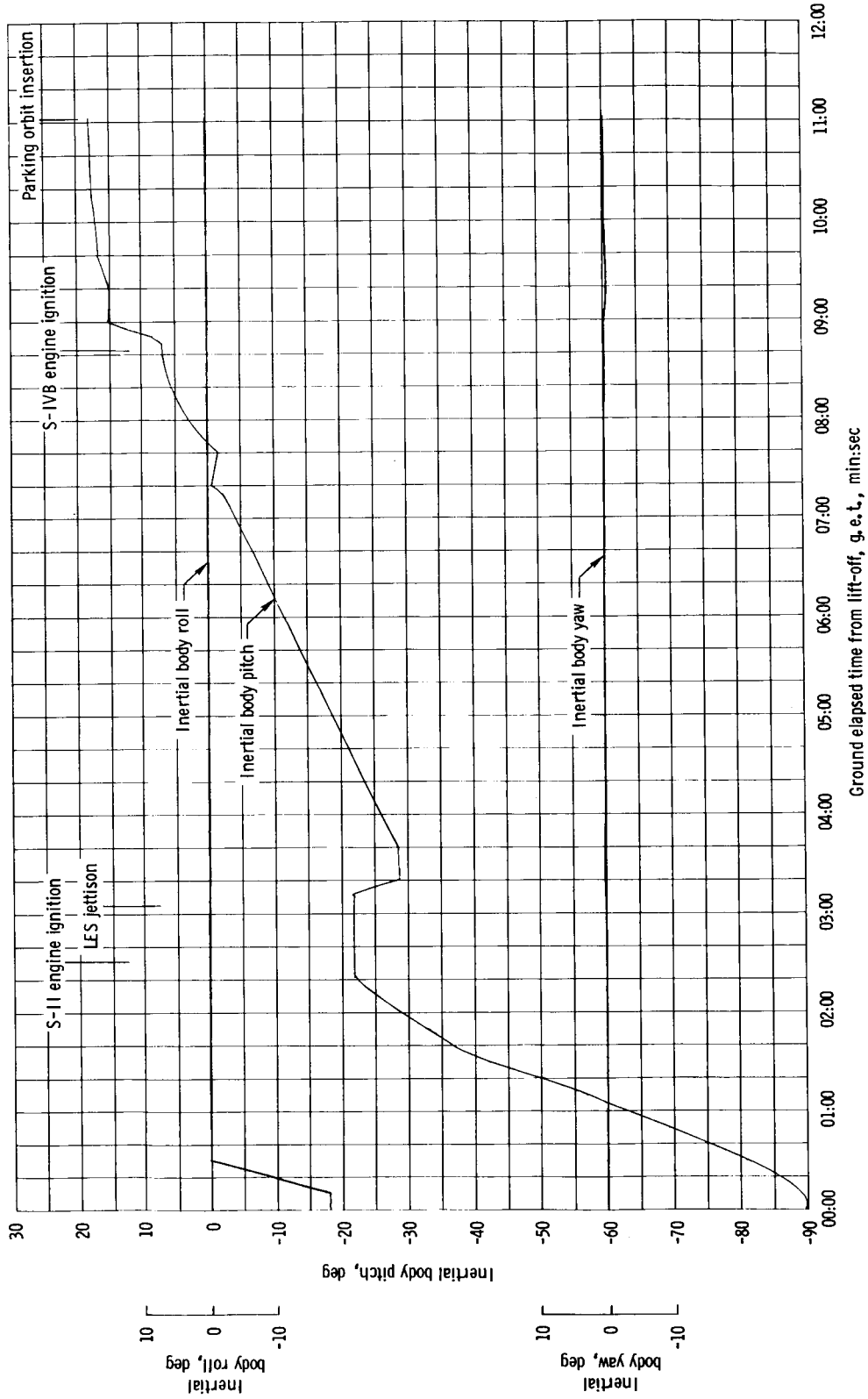
(d) Altitude, Mach number, and dynamic pressure.

Figure 3-4. - Continued.



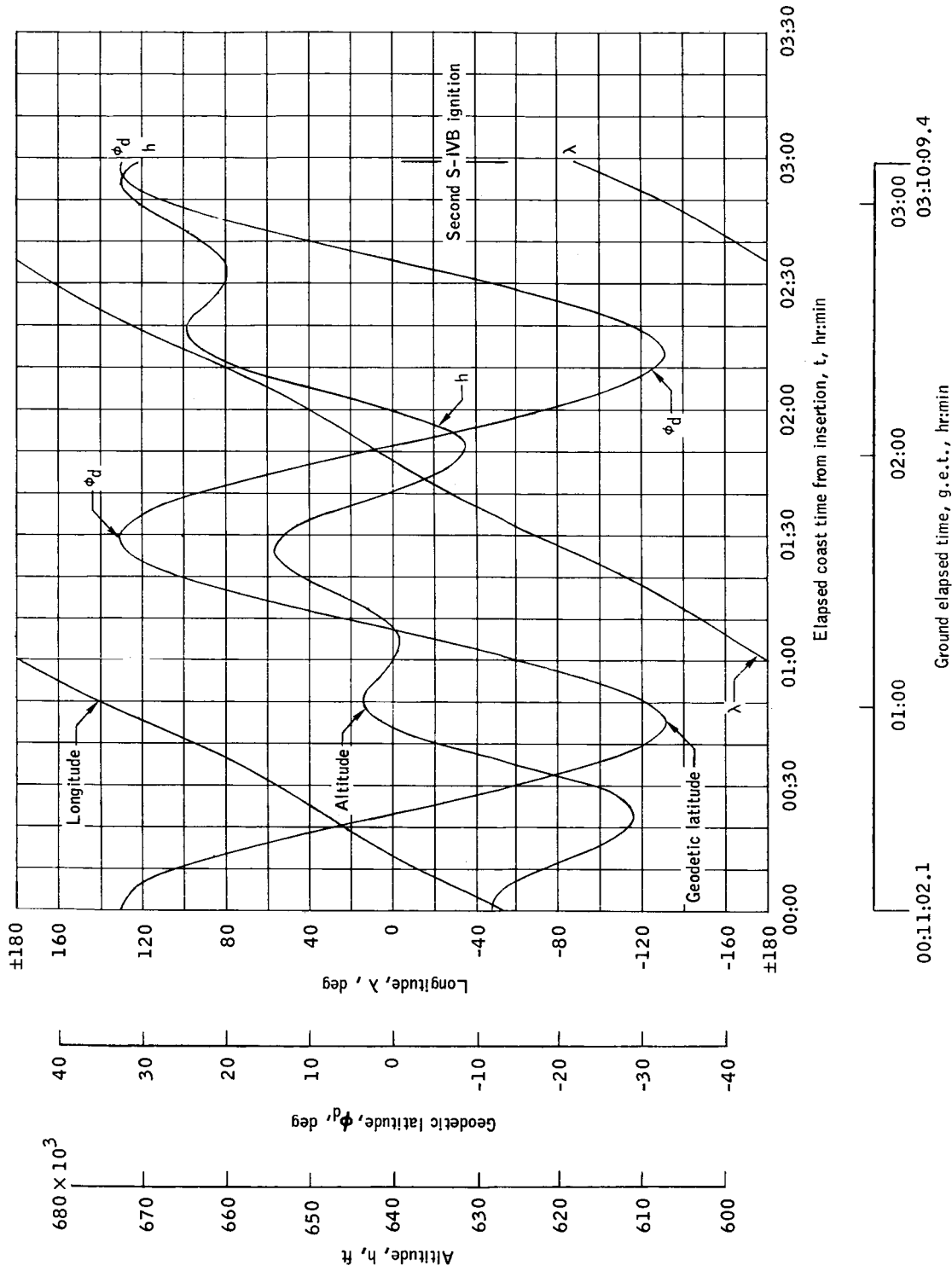
(e) Pitch angle of attack.

Figure 3-4. - Continued.



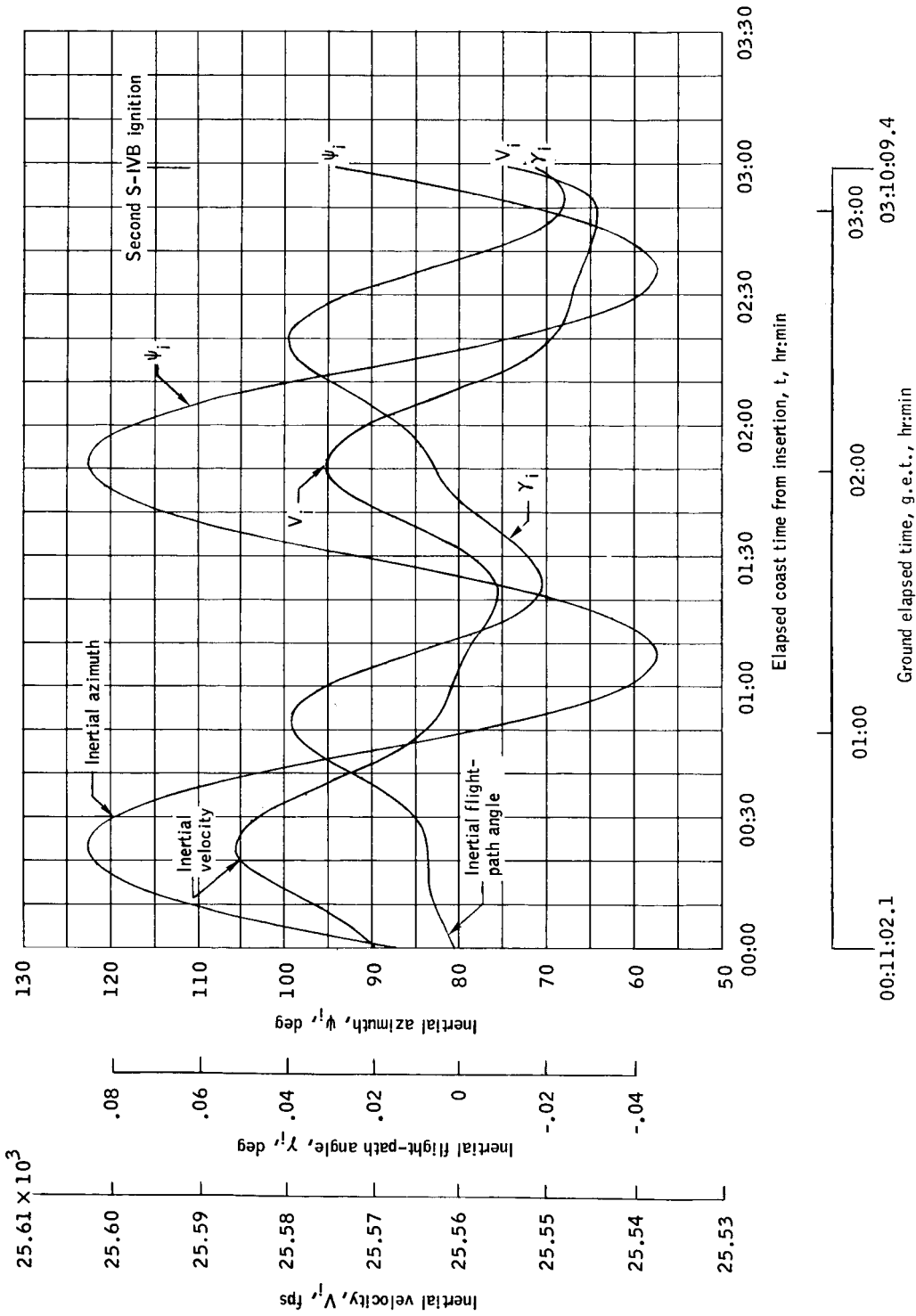
(f) Inertial yaw, pitch and roll.

Figure 3-4, - Concluded.



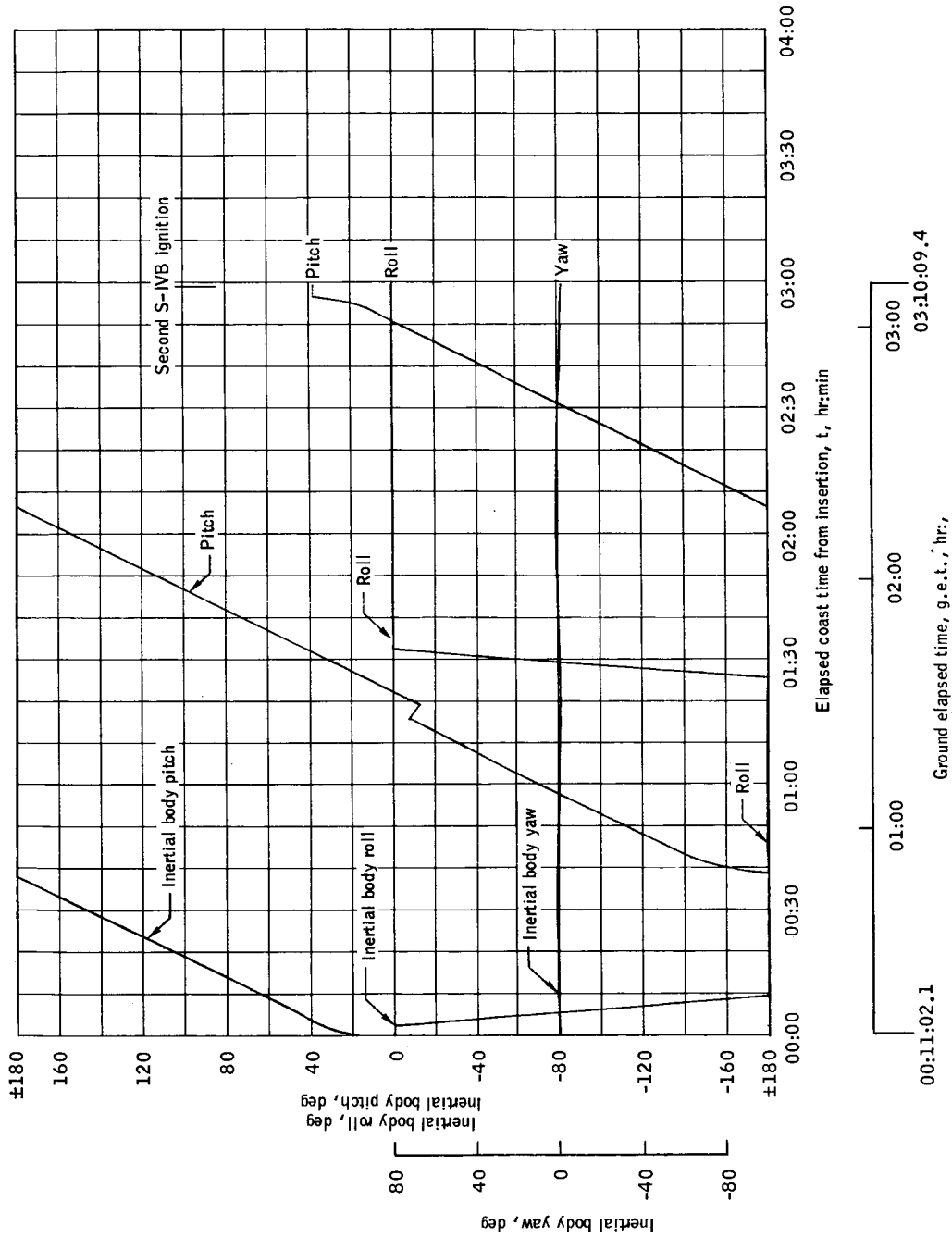
(a) Altitude, latitude, and longitude.  
 Figure 3-5.- Earth parking orbit.





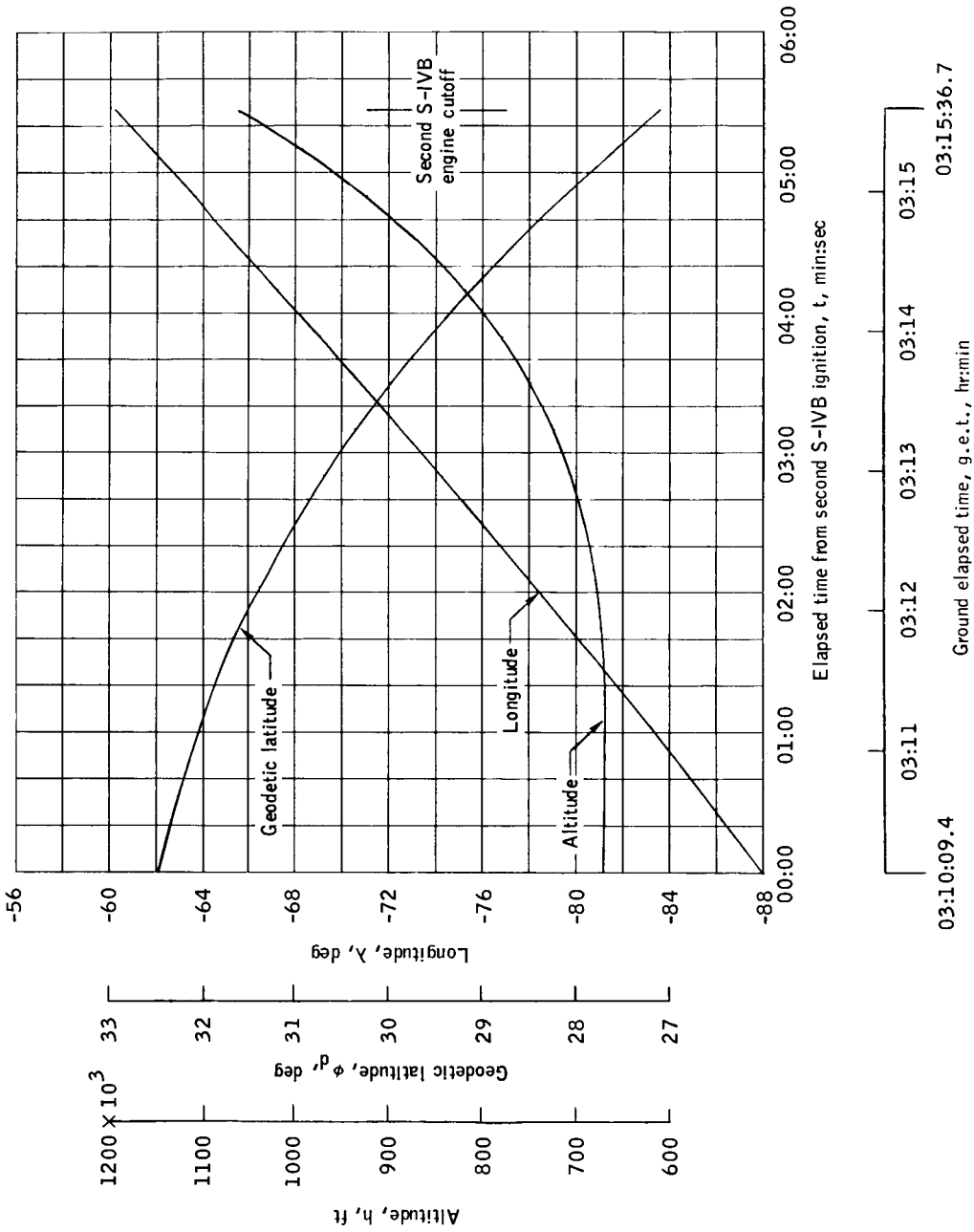
(b) Inertial velocity, flight-path angle, and azimuth.

Figure 3-5.- Continued.



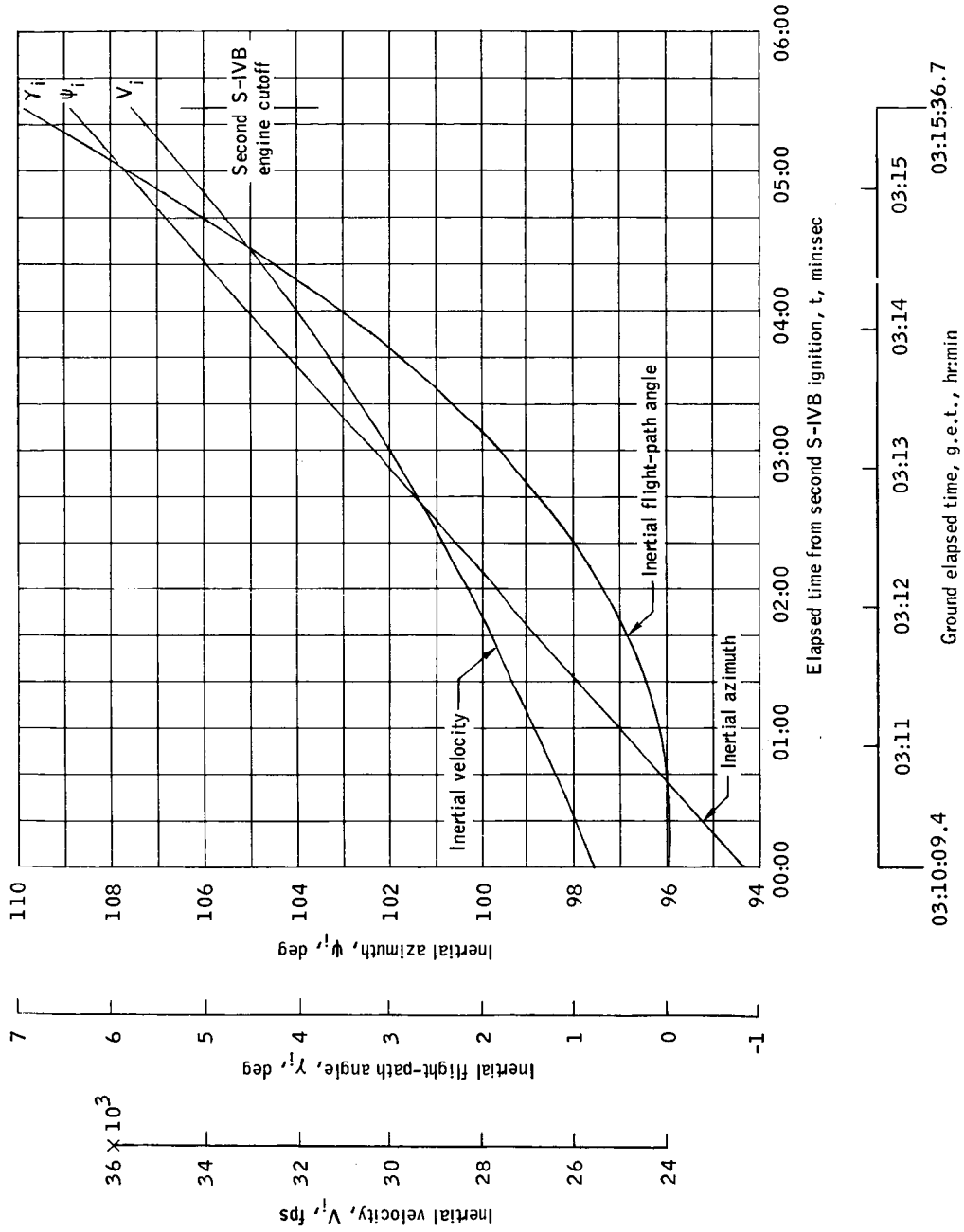
(c) Inertial yaw, pitch, and roll.

Figure 3-5.- Concluded.



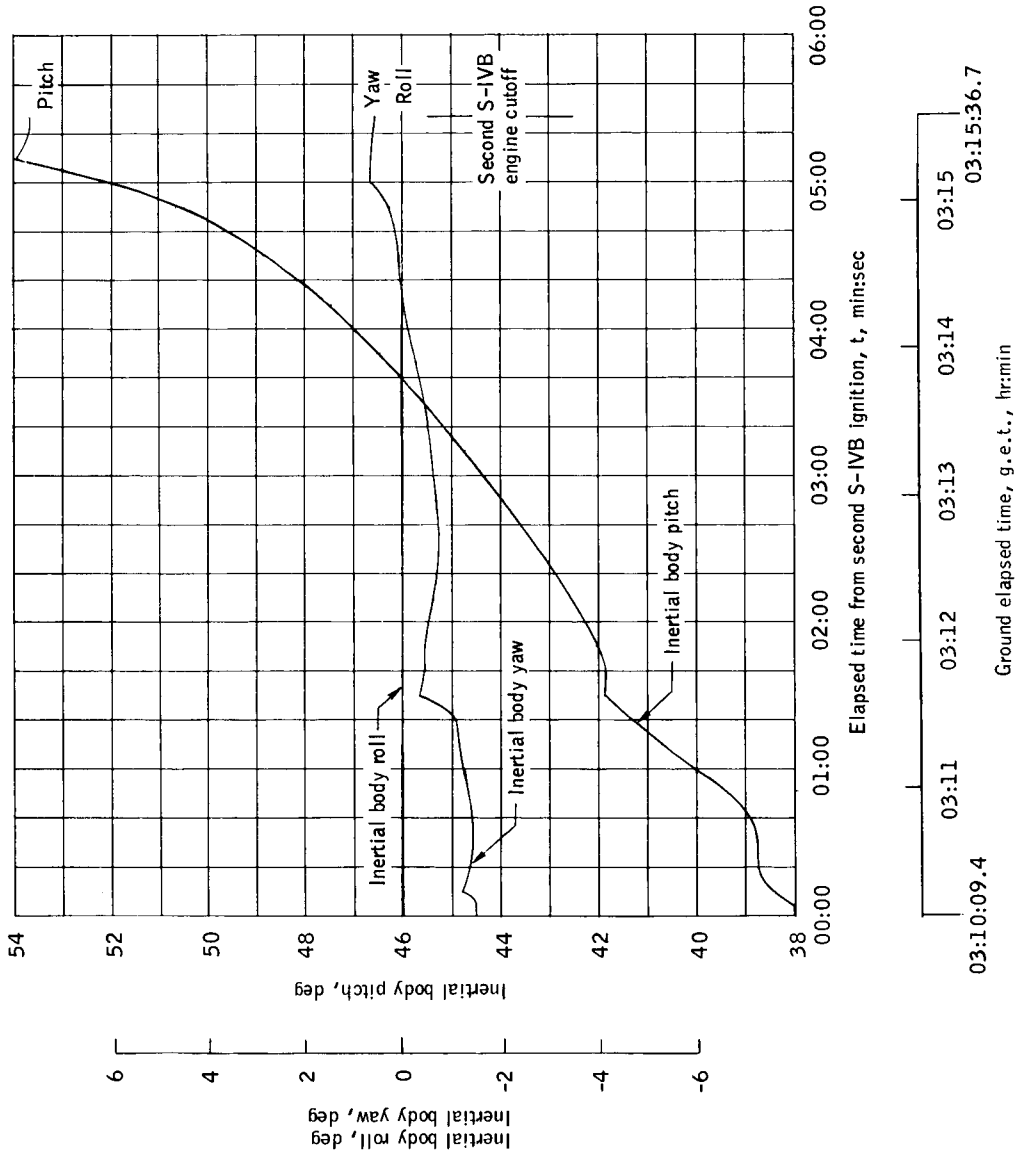
(a) Altitude, latitude, and longitude.

Figure 3-6.- Second S-IVB burn.



(b) Inertial velocity, flight-path angle, and azimuth.

Figure 3-6.- Continued



(c) Inertial yaw, pitch, and roll.

Figure 3-6.- Concluded.

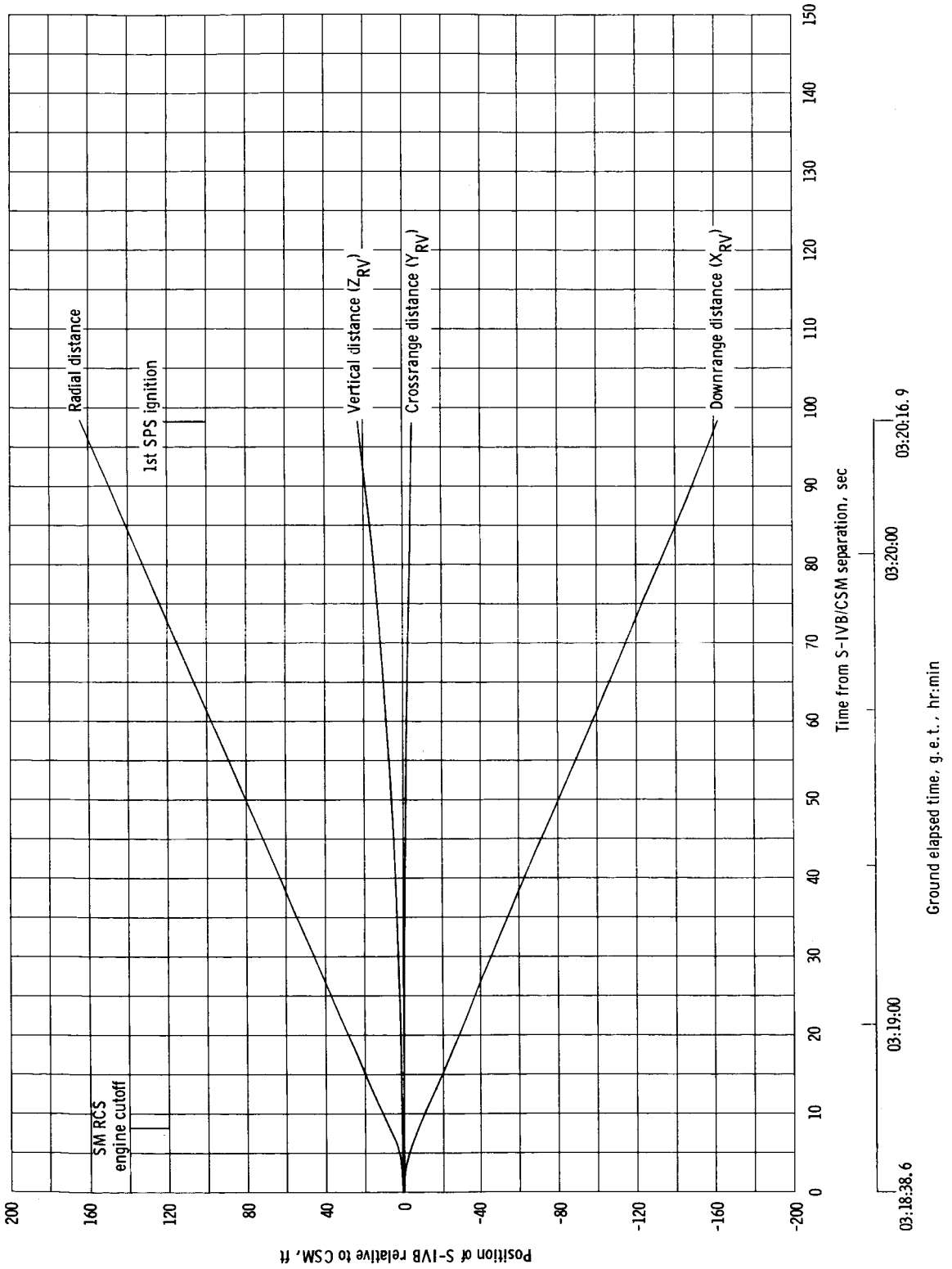


Figure 3-7. - CSM/S-IVB separation characteristics.

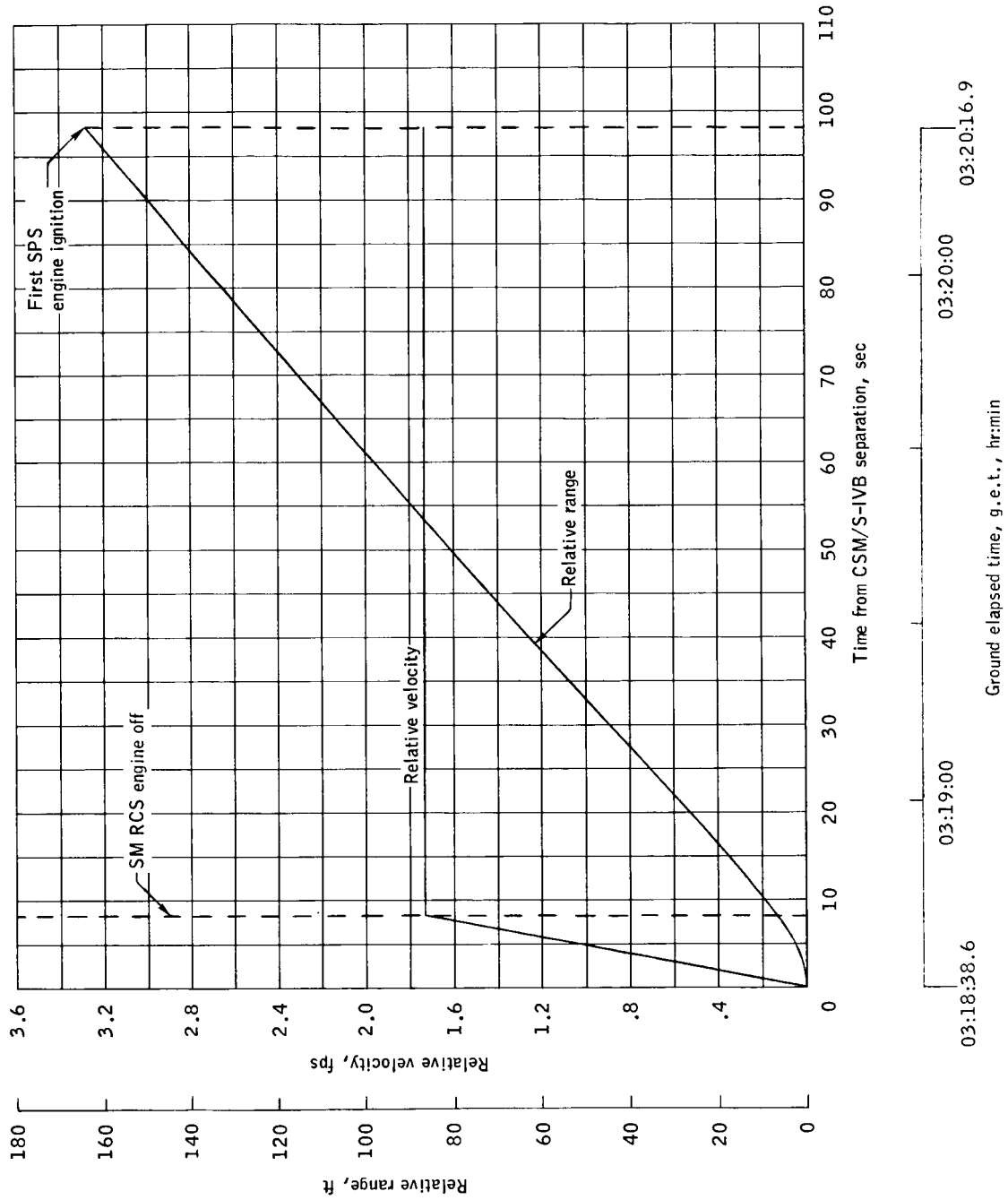


Figure 3-8.- Time history of CSM/S-IVB relative velocity and separation distance.

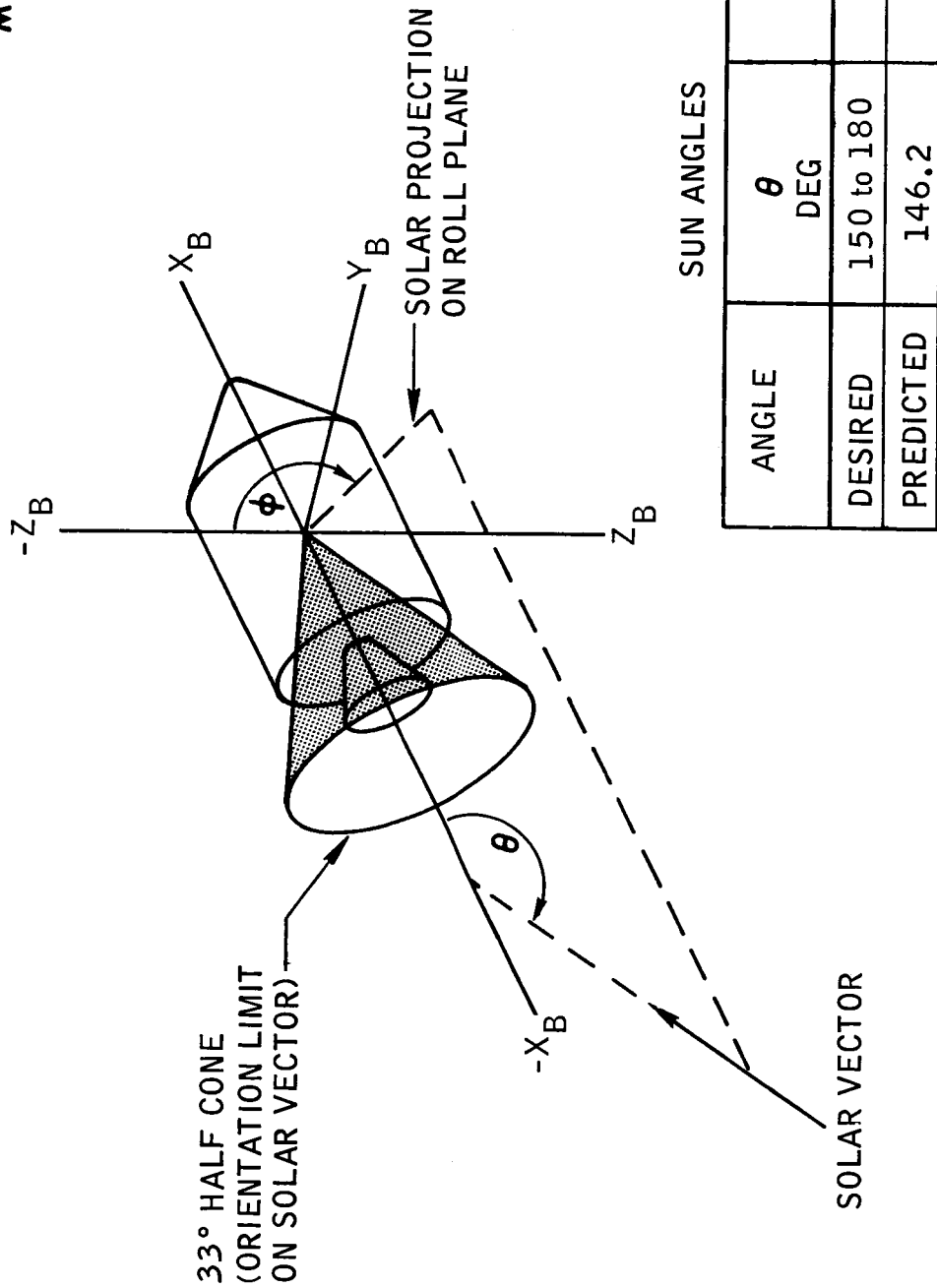
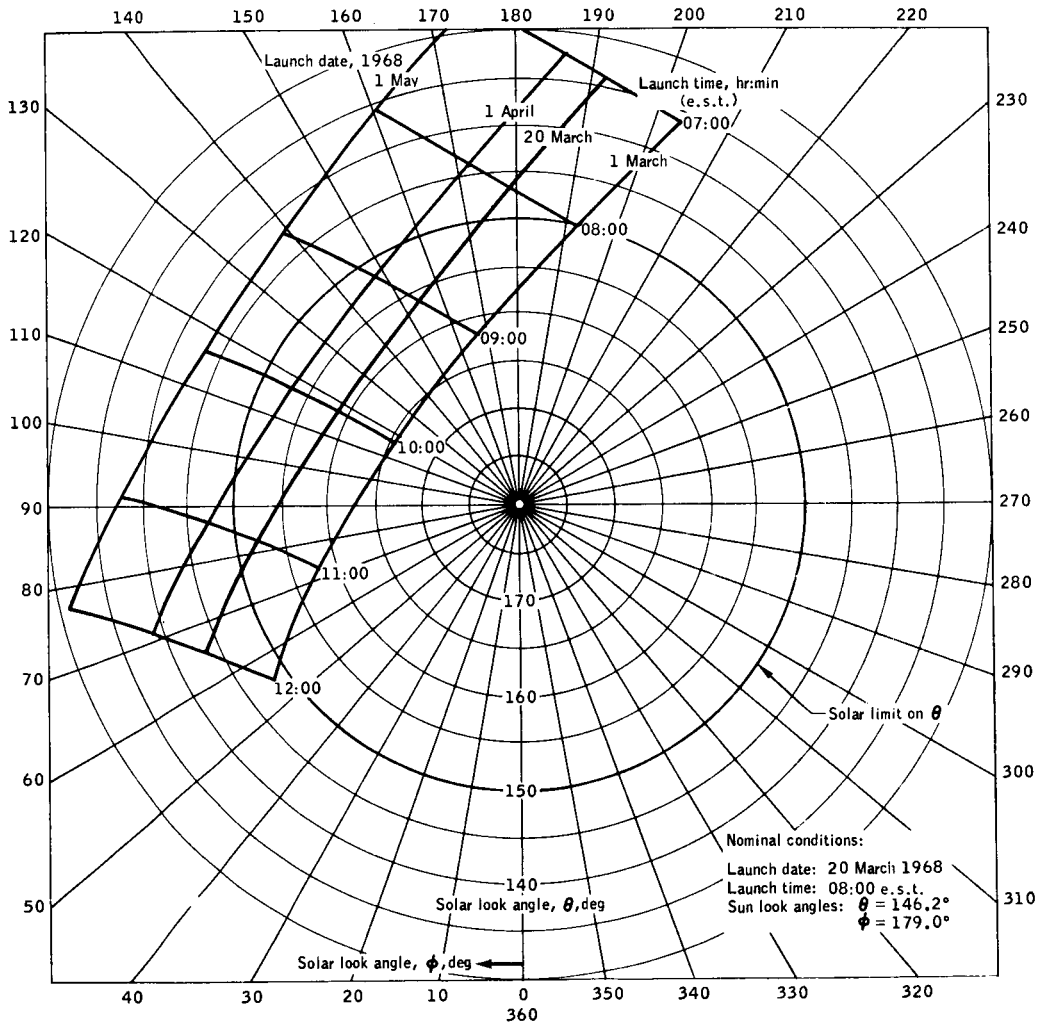


Figure 3-9.- Spacecraft attitude orientation requirements during earth intersecting coast.

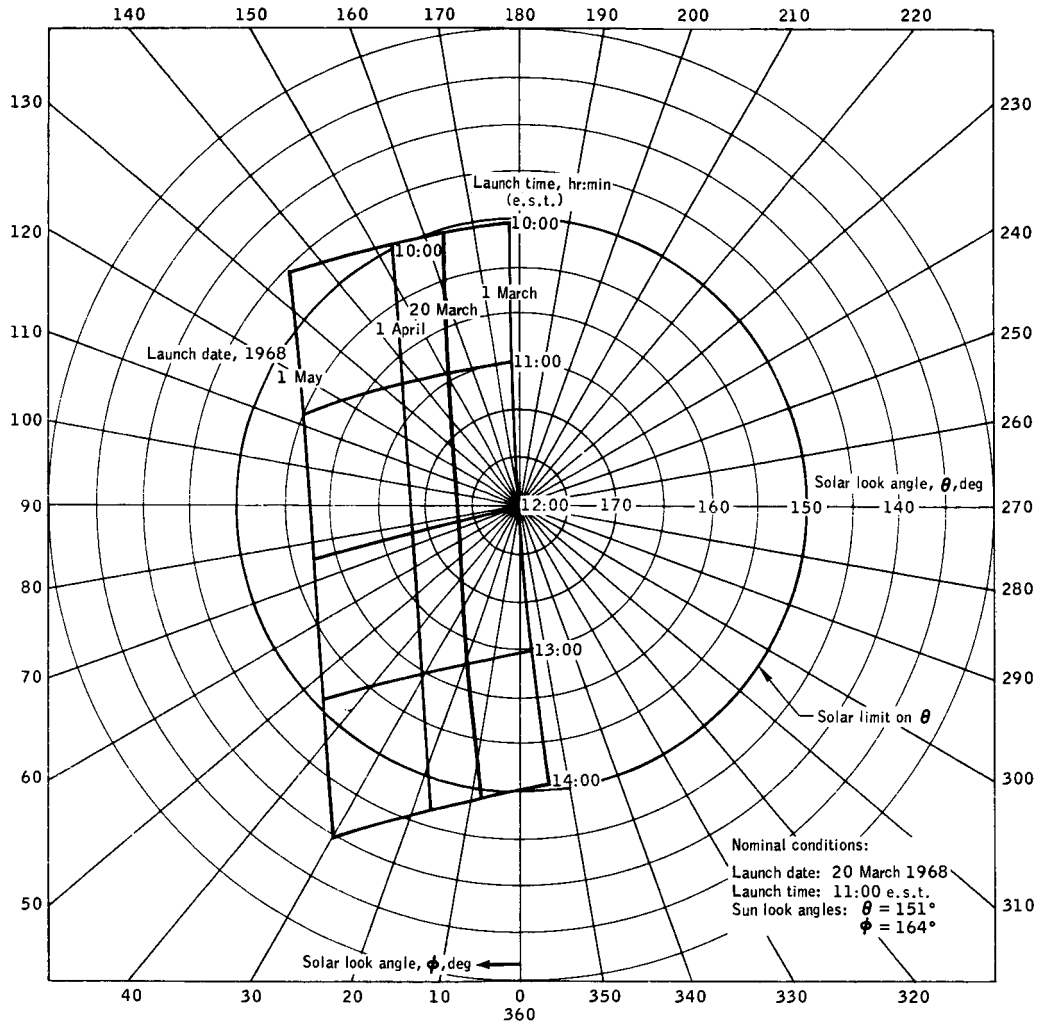




(a) Primary solar soak attitude.

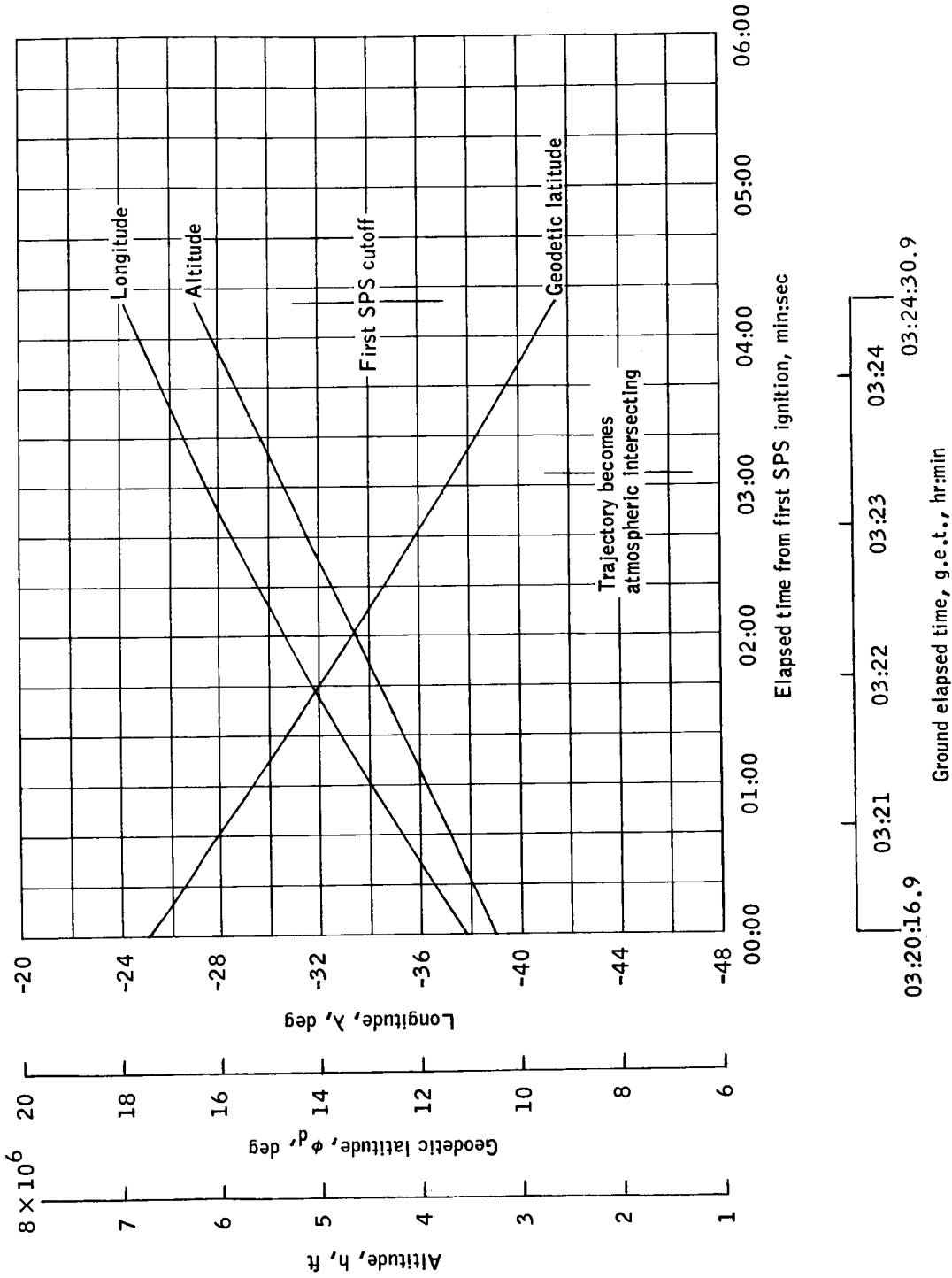
Figure 3-10.- Effect of launch delay on sun look angles.

MPAD 3180 S



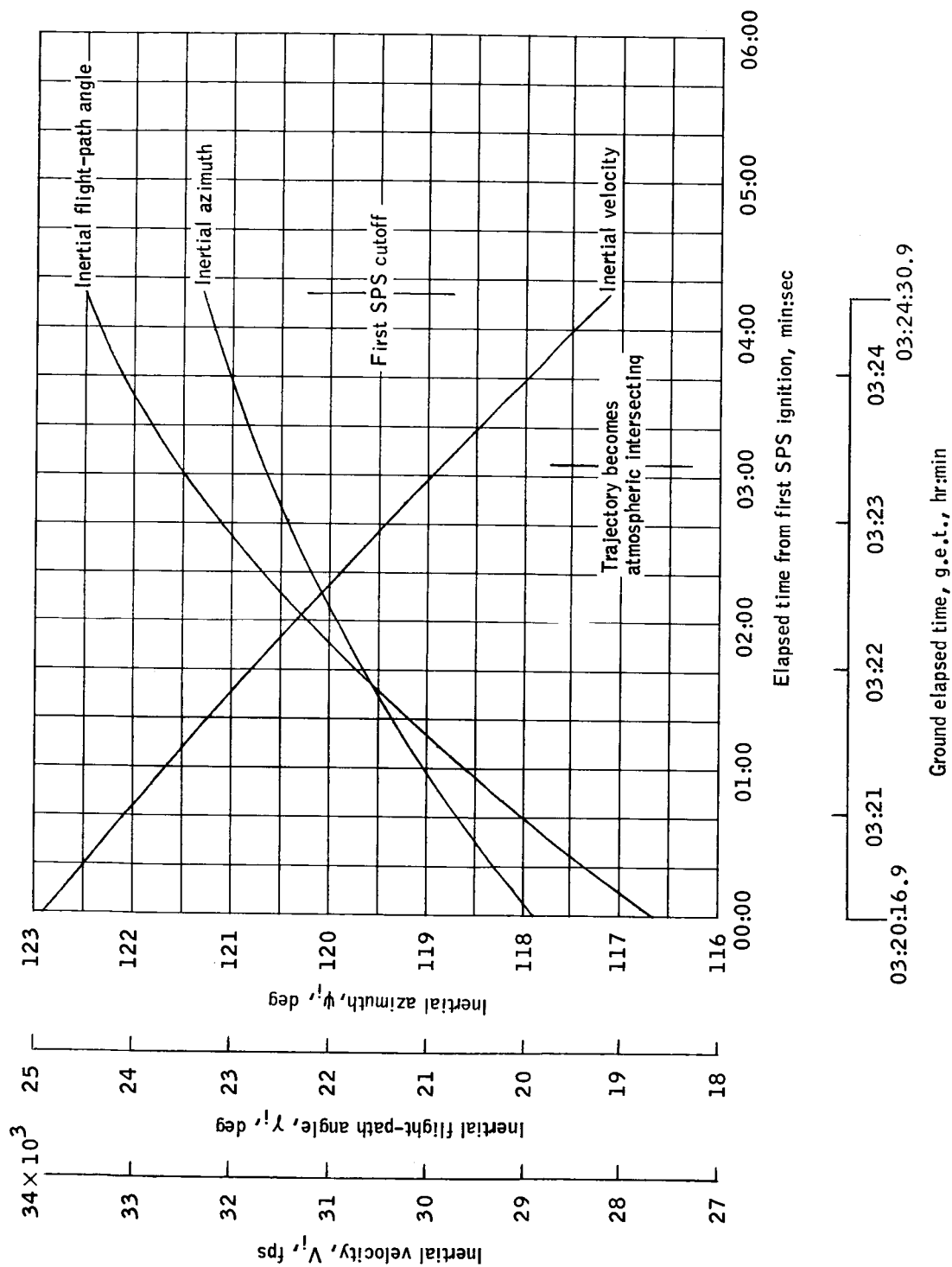
(b) Secondary solar soak attitude.

Figure 3-10.- Concluded



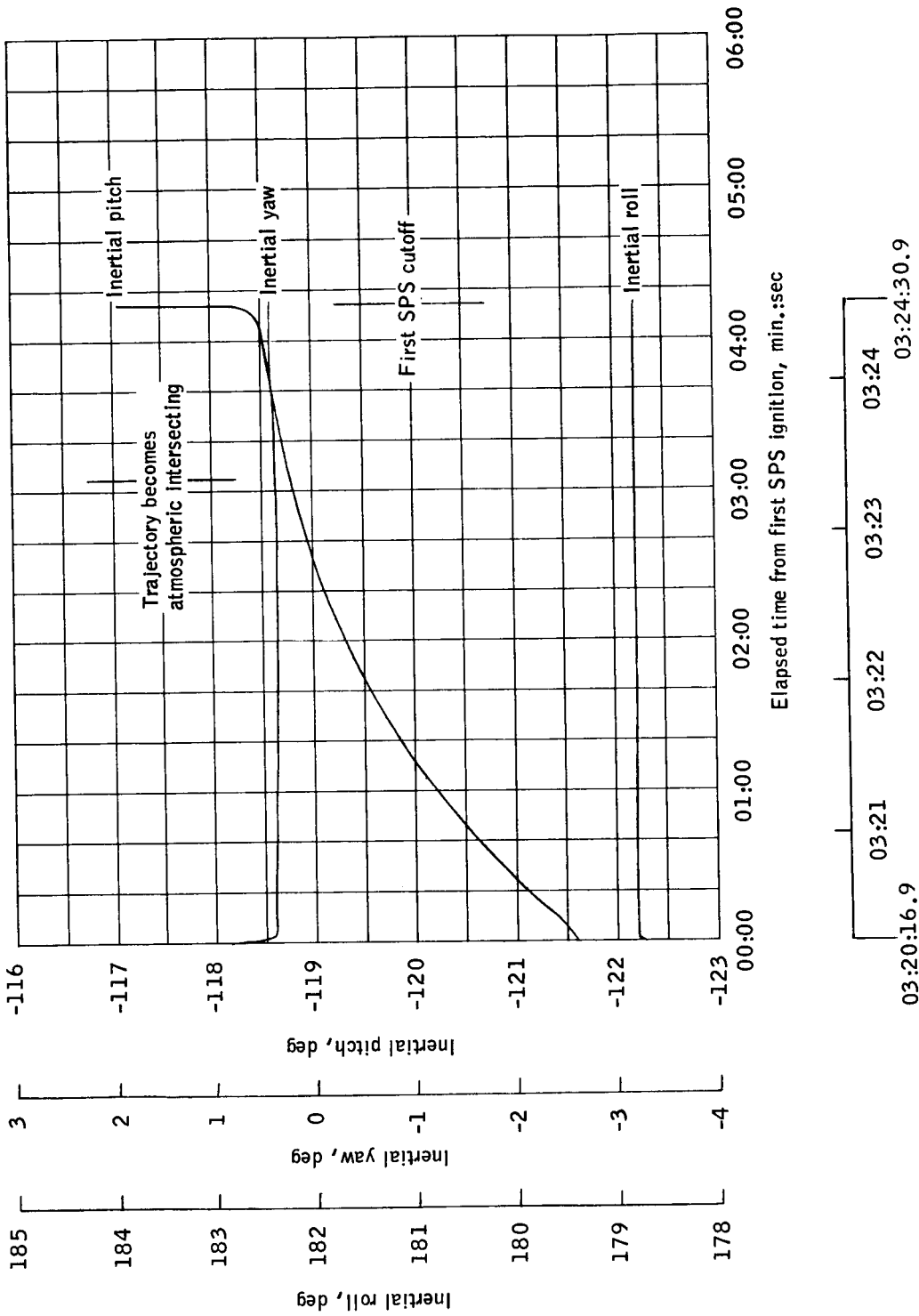
(a) Altitude, latitude, and longitude.

Figure 3-11.- First SPS burn.



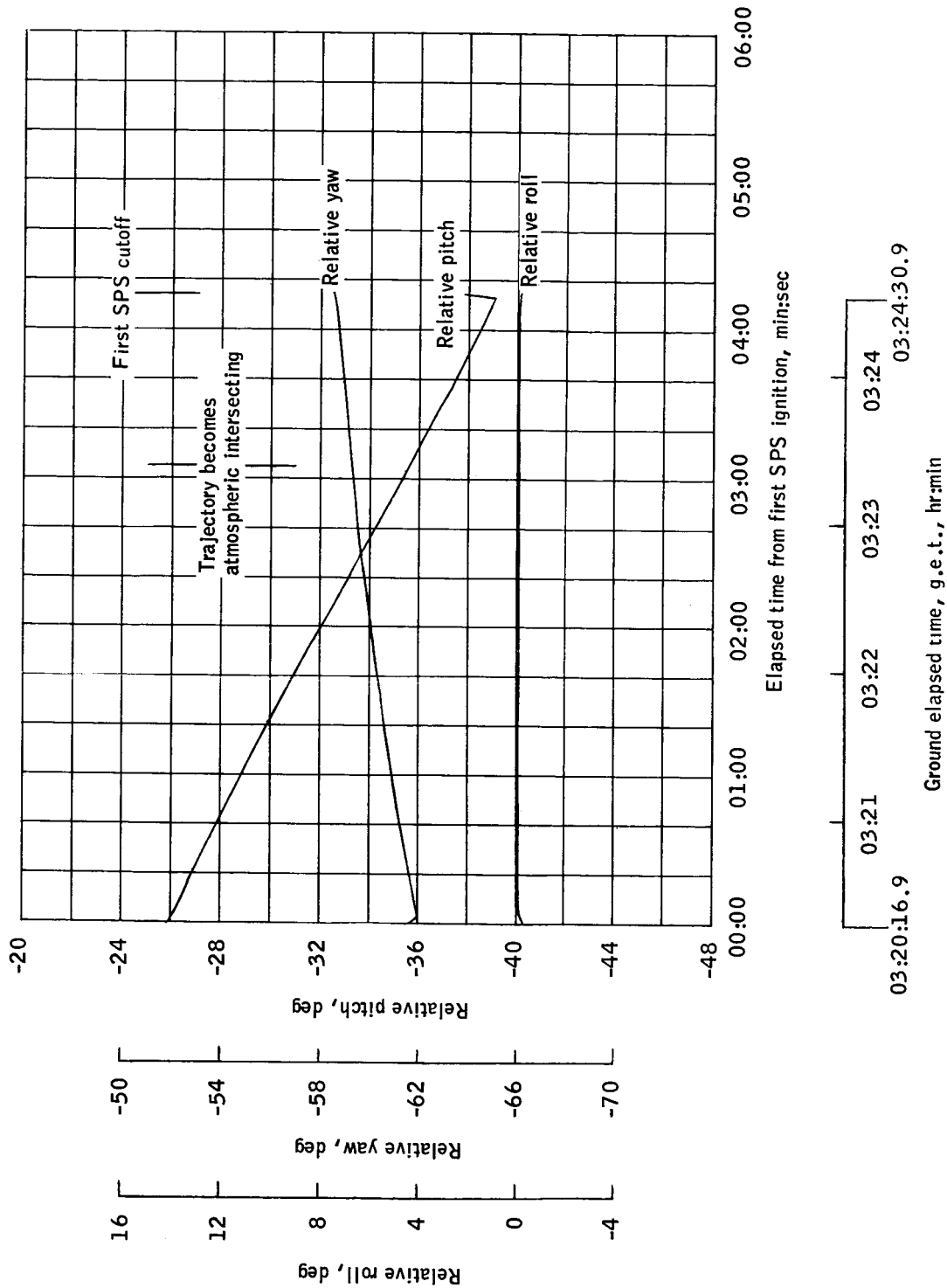
(b) Inertial velocity, flight-path angle, and azimuth.

Figure 3-11.- Continued.



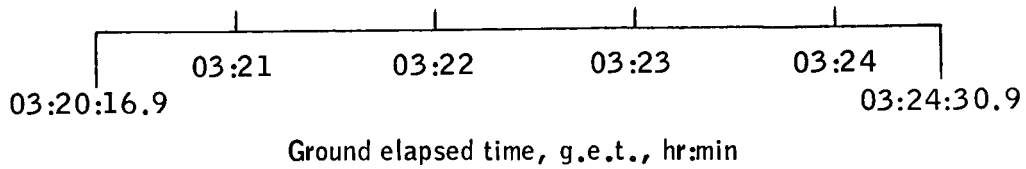
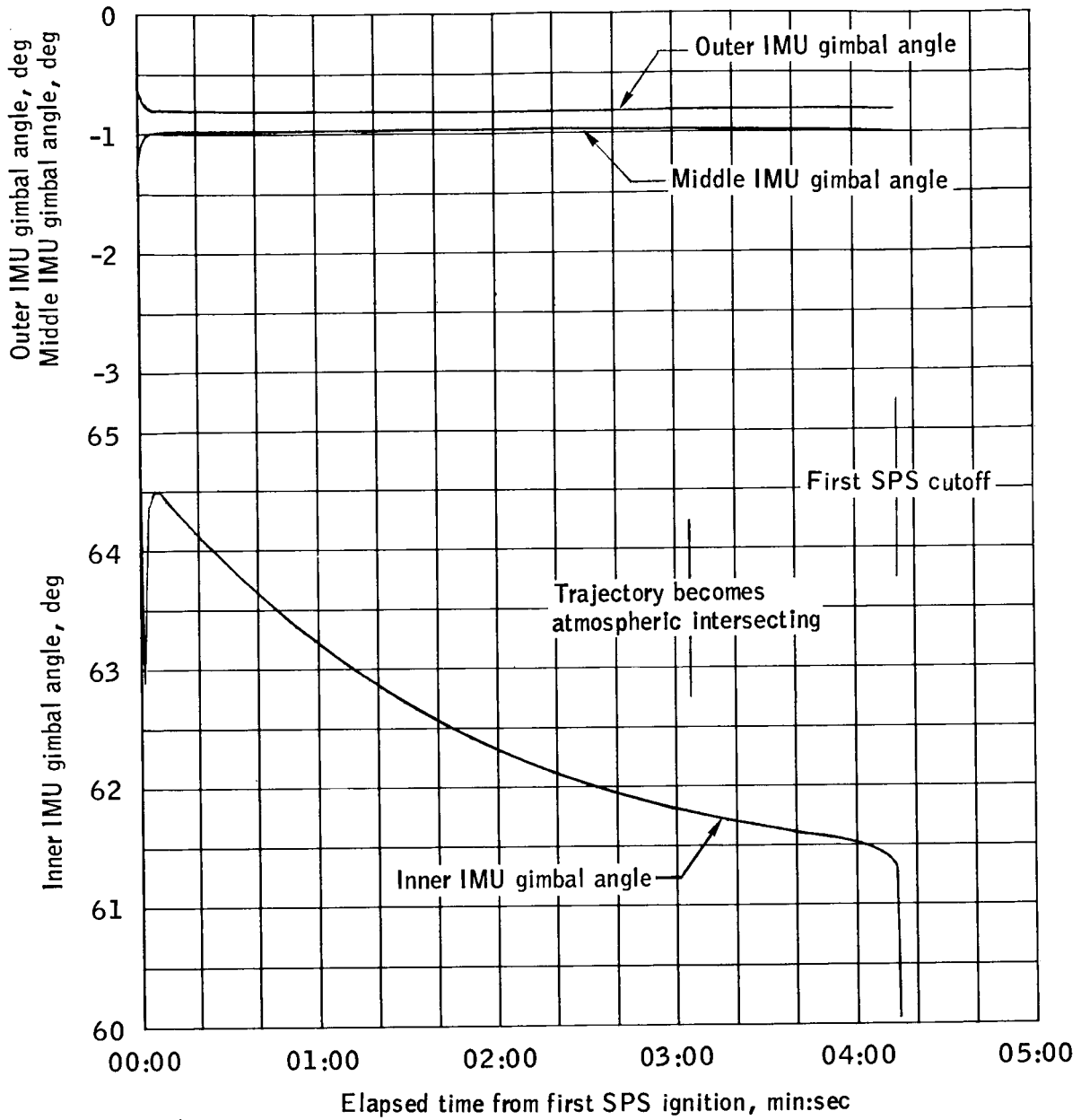
(c) Inertial yaw, pitch, and roll.

Figure 3-11.- Continued.



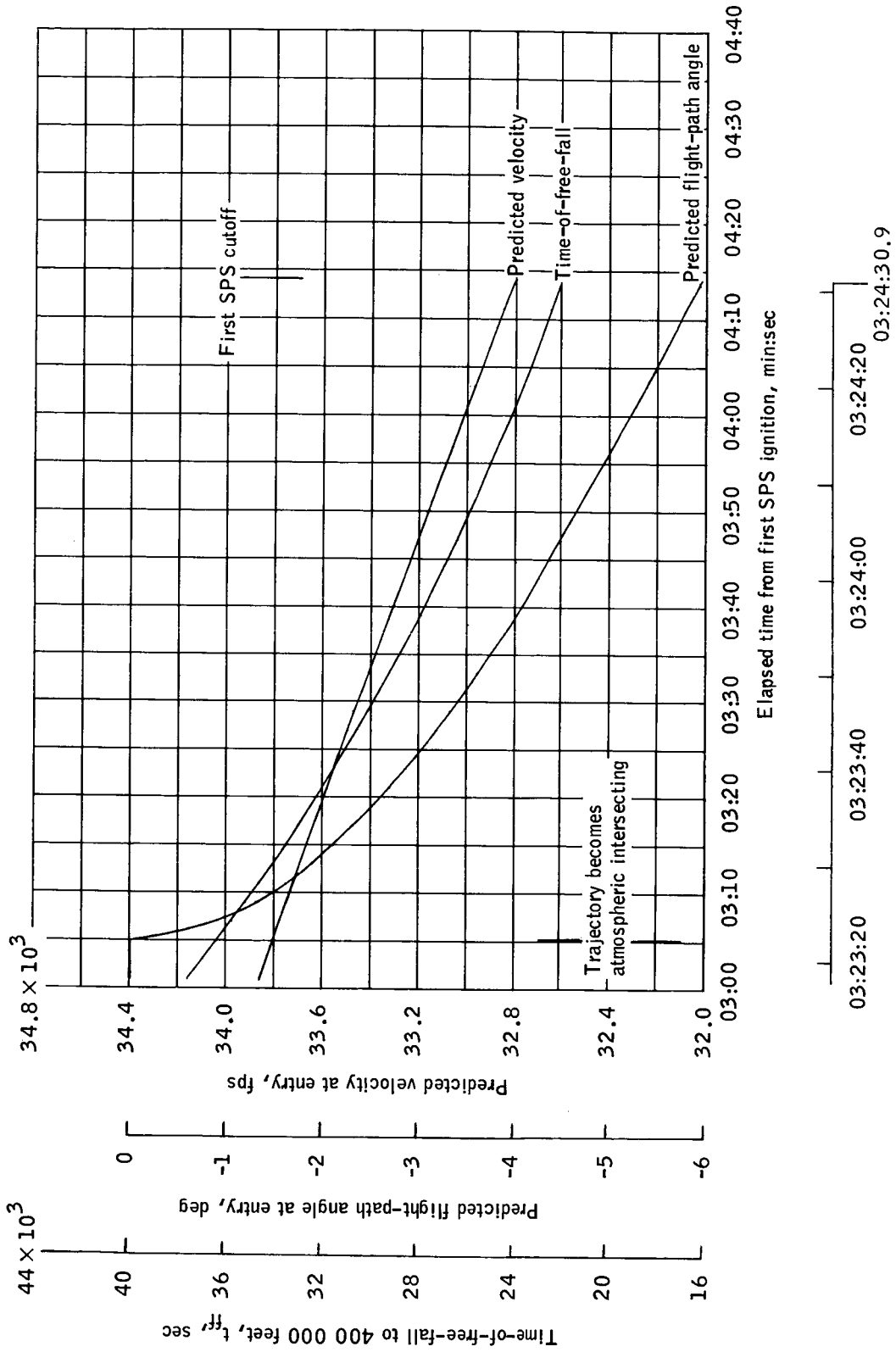
(d) Relative yaw, pitch, and roll.

Figure 3-11.- Continued.



(e) IMU gimbal angles.

Figure 3-11.- Continued.

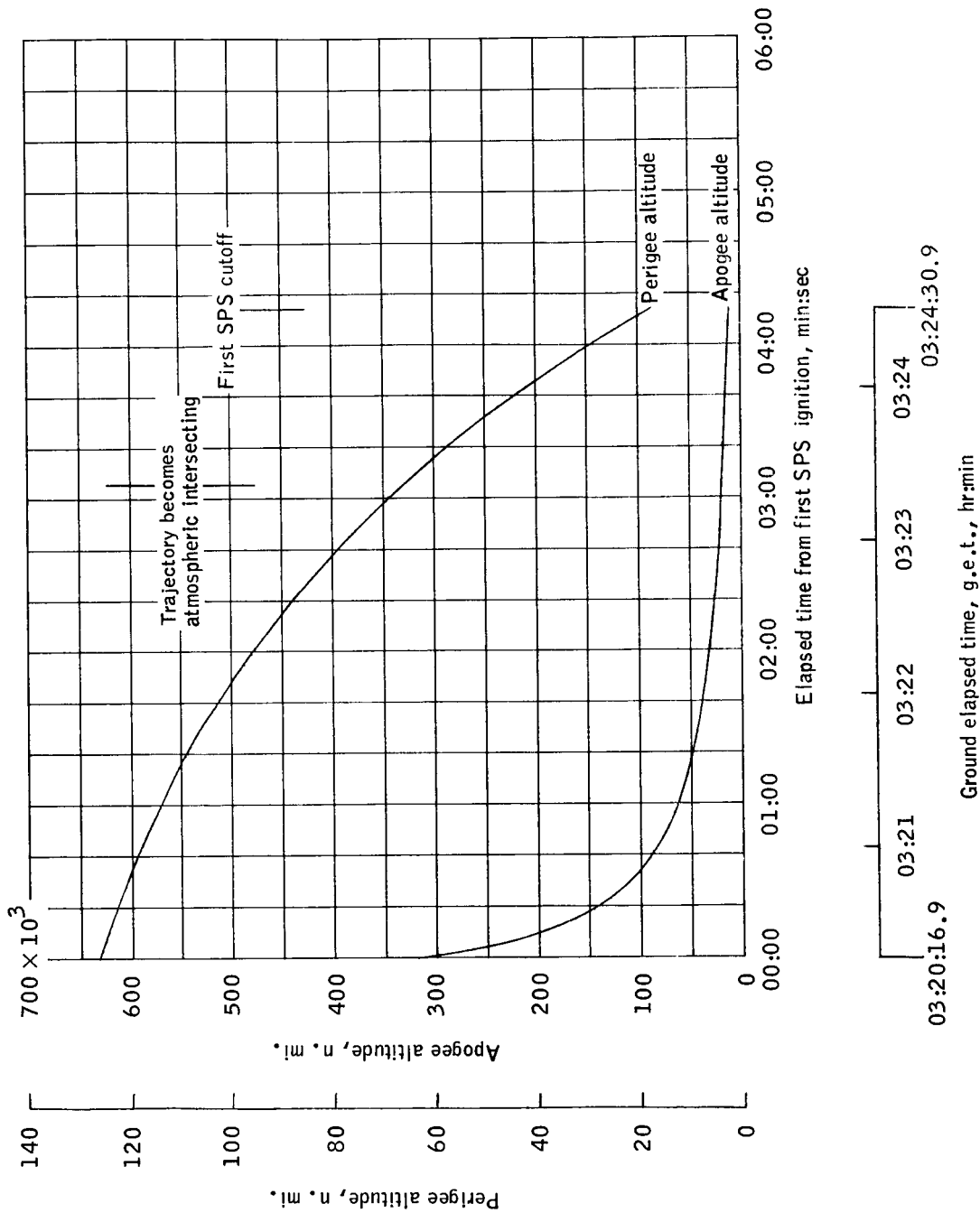


Ground elapsed time, g.e.t., hr:min

(f) Time of free fall to reentry, predicted velocity and flight-path angle at entry.

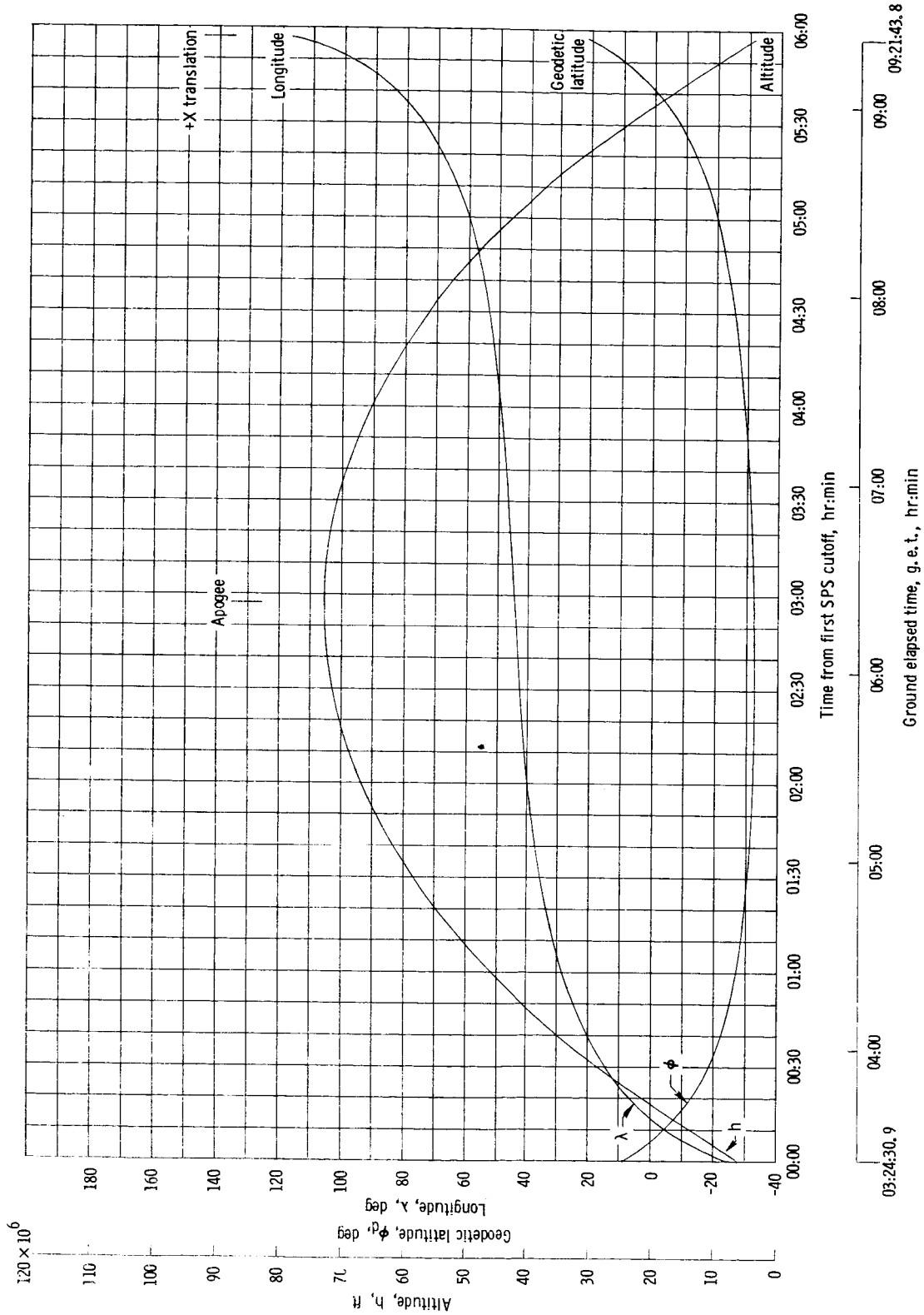
Figure 3-11.- Continued.





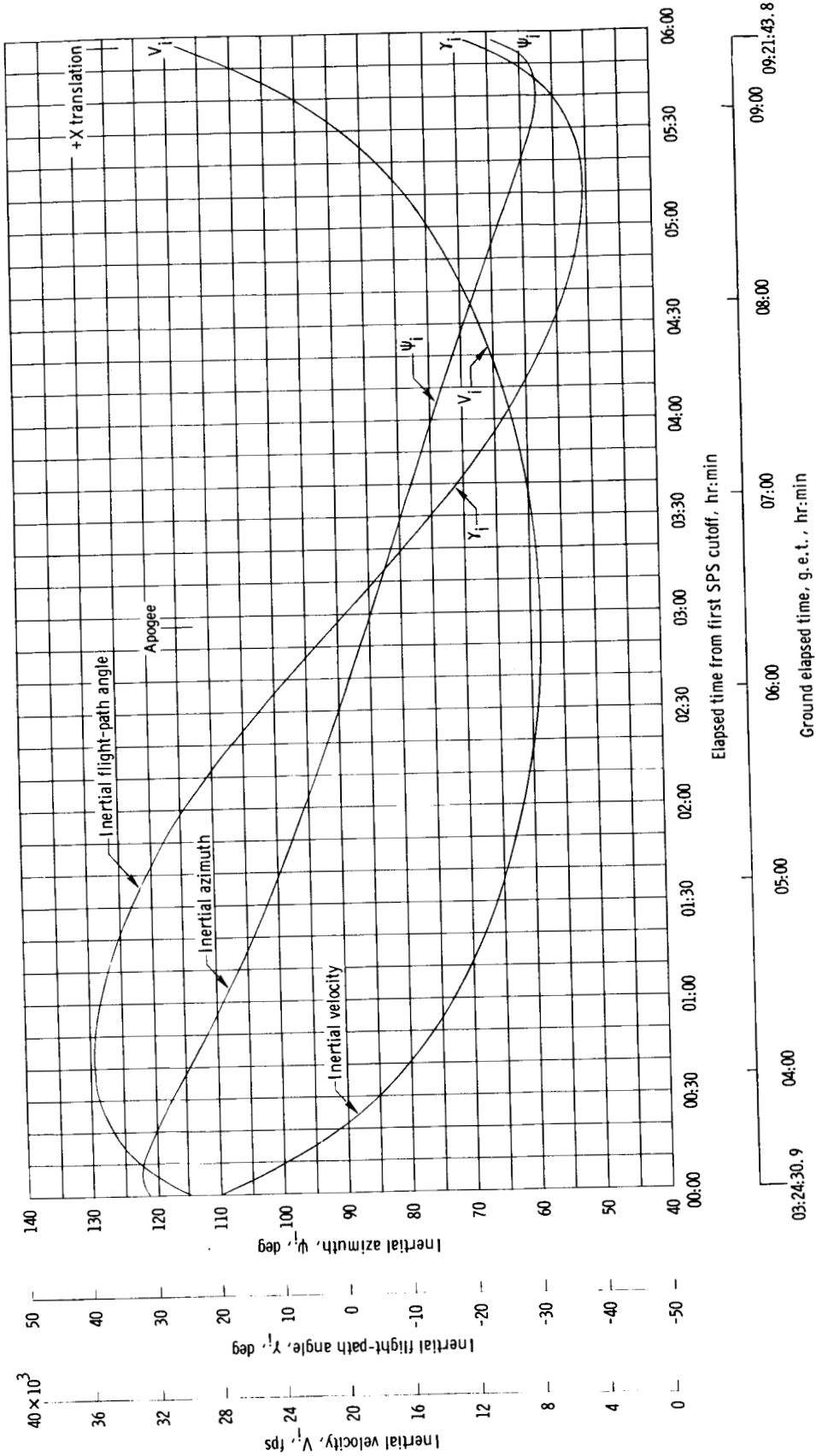
(g) Instantaneous apogee and perigee altitude.

Figure 3-11.- Concluded.



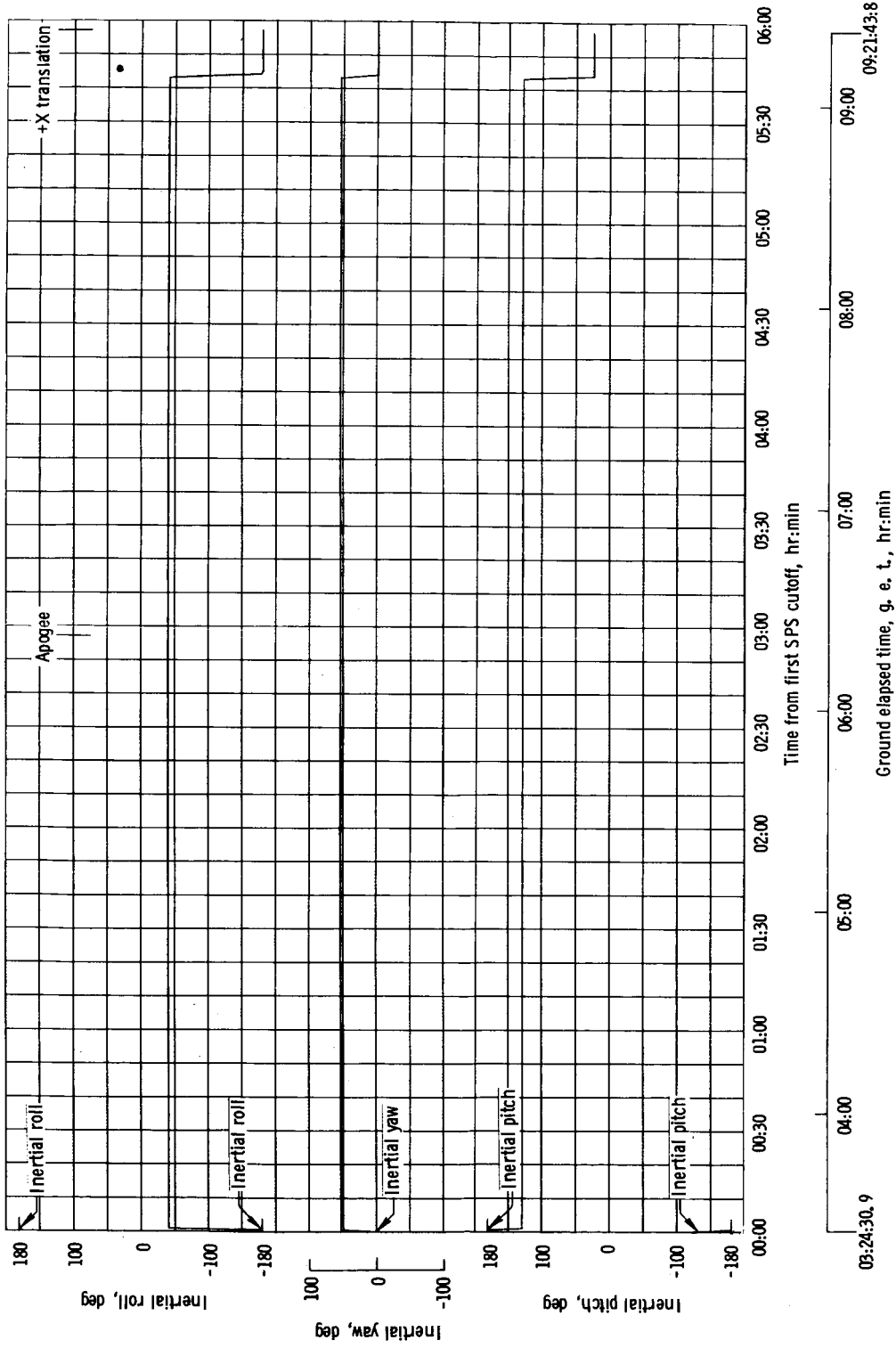
(a) Altitude, latitude, and longitude.

Figure 3-12. - Earth intersecting coast.



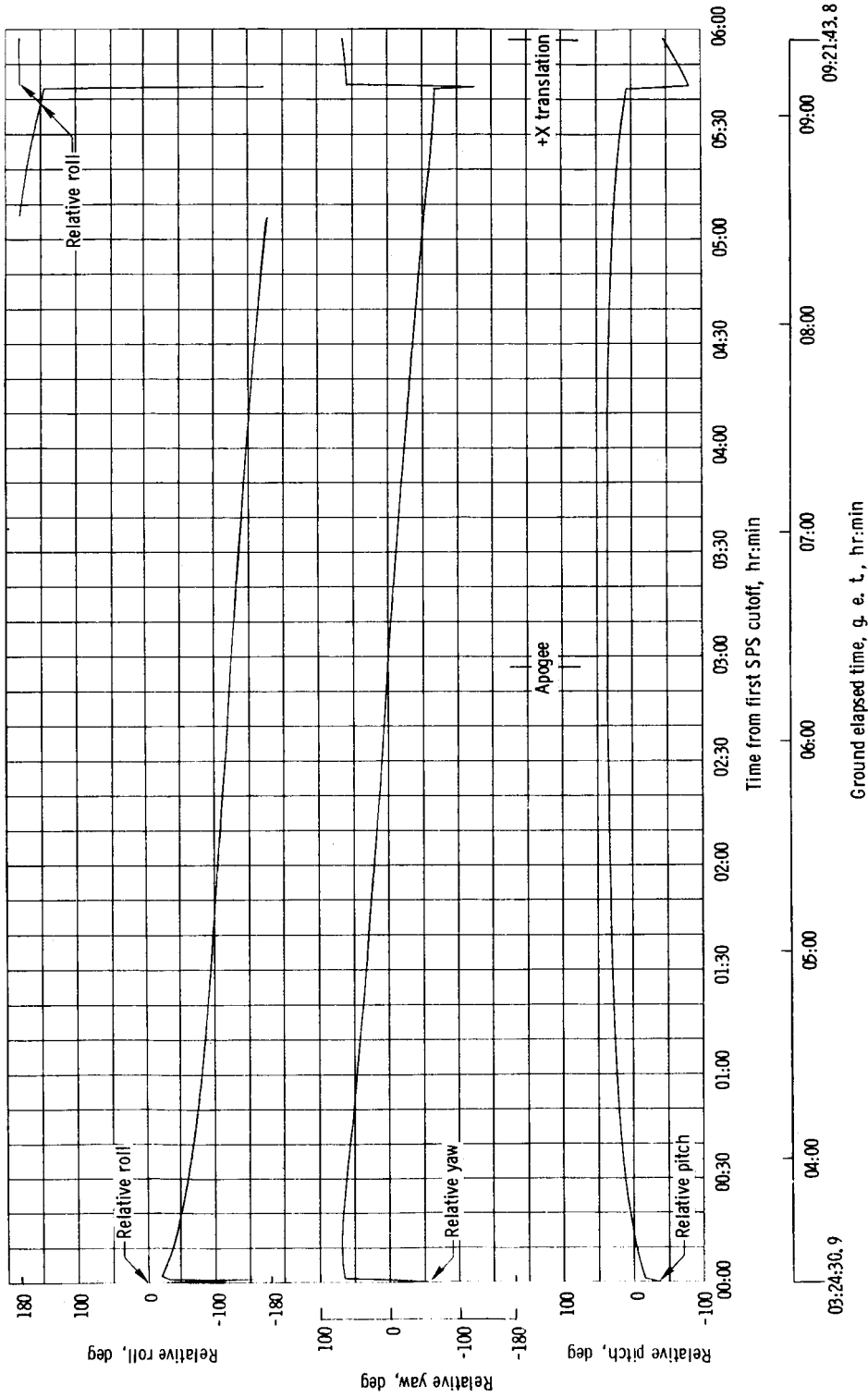
(b) Inertial velocity, azimuth, and flight-path angle.

Figure 3-12. - Continued.



(c) Inertial yaw, pitch, and roll.

Figure 3-12. - Continued.



(d) Relative yaw, pitch, and roll.

Figure 3-12. - Continued.

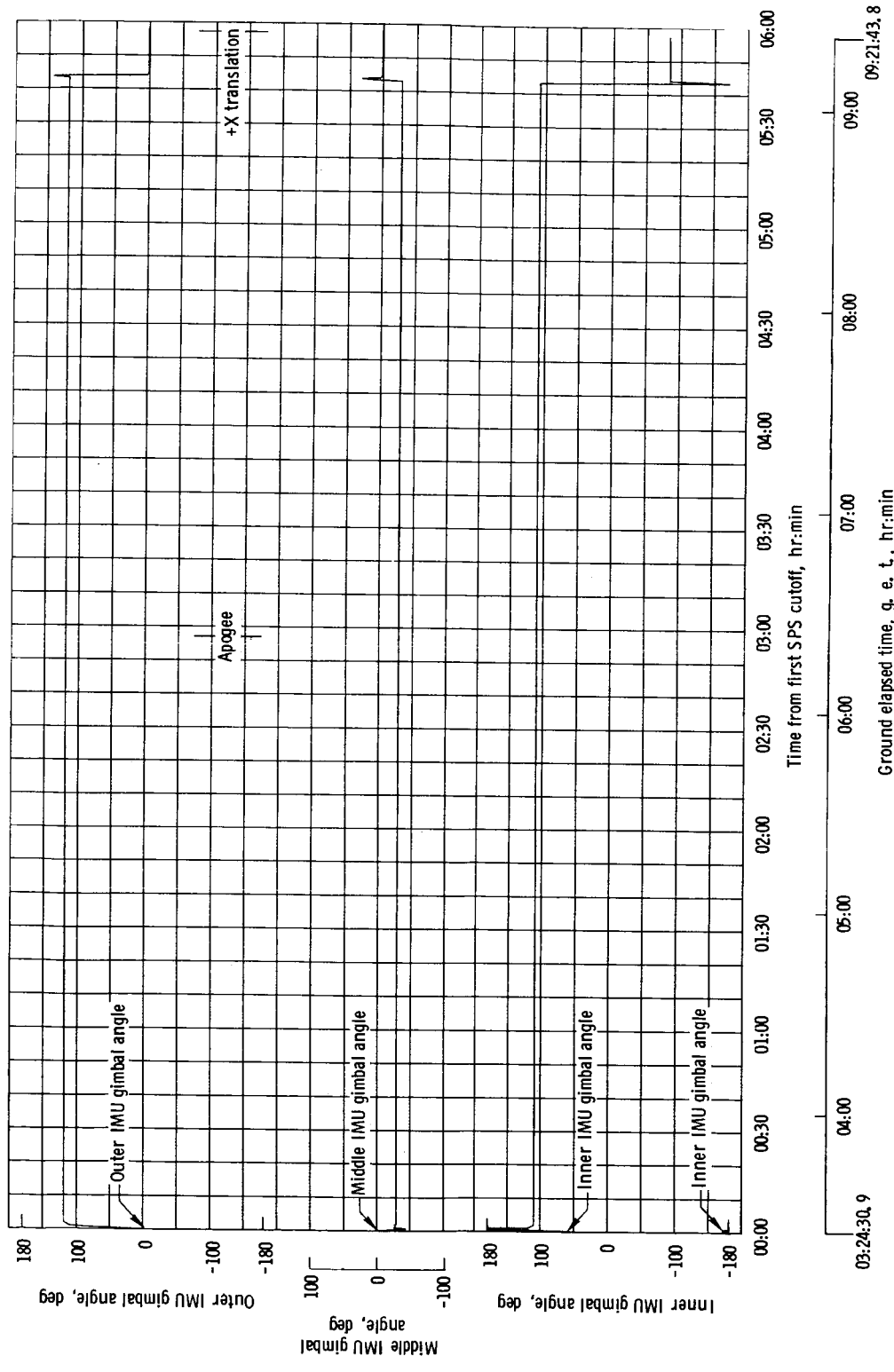
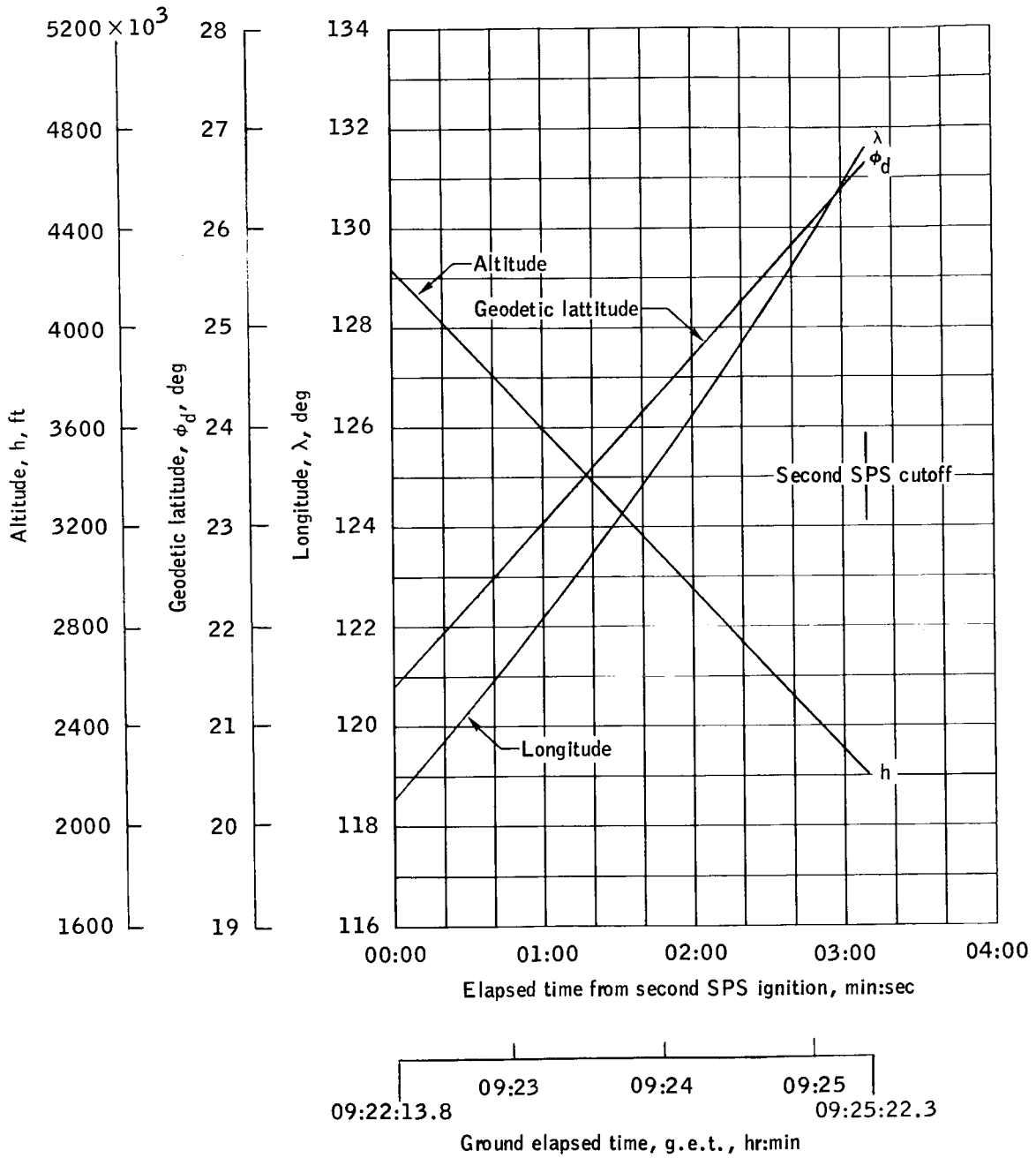


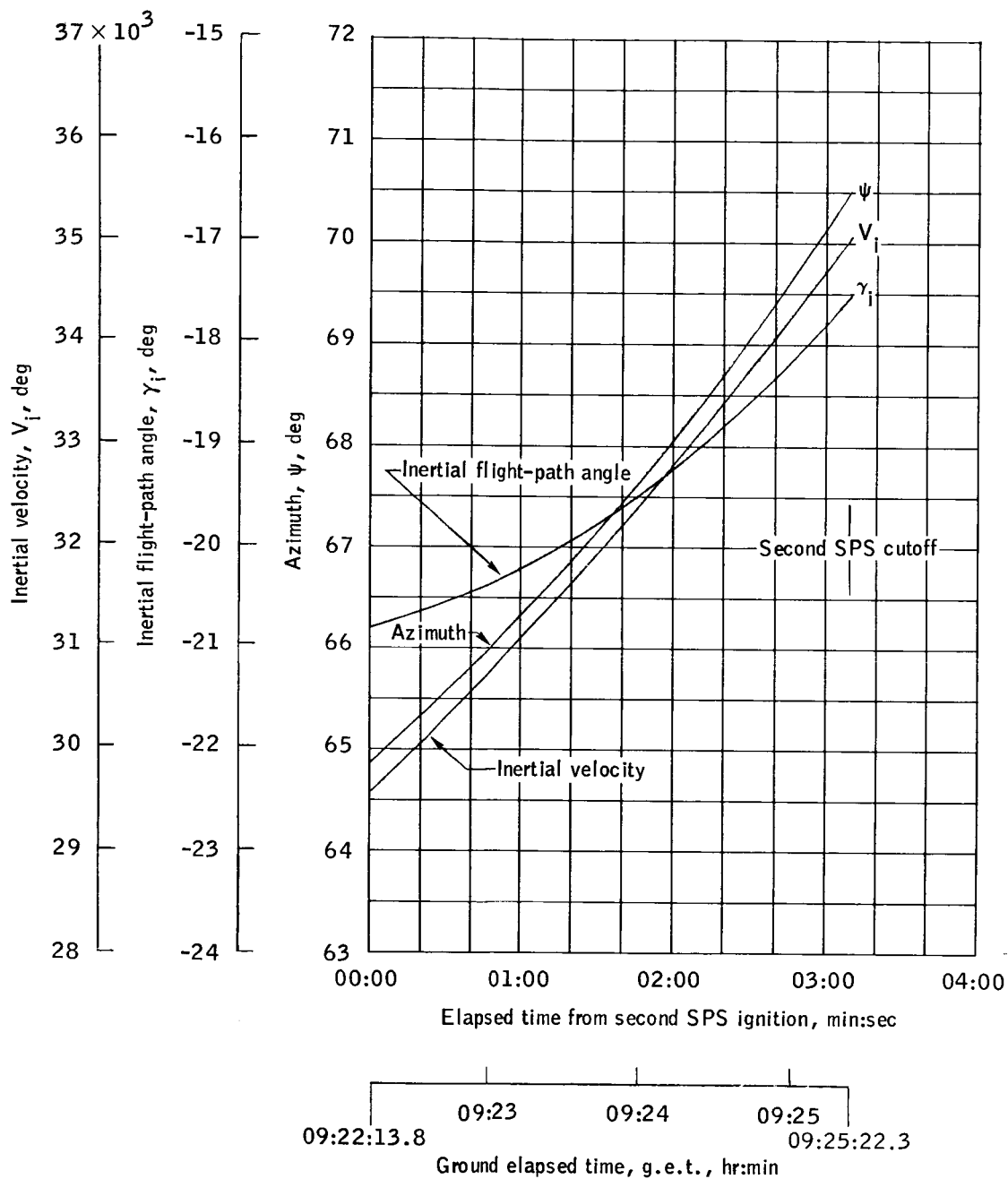
Figure 3-12. - Concluded.

(e) IMU gimbal angles.



(a) Altitude, latitude, and longitude.

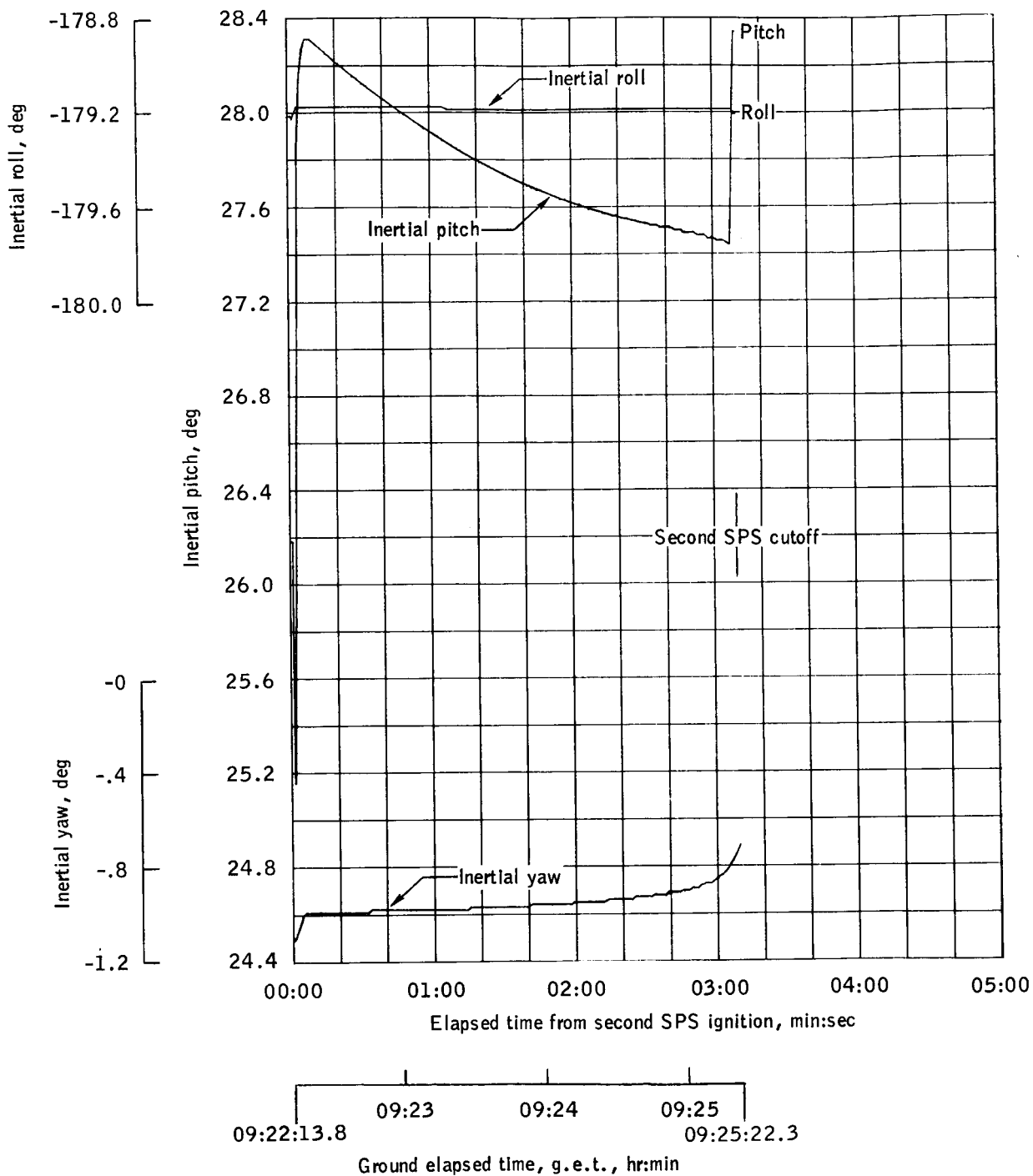
Figure 3-13.- Second SPS burn.



(b) Inertial velocity, flight-path angle, and azimuth.

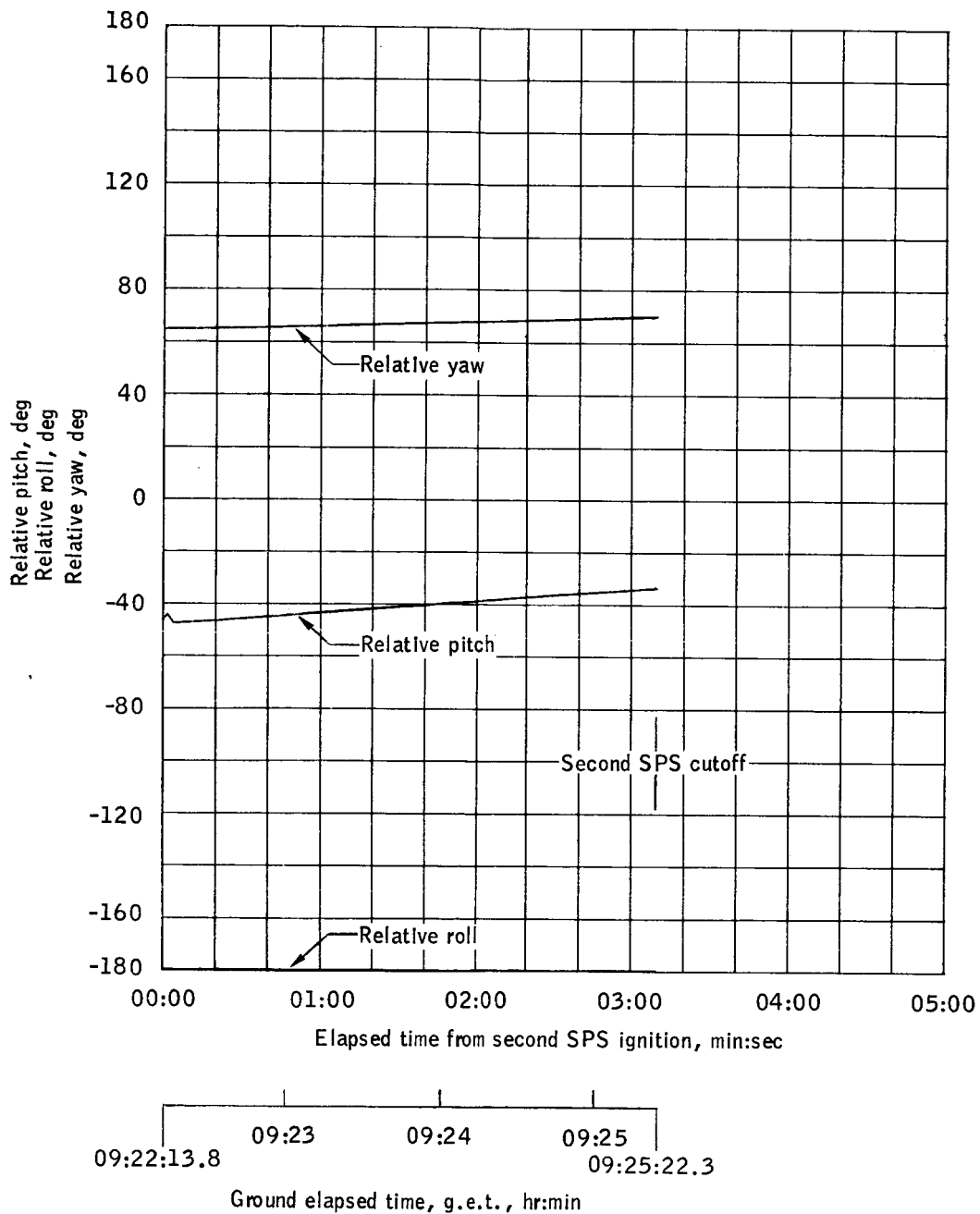
Figure 3-13.- Continued.





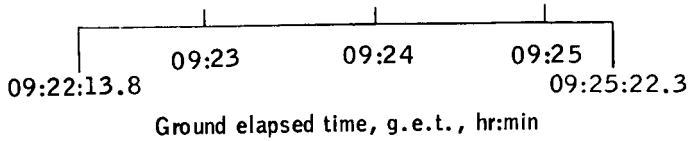
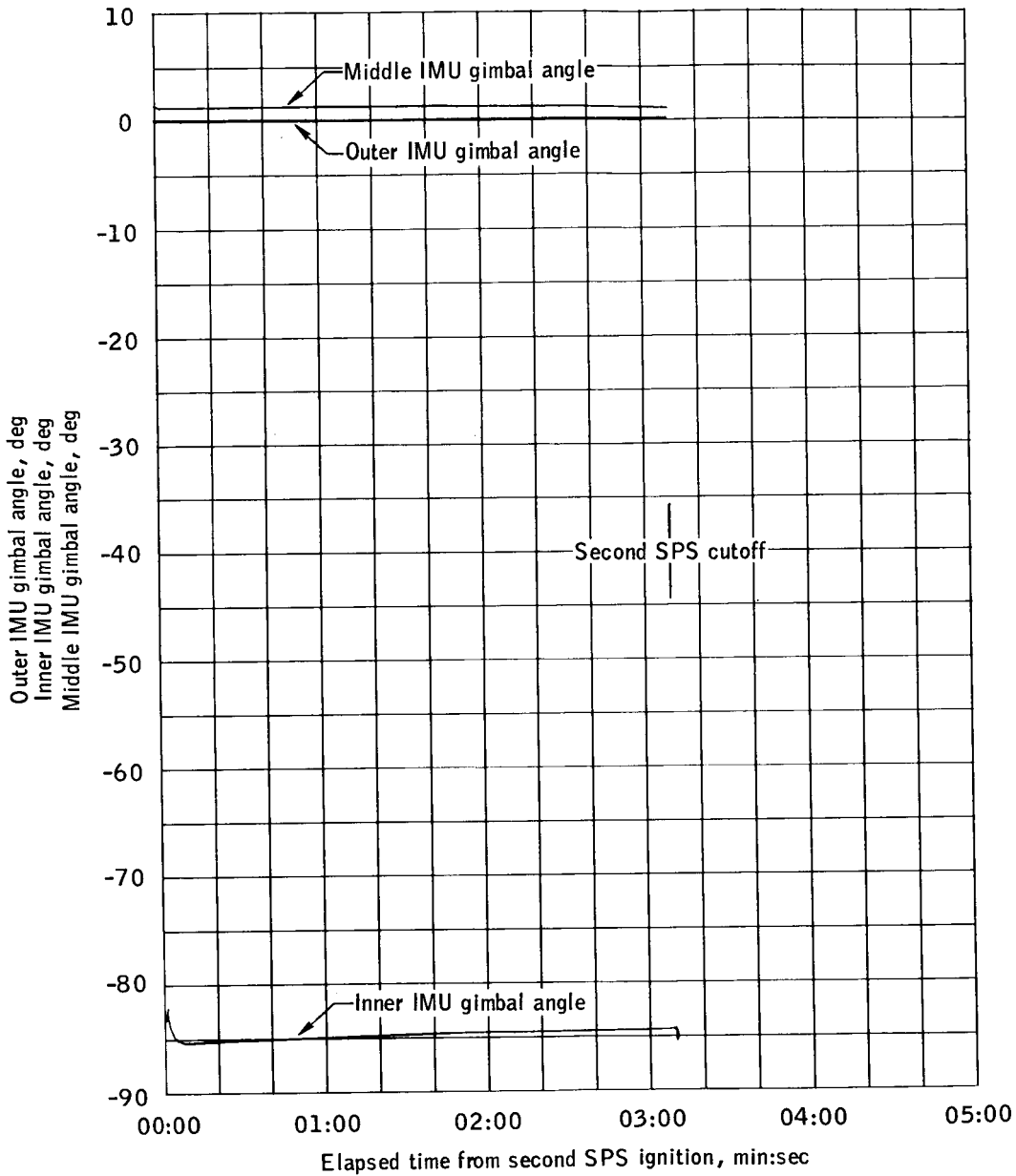
(c) Inertial yaw, pitch, and roll.

Figure 3-13.- Continued.



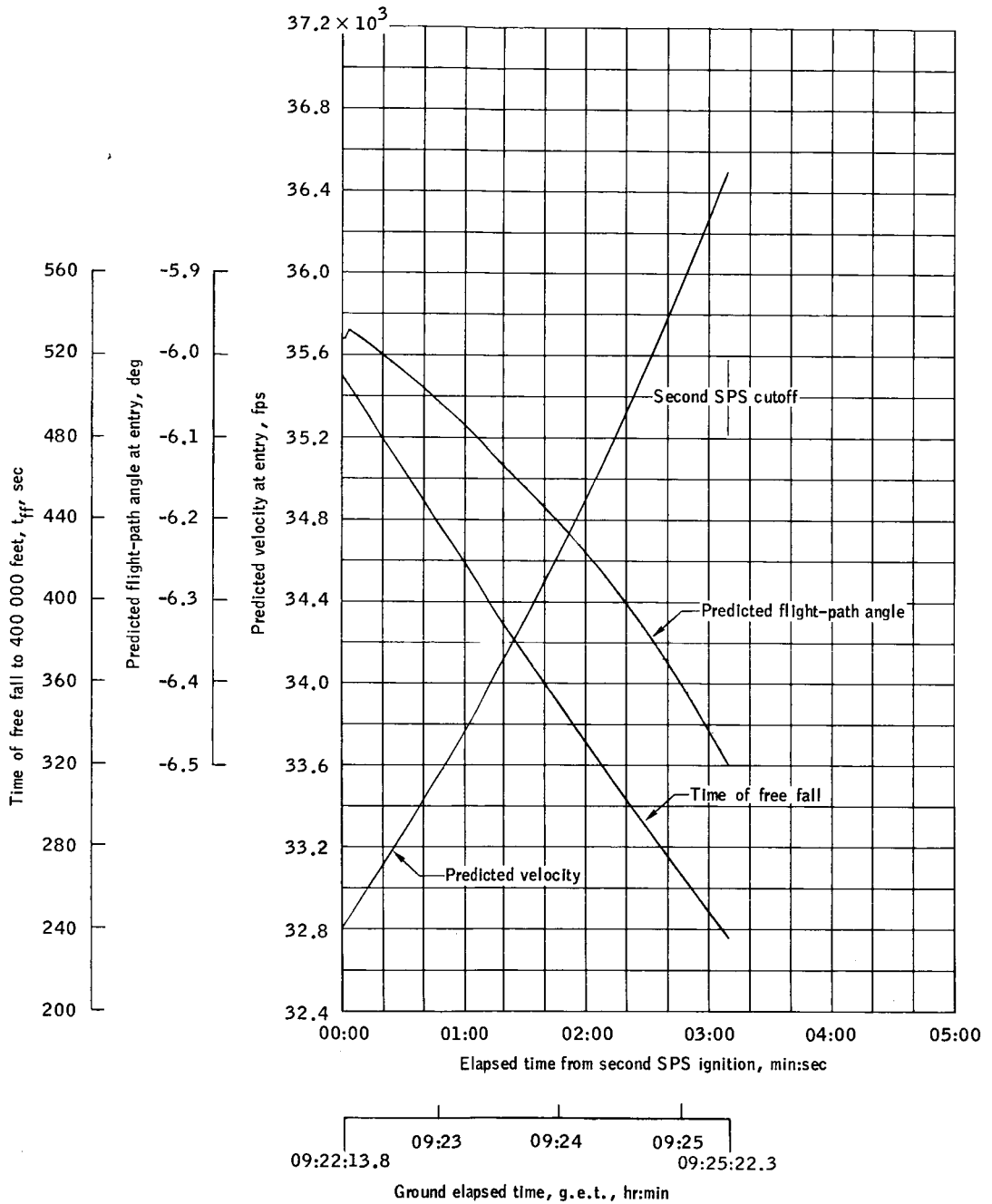
(d) Relative yaw, pitch, and roll.

Figure 3-13.- Continued.



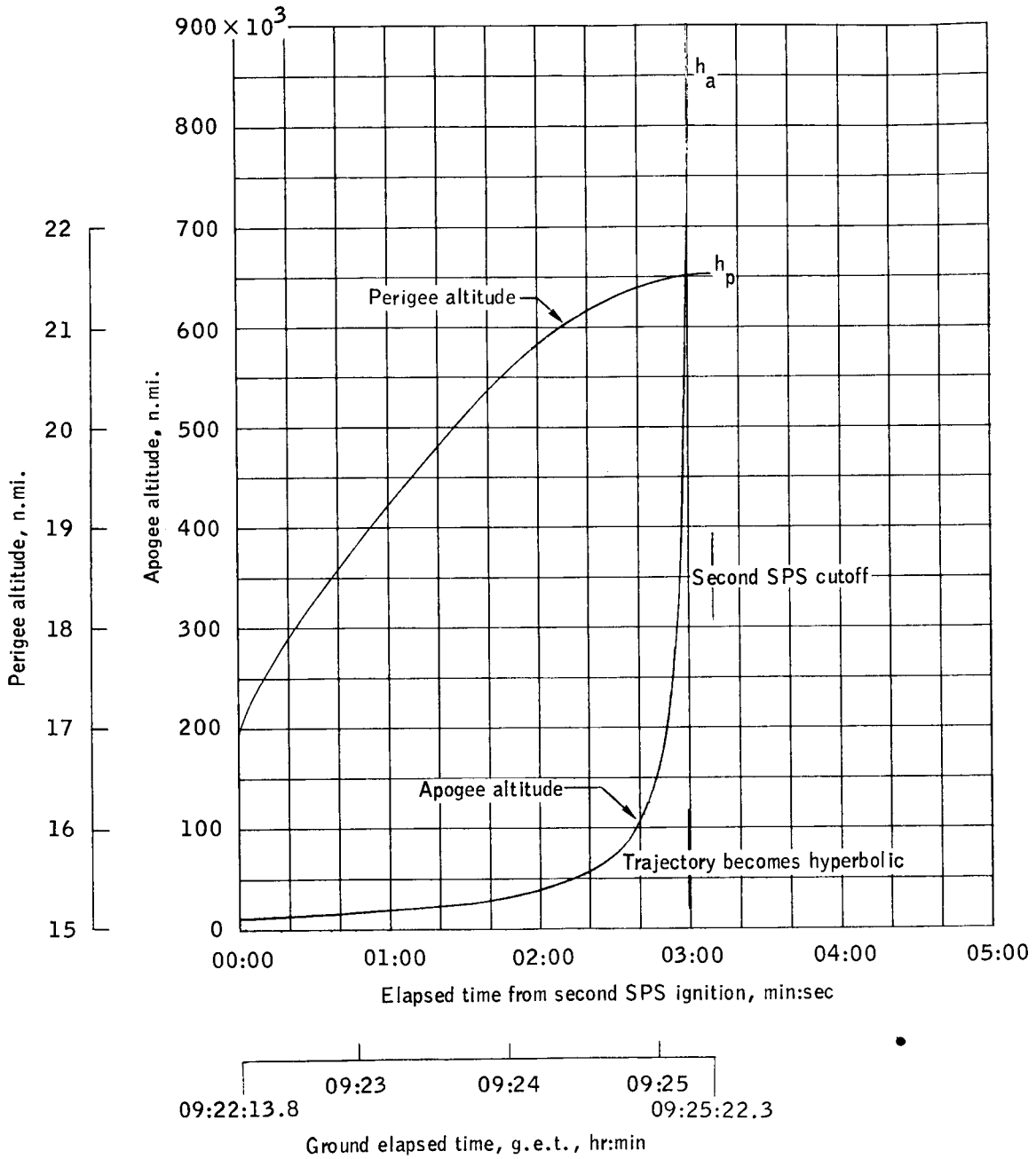
(e) IMU gimbal angles.

Figure 3-13.- Continued.



(f) Time of free fall to reentry, predicted velocity and flight-path angle at entry.

Figure 3-13.- Continued.



(g) Instantaneous apogee and perigee altitude.

Figure 3-13.- Concluded.

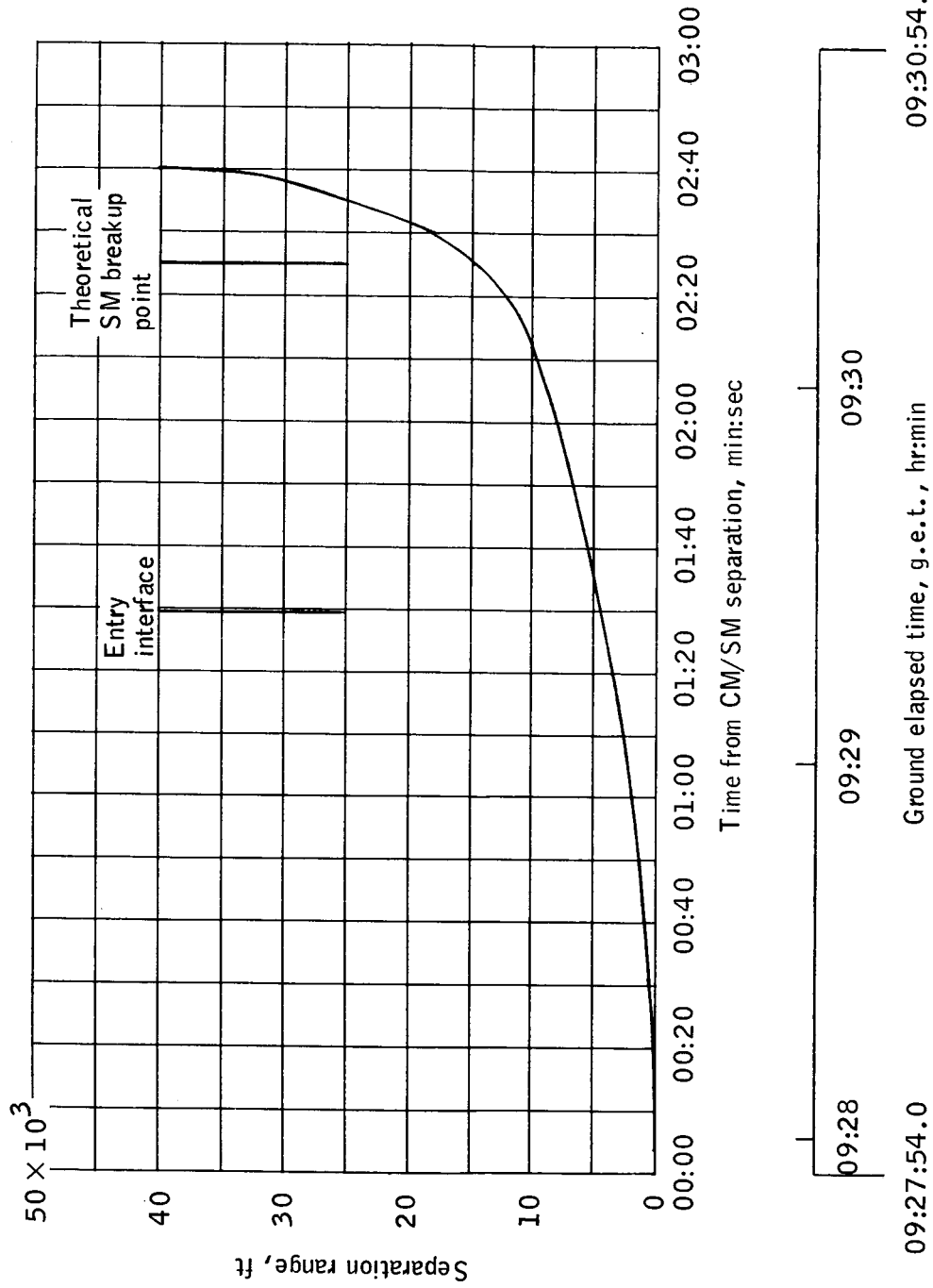
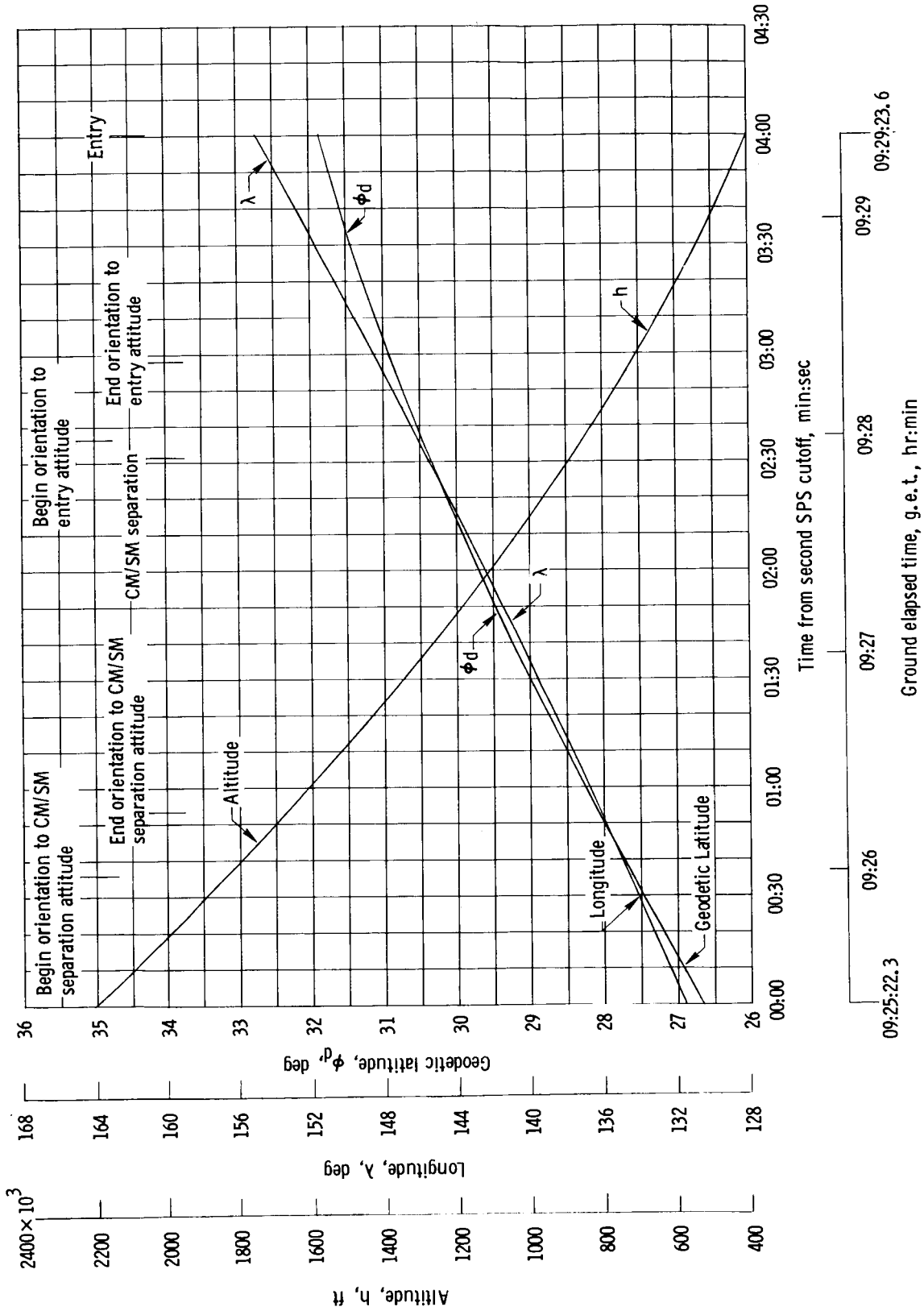
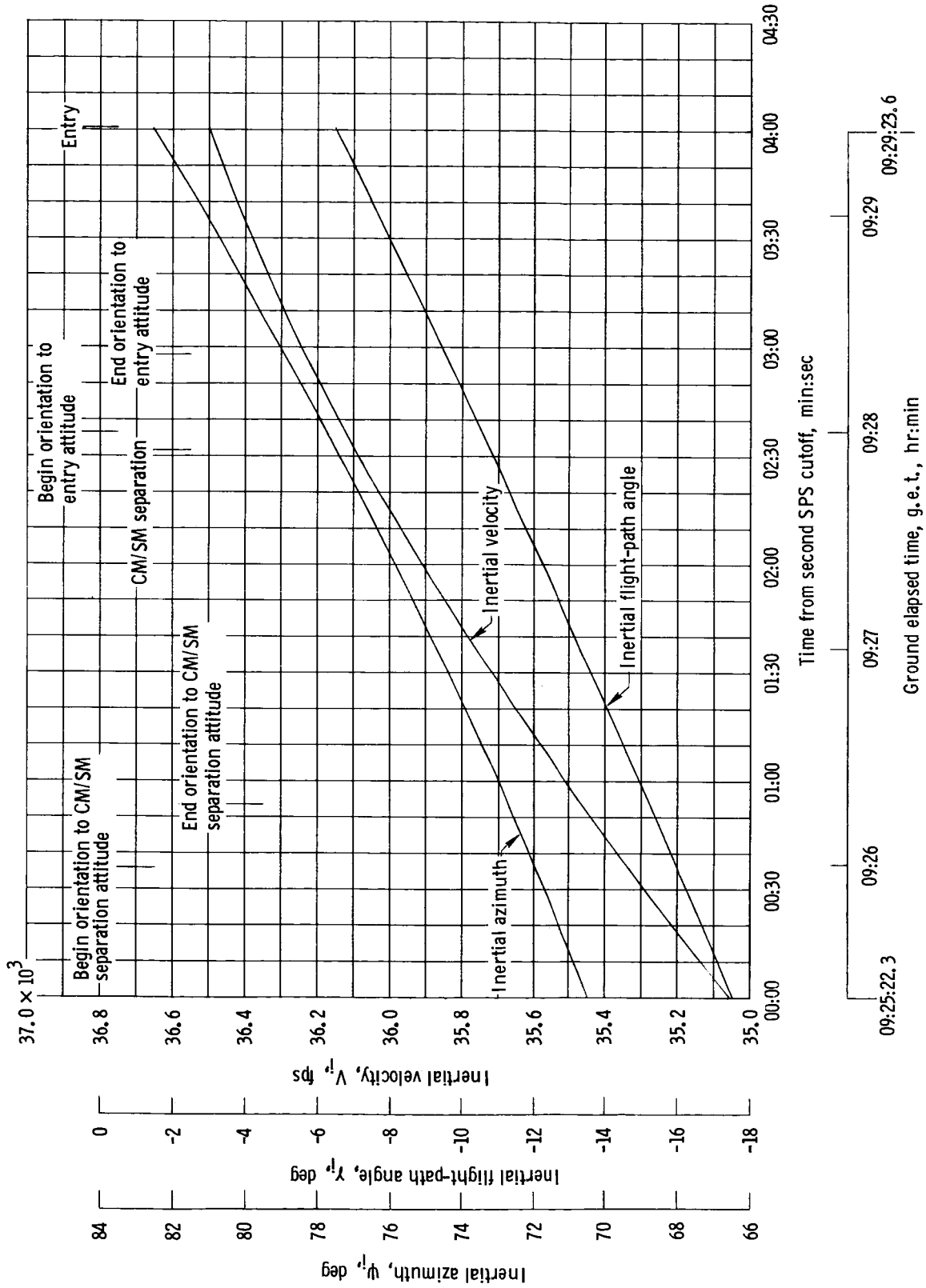


Figure 3-14.- CM/SM separation distance.



(a) Altitude, latitude, and longitude.

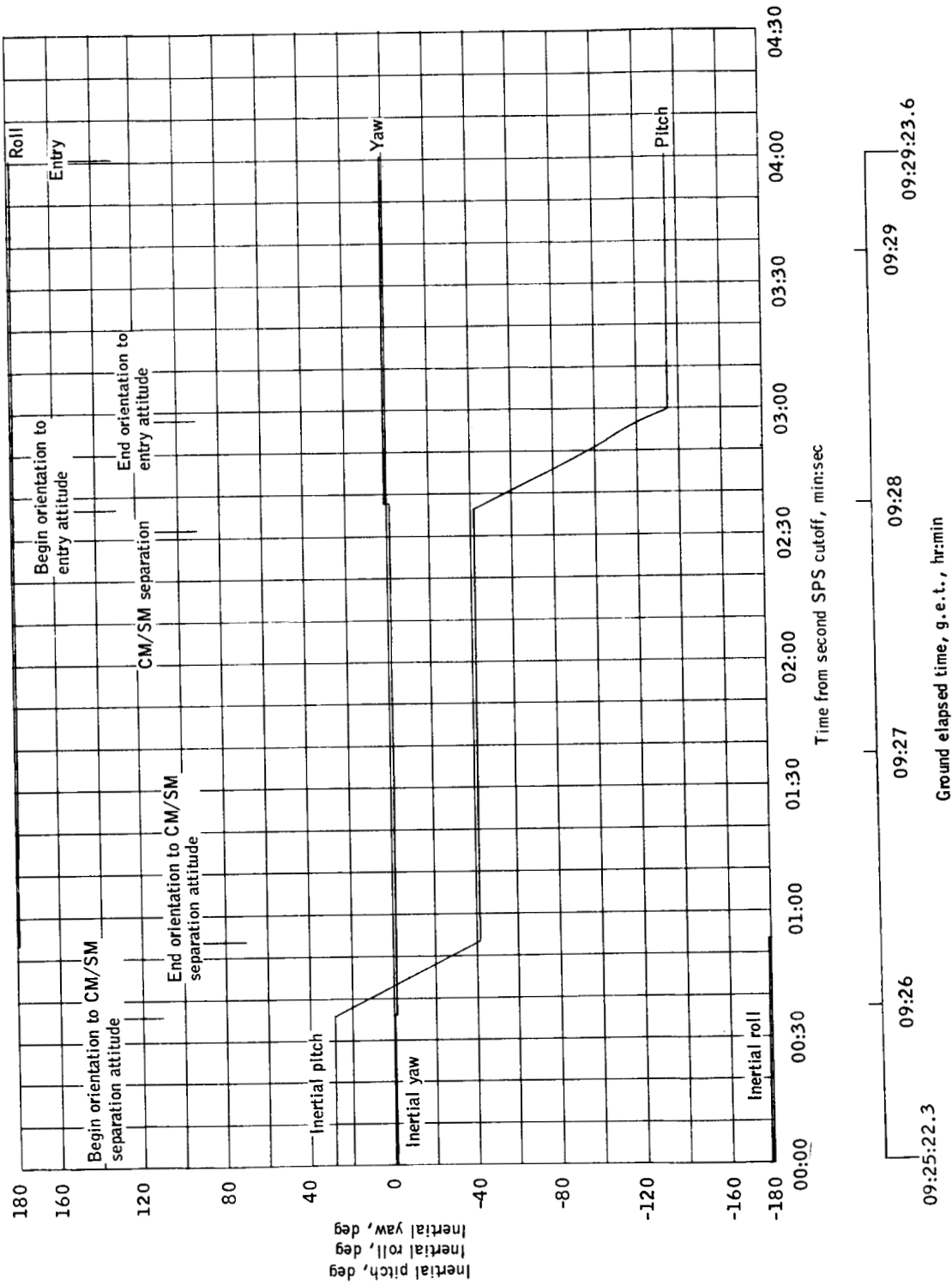
Figure 3-15. - Preentry sequence.



(b) Inertial velocity, flight-path angle, and azimuth.

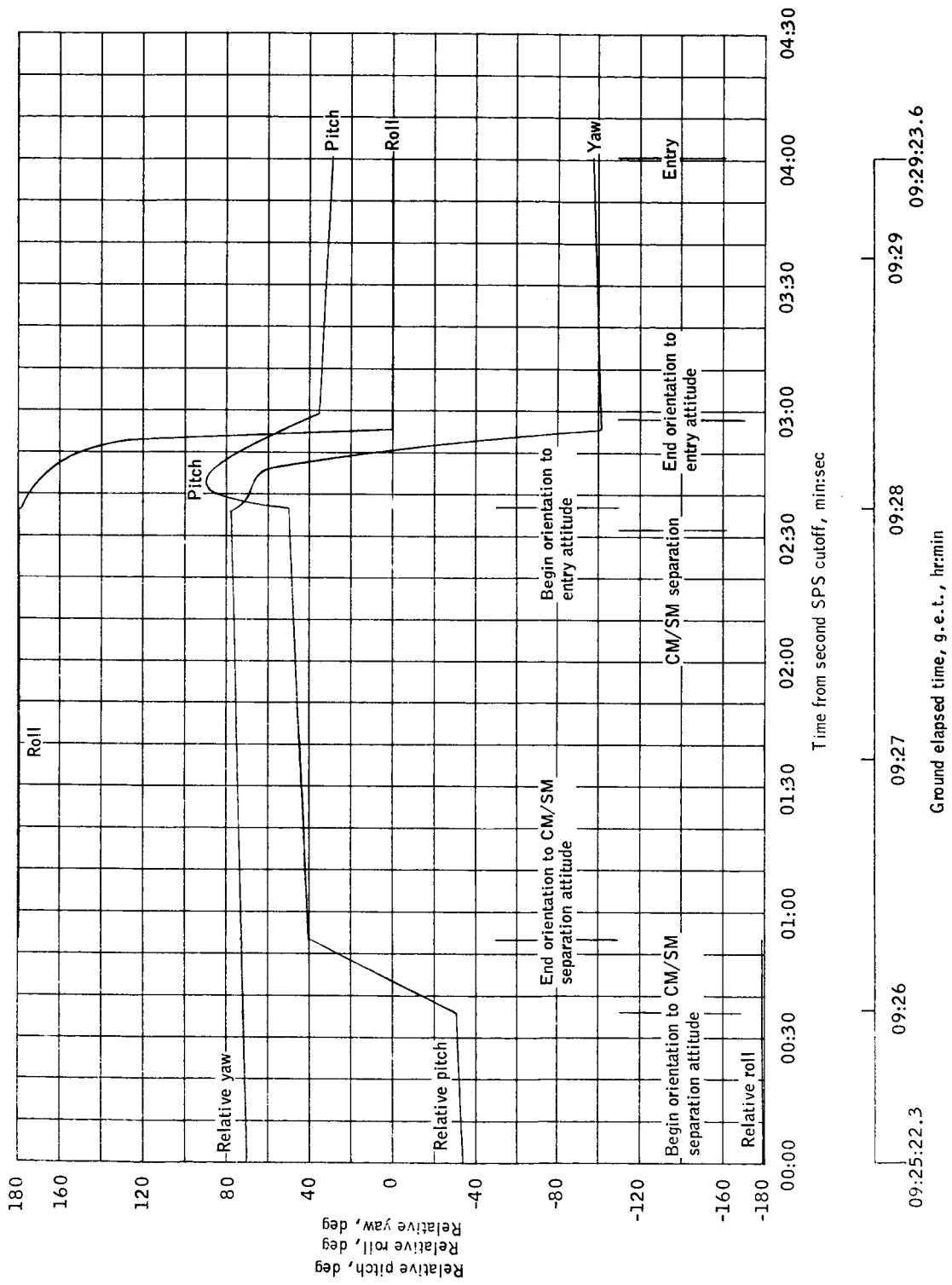
Figure 3-15, - Continued.





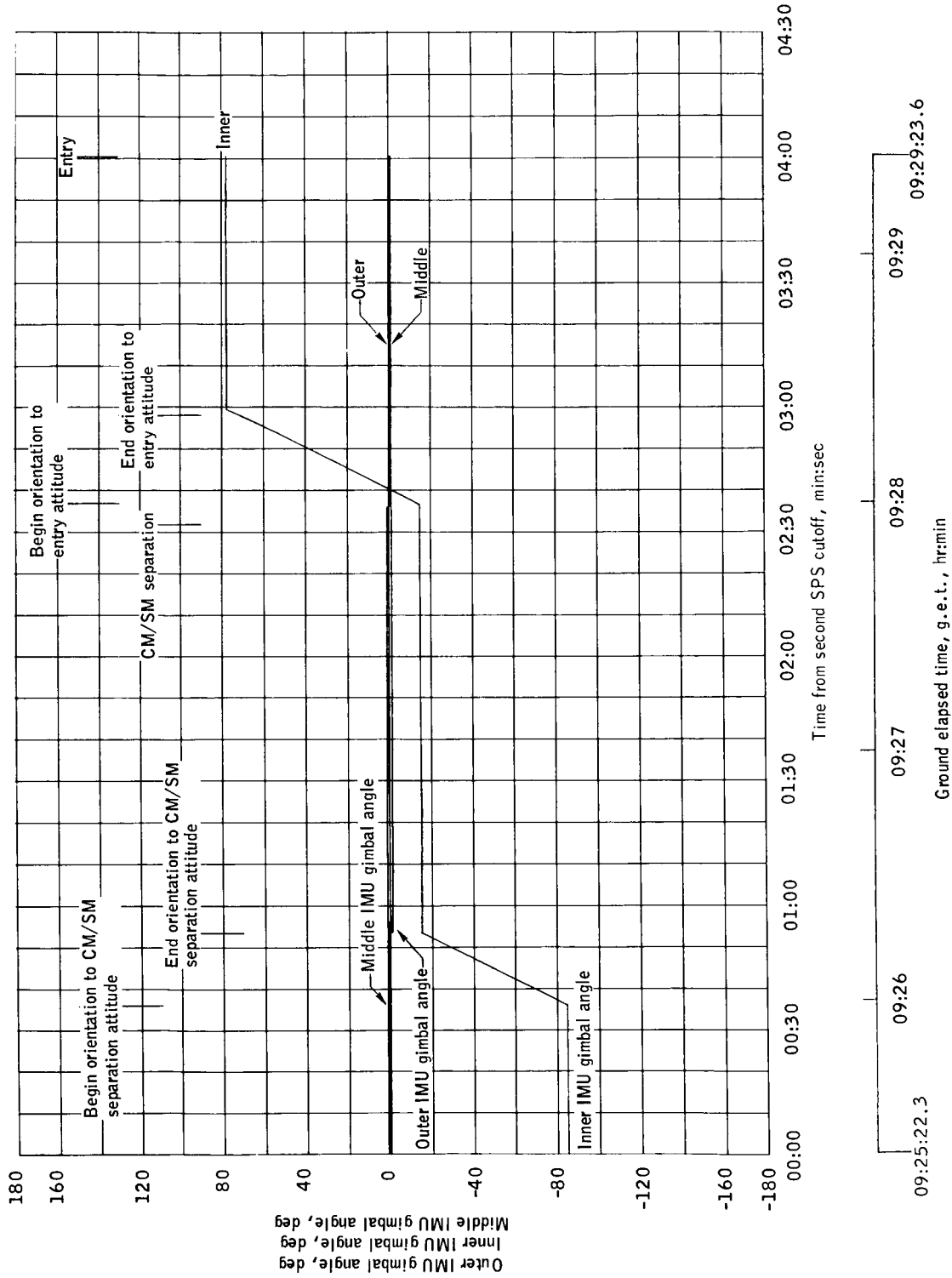
(c) Inertial yaw, pitch, and roll.

Figure 3-15.- Continued.



(d) Relative yaw, pitch, and roll.

Figure 3-15.- Continued.



(e) IMU gimbal angles.

Figure 3-15.- Concluded.

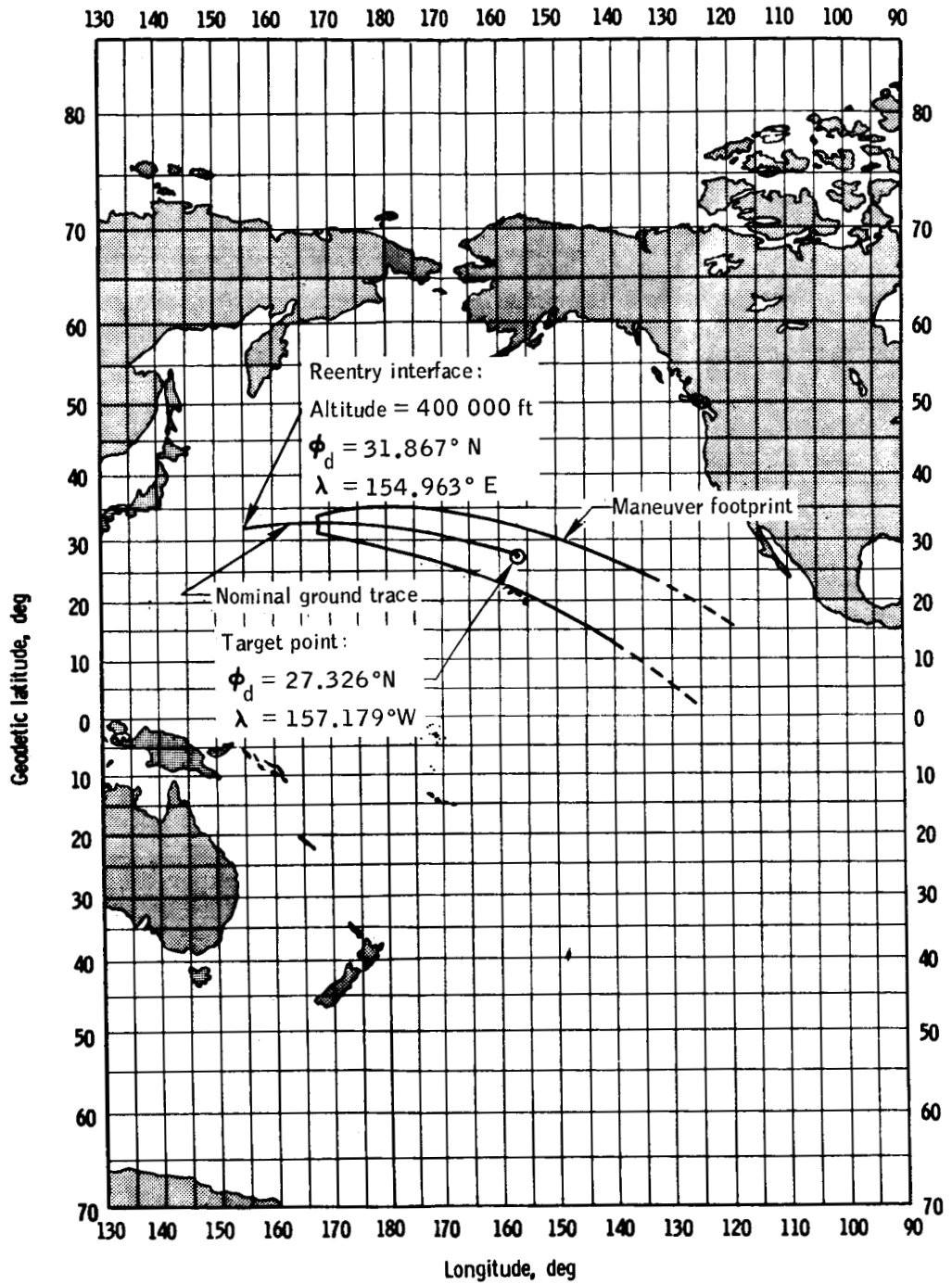


Figure 3-16.- Spacecraft landing footprint.

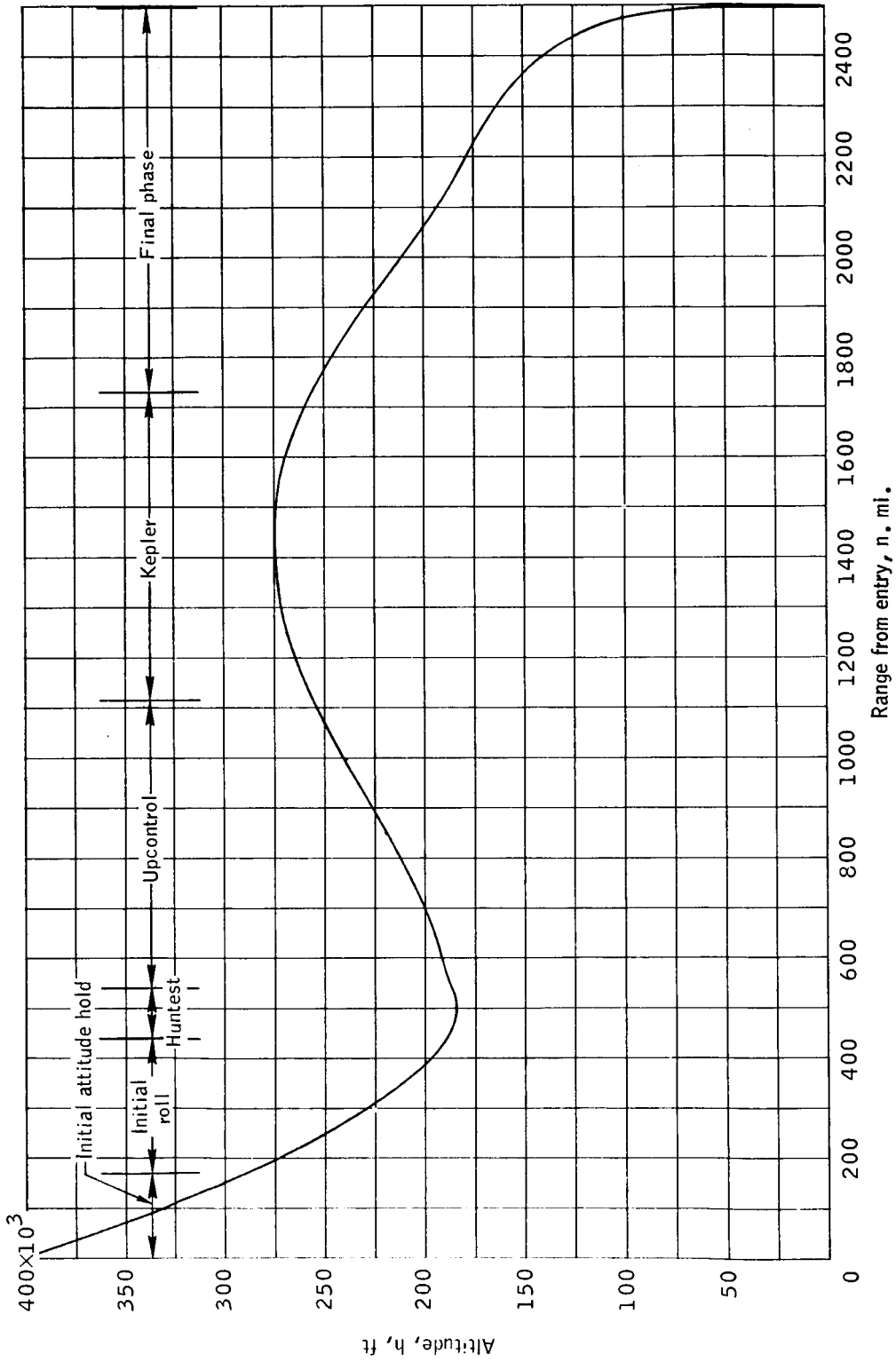
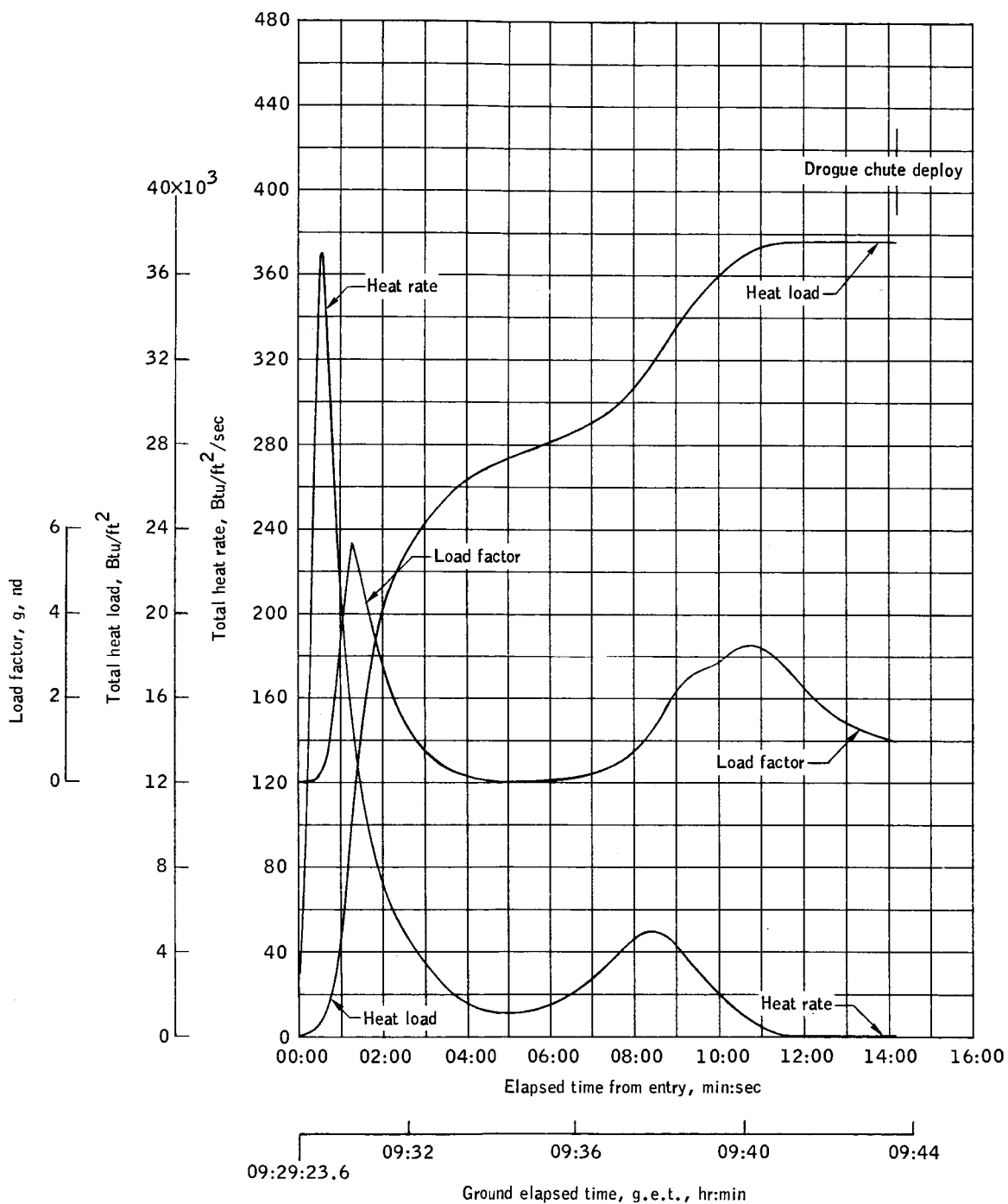
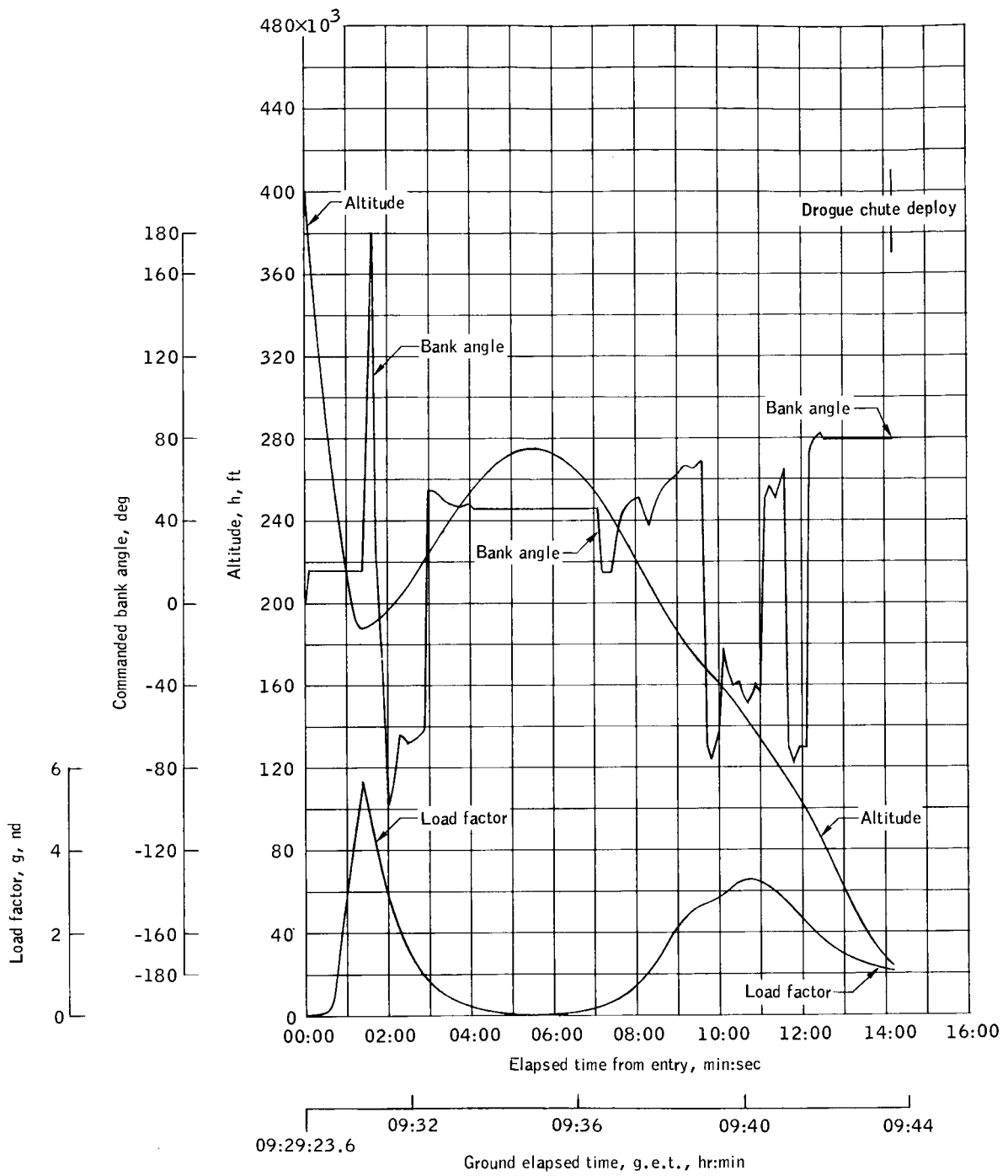


Figure 3-17.- Reentry altitude range profile.



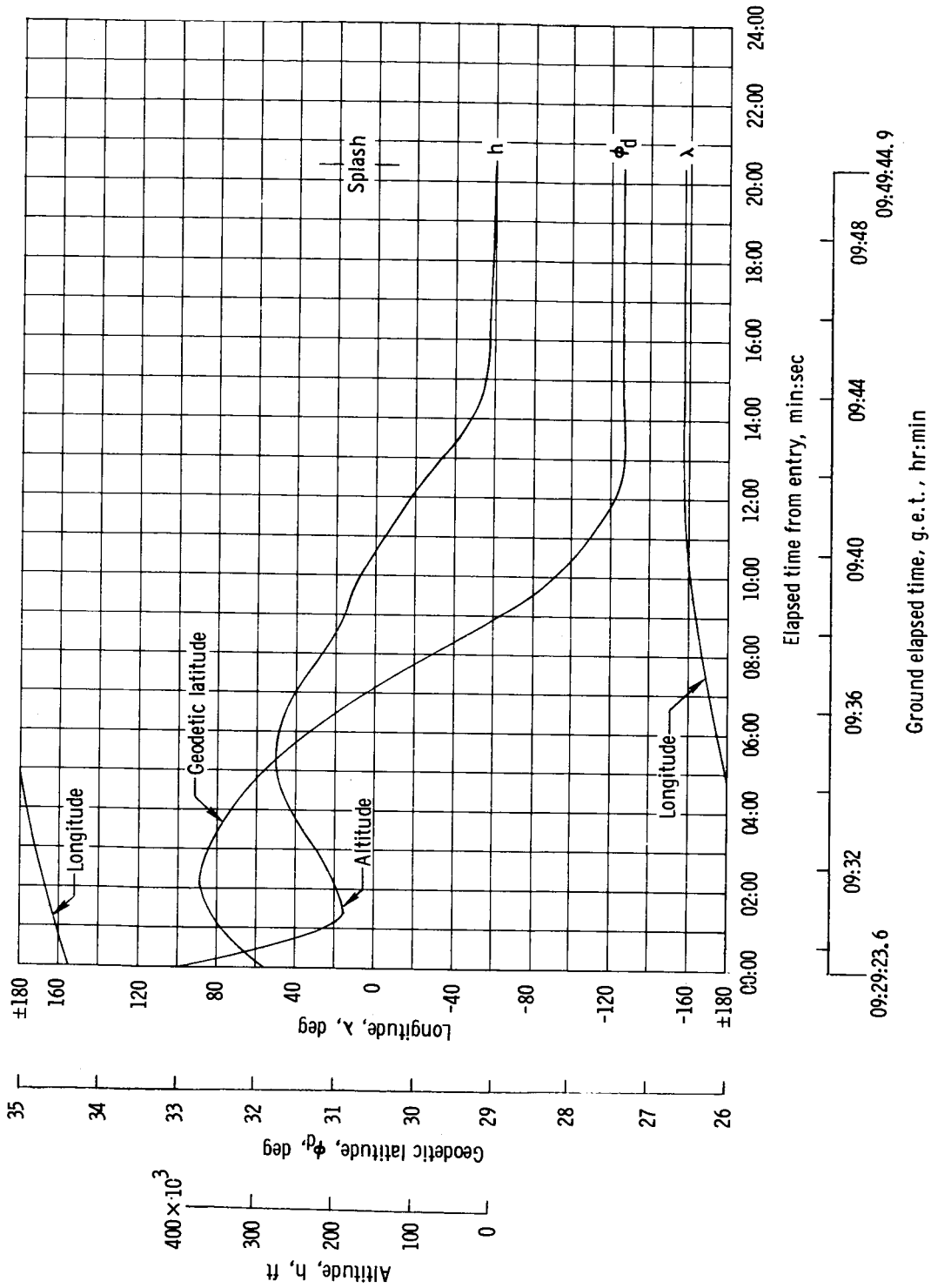
(a) Heat rate, heat load, and load factor.

Figure 3-18.- Atmospheric entry.



(b) Altitude, bank angle, and load factor.

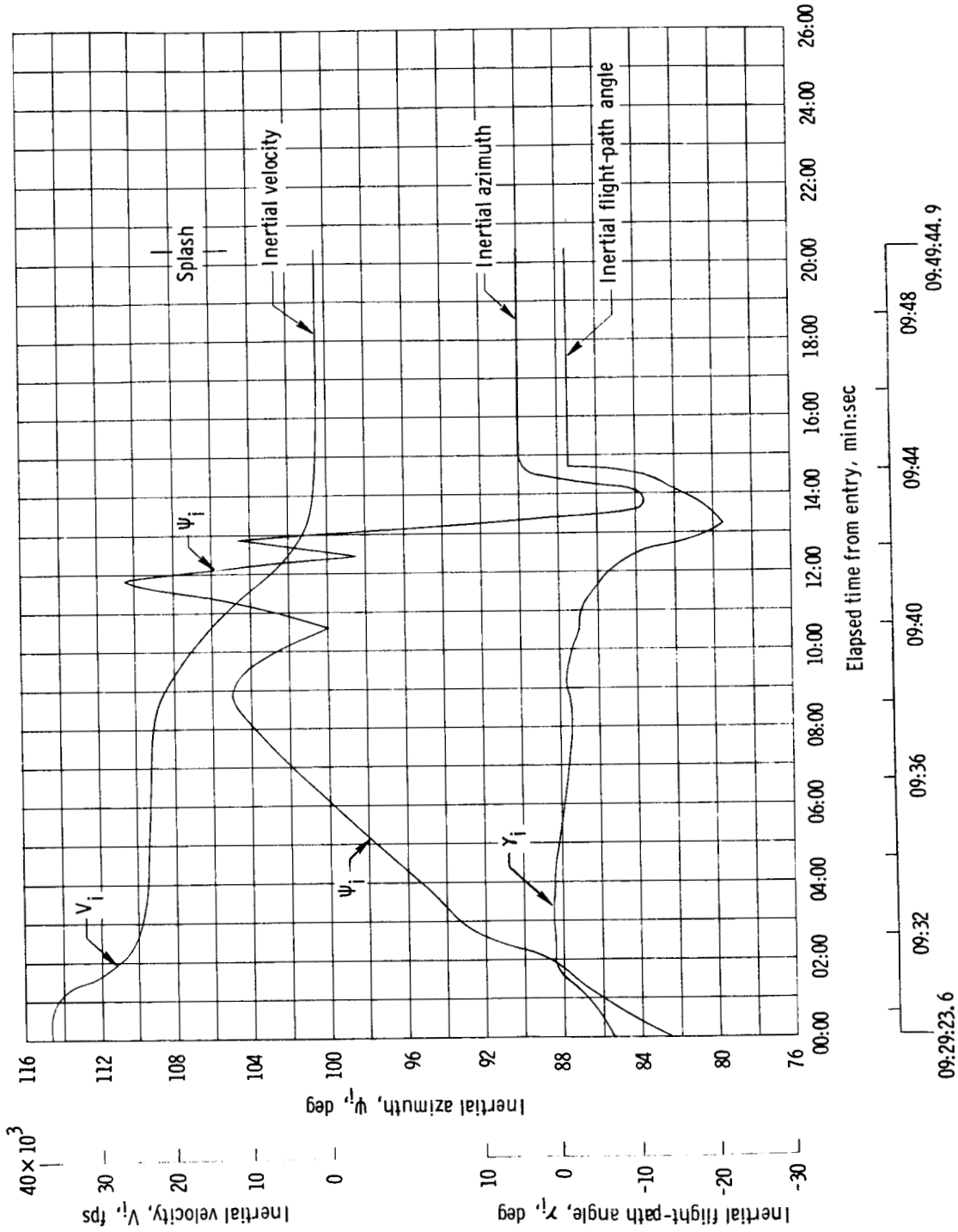
Figure 3-18.- Continued.



(c) Altitude, latitude, and longitude.

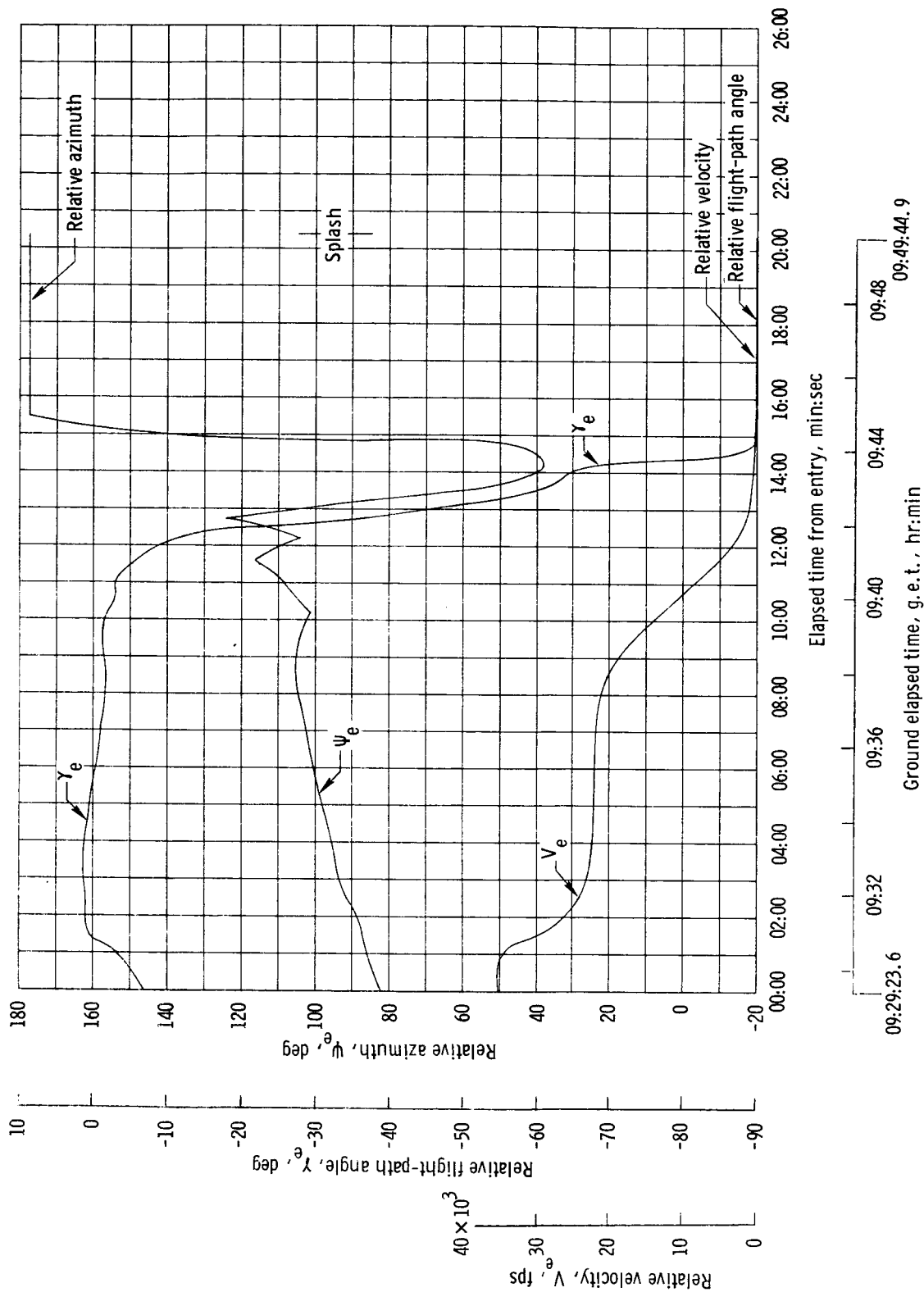
Figure 3-18. - Continued.





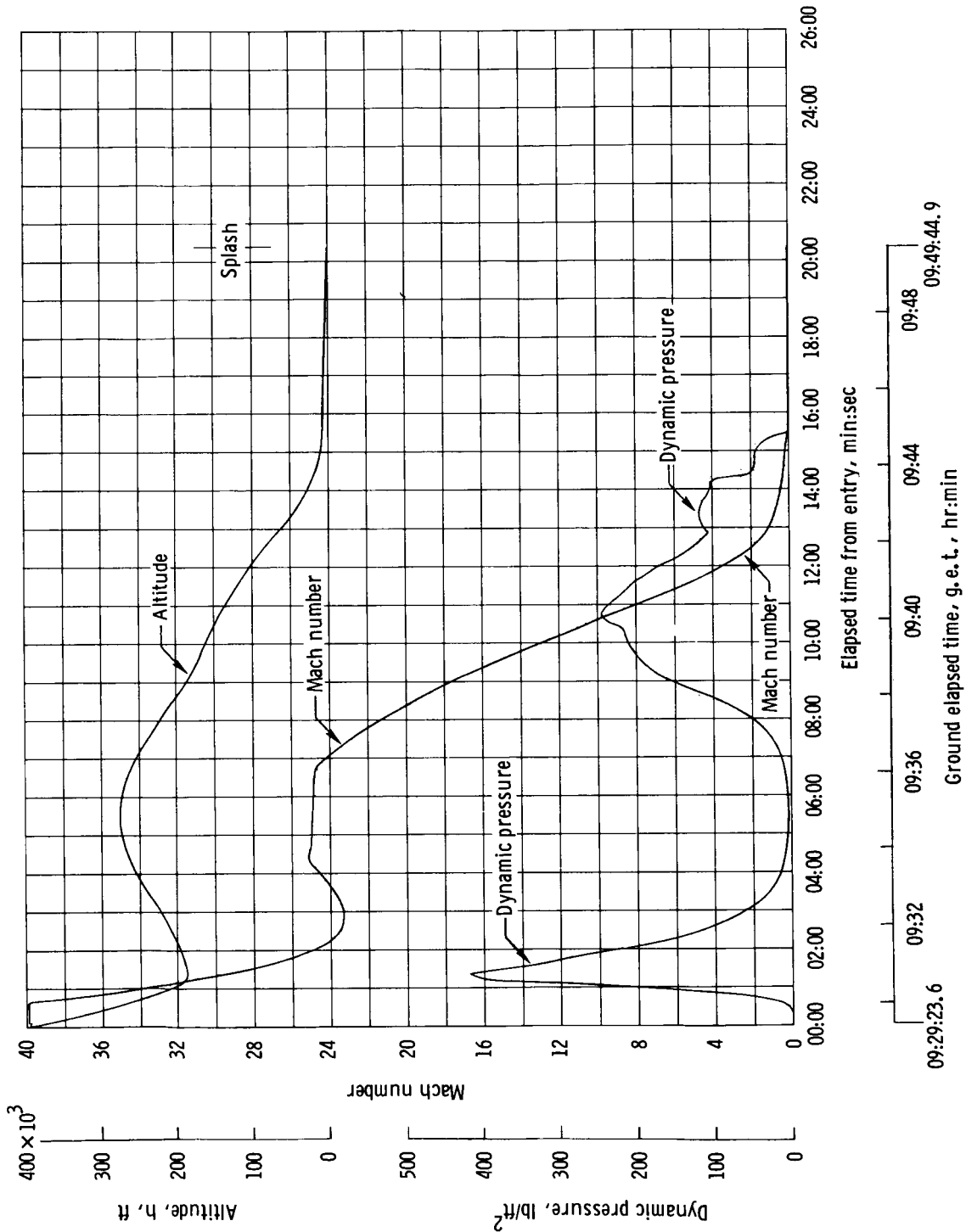
(d) Inertial velocity, flight-path angle, and azimuth.

Figure 3-18. - Continued.



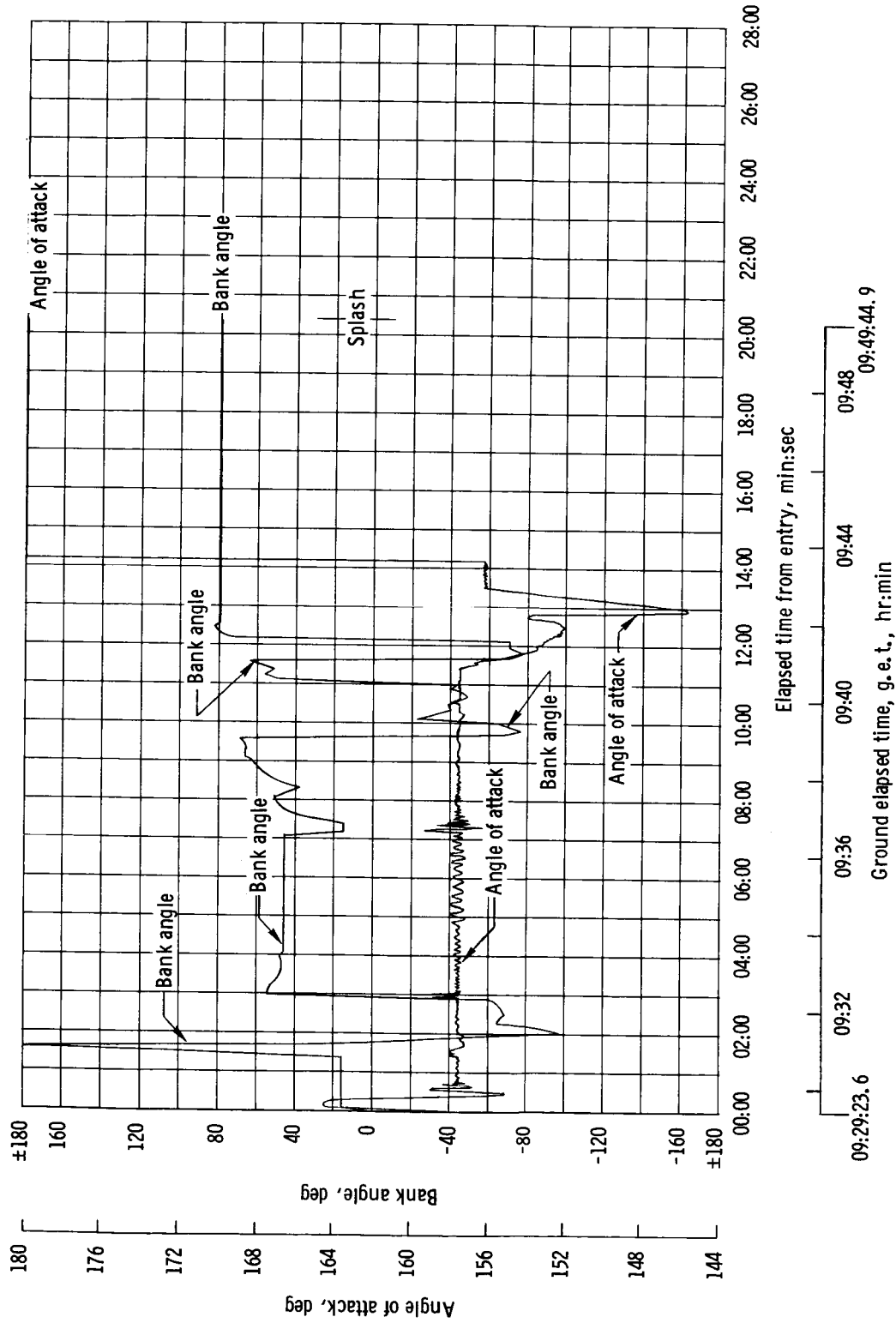
(e) Relative velocity, flight-path angle, and azimuth.

Figure 3-18. - Continued.



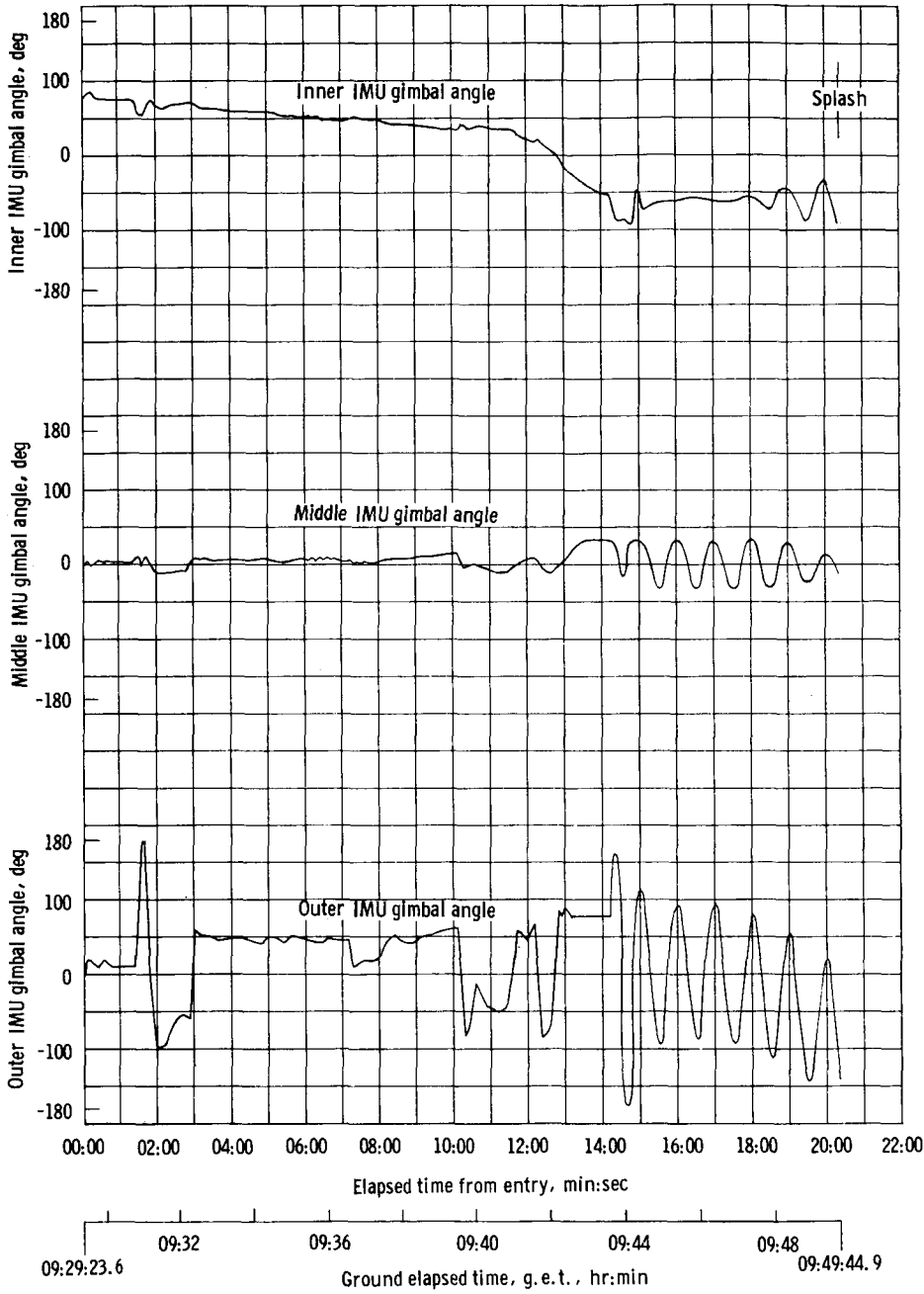
(f) Altitude, dynamic pressure, and Mach number.

Figure 3-18. - Continued.



(g) Bank angle and trim angle of attack.

Figure 3-18. - Continued.



(h) IMU gimbal angles.

Figure 3-18. - Concluded.

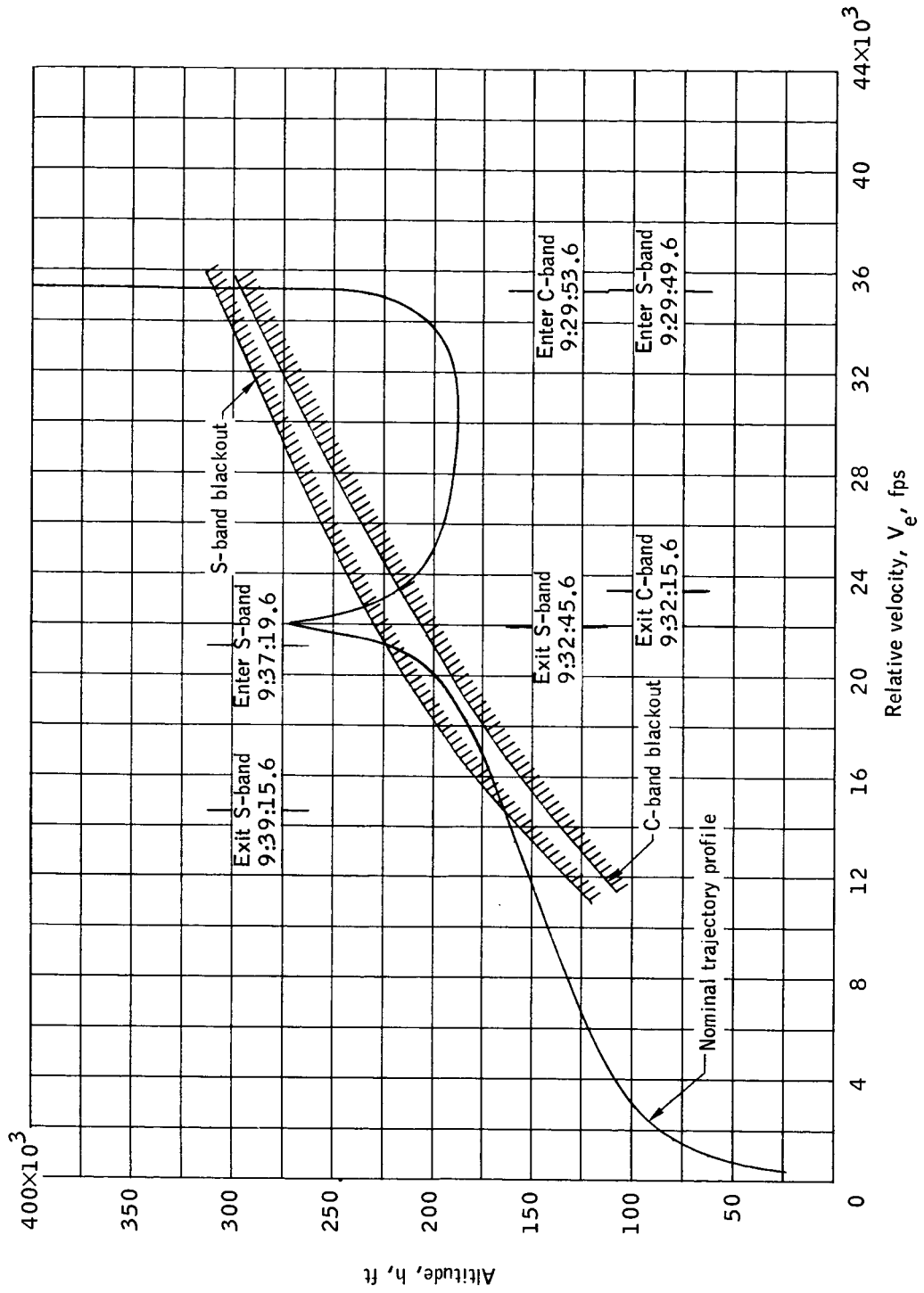


Figure 3-19.- Entry communications blackout.

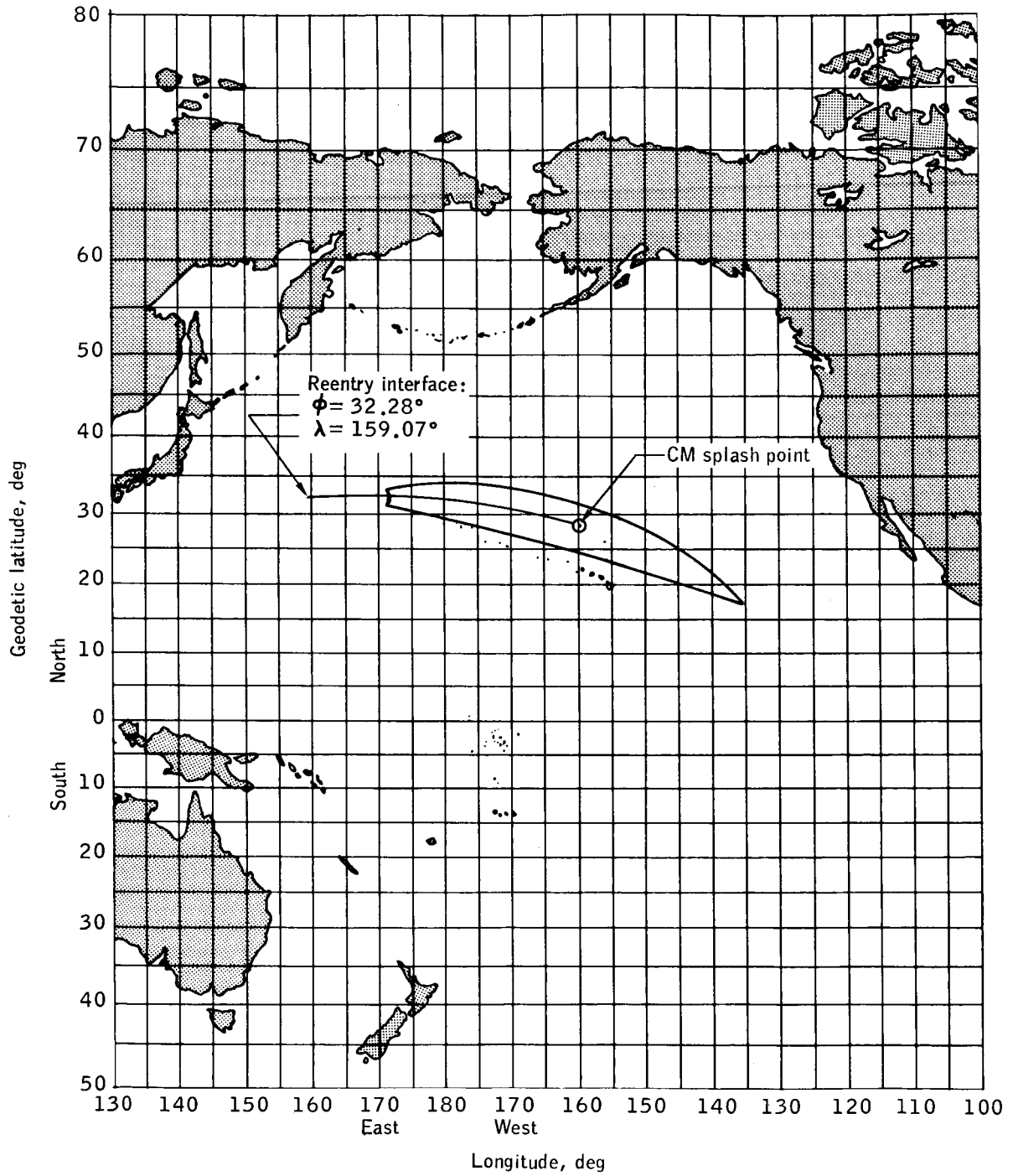


Figure 4-1.- Spacecraft landing footprint - no second SPS burn.

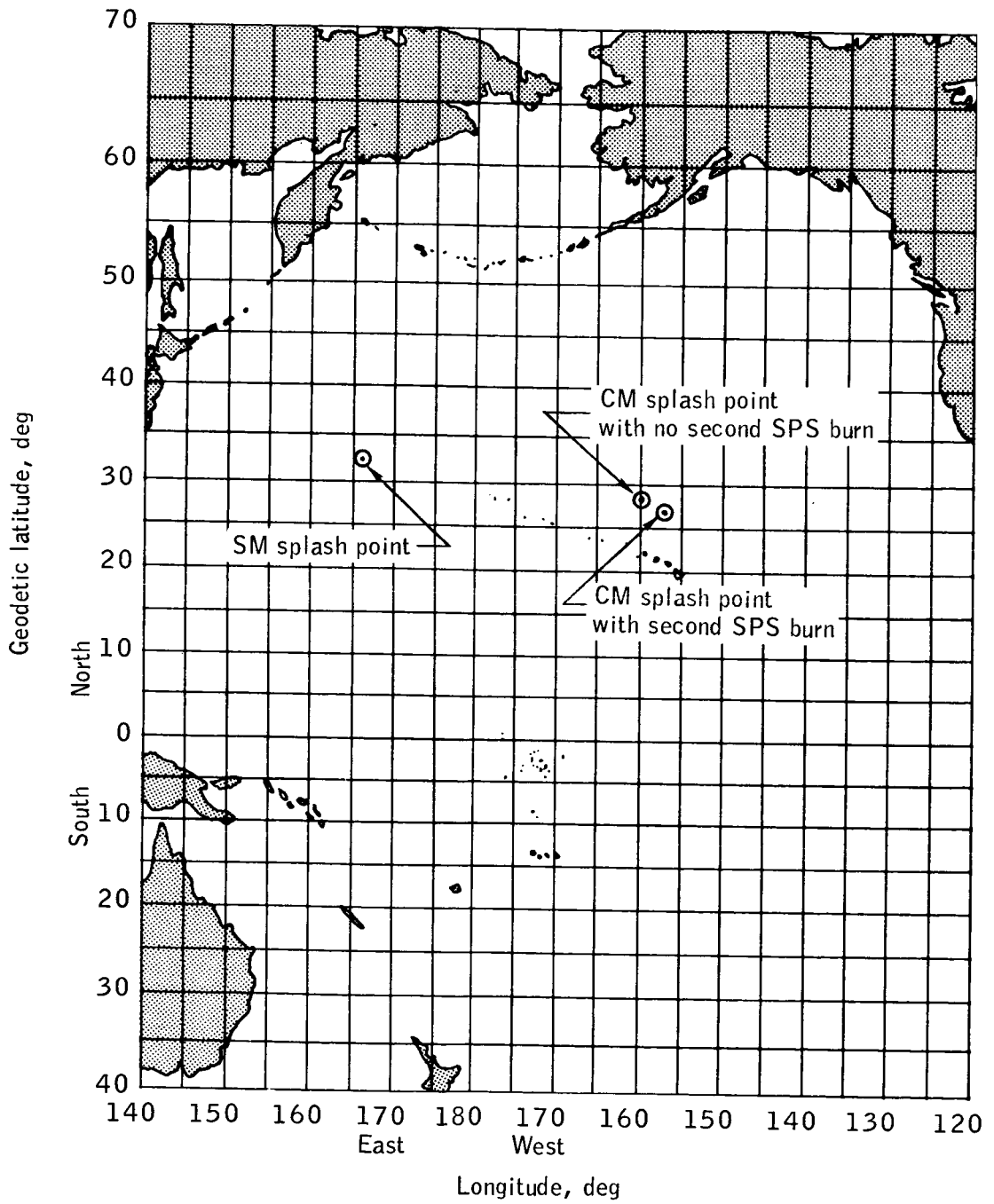
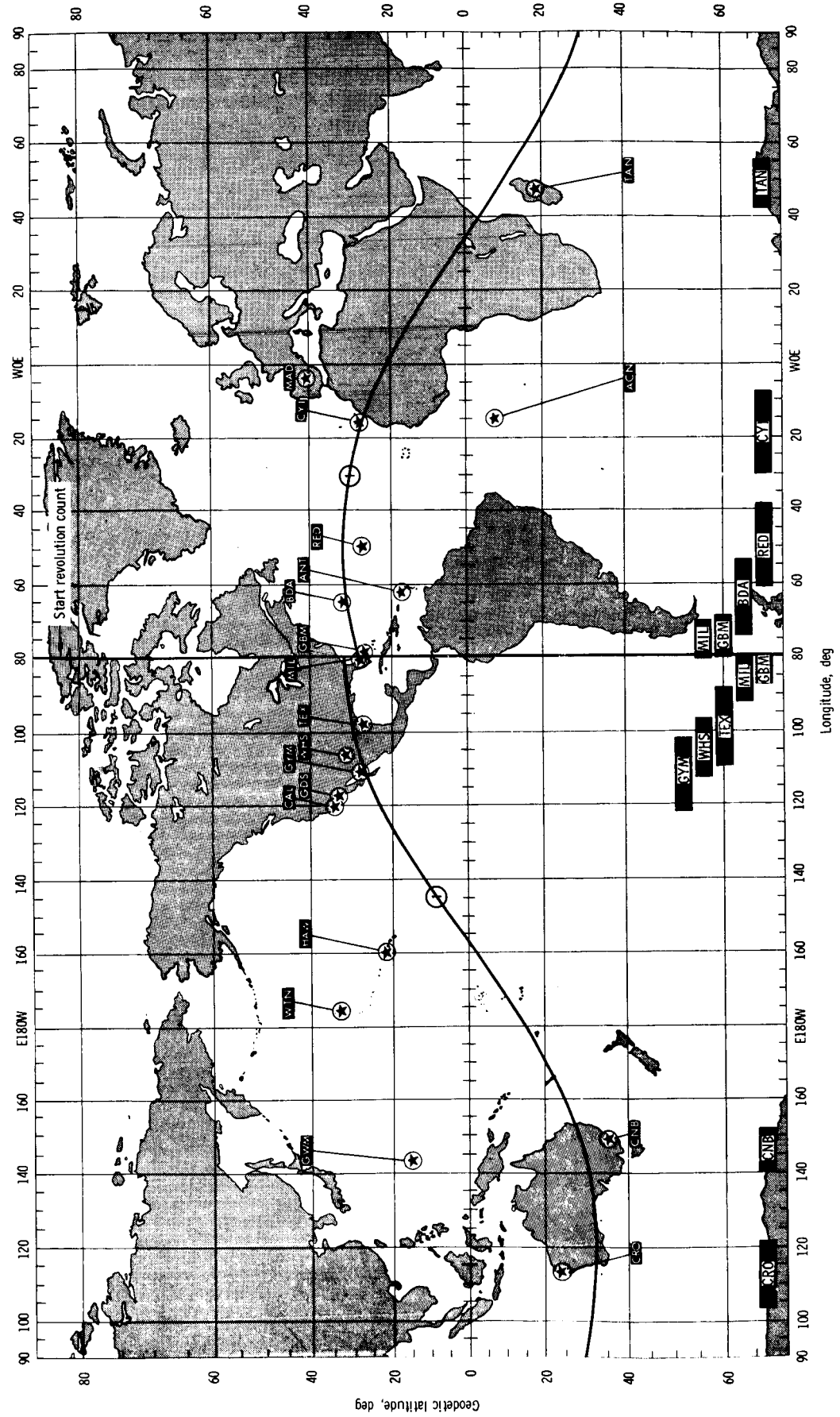


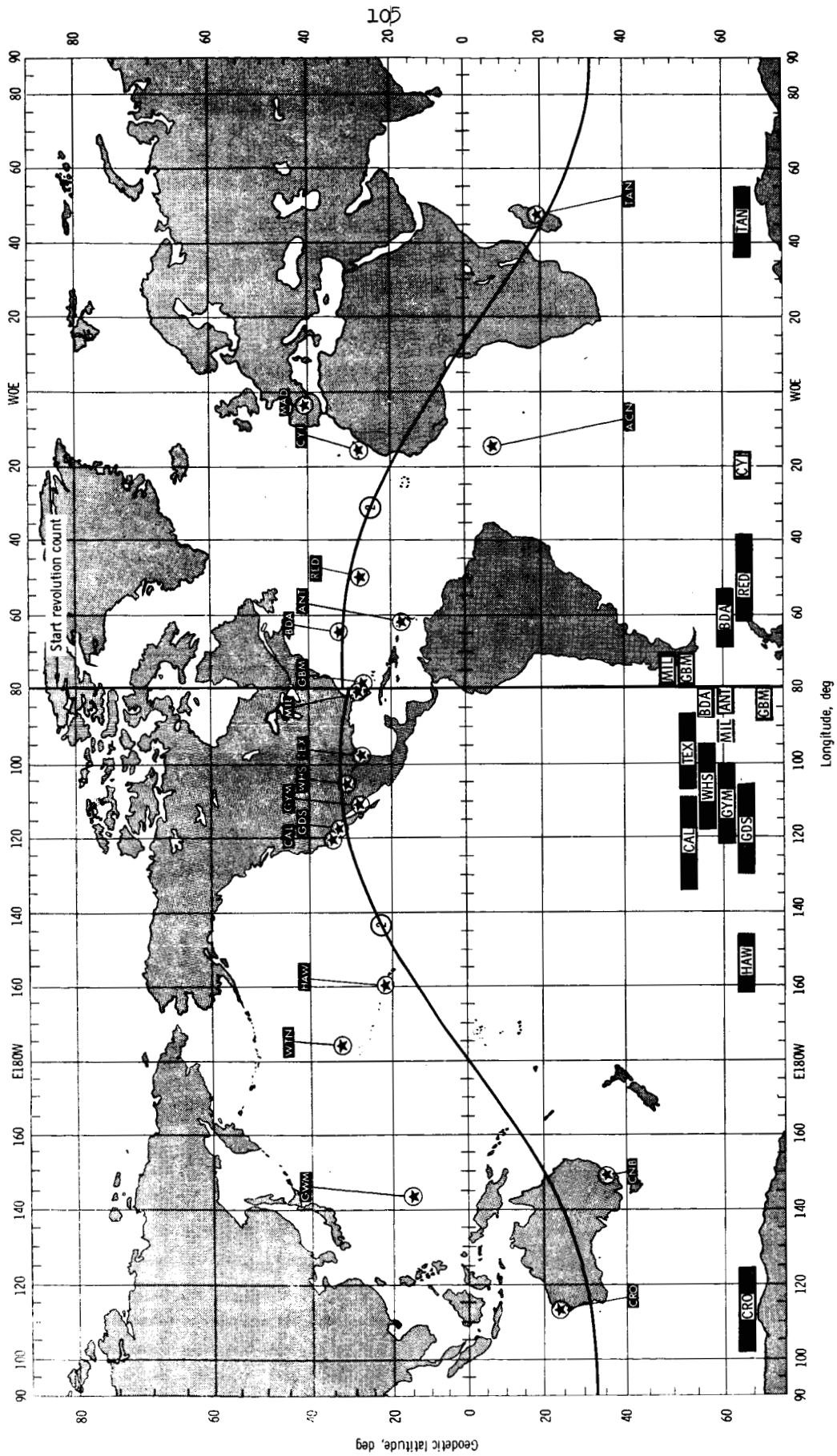
Figure 4-2.- Summary of splash points.





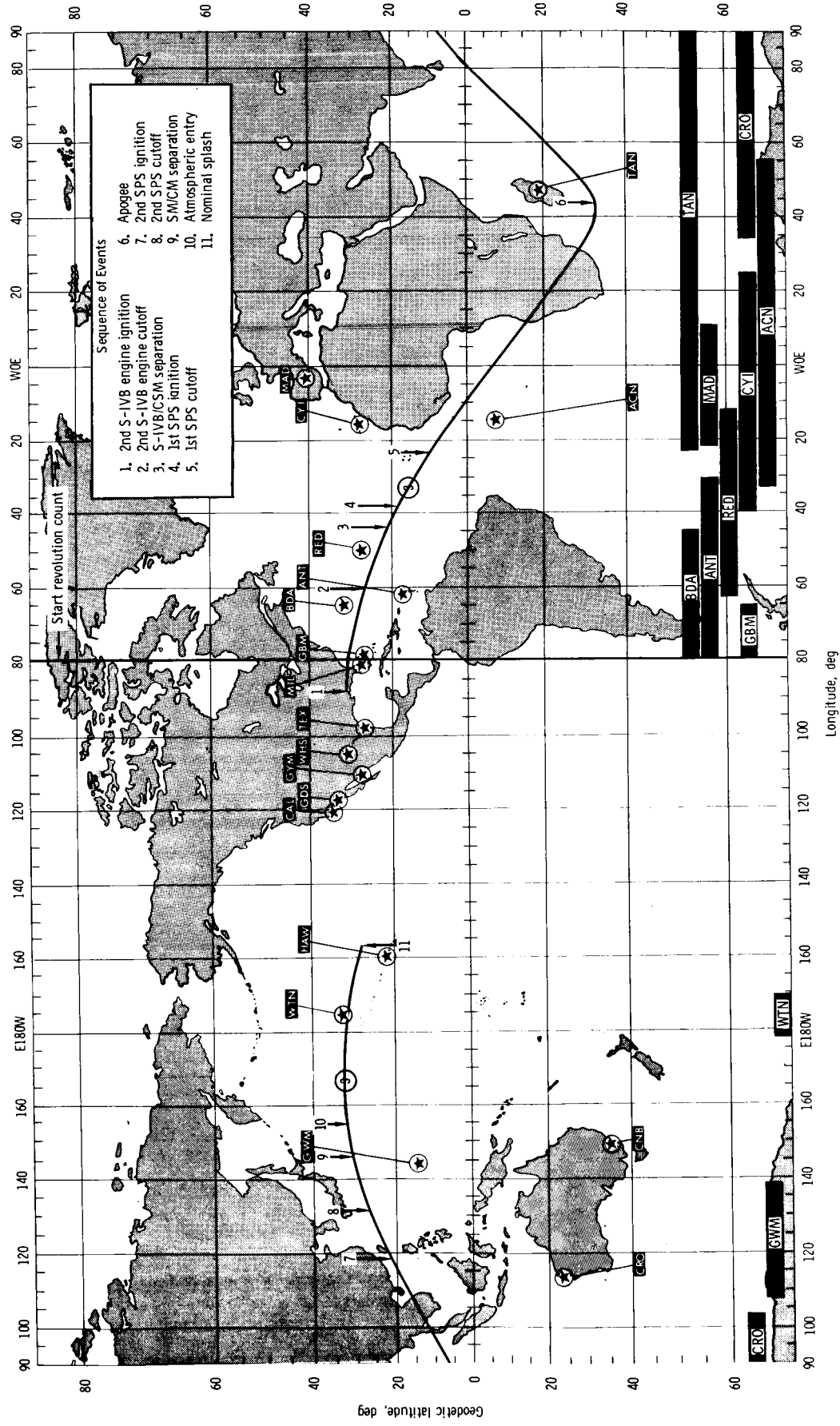
(a) First revolution.

Figure 5-1. - Ground track and radar coverage.



(b) Second revolution.

Figure 5-1 - Continued.



(c) Third revolution.

Figure 5-1. - Concluded.

## REFERENCES

1. Bennett, William J.; Moore, Ronny H.; and Scott, Walter, Jr.: AS-502 Spacecraft Reference Trajectory, Volume I, II, III,: MSC IN 66-FM-67. July 7, 1966.
2. NASA: Apollo 4 and 6 Mission Requirements. Revision, NAS 9-4810, September 27, 1967.
3. Boeing: Saturn V, AS-502 Launch Vehicle Operational Flight Trajectory Final Volumes I and II, Boeing Company. December 12, 1967.
4. Memo: The latest on AS-502/020, Apollo 6. Mission Design Manager Memo 68-FM-H-12. January 21, 1968.
5. Memo: Revision #2 to the Apollo Mission Data Specification (AMDS) "D" for AS-502. PD/Chief, Systems Engineering Division Memo PD7/M-283/67.
6. TRW: Apollo Mission Data Specification "D". Apollo Saturn 501 (U). TRW No. 2131-H009-R8-000, Confidential.
7. Flight Software Branch: Station Characteristics for Apollo Mission Support. Flight Support Division, May 1967.
8. Apollo Missions and Navigation Systems Characteristics. Technical Report #AN-1.3. December 15, 1967.
9. MIT: Guidance System Operational Plan, AS-501, Volume I. MIT R-537, Revision 1. December 1966.
10. Kotanchik, Joseph N.: Apollo 6 Launch Time Versus Heat Shield Test Degradation and Minimum Temperature Deviation. MSC Memo ES161/2-23/99, February 23, 1968.
11. TRW: AS-502 Cold Soak Attitude for December 1, 1967. TRW IOC 3423.9-46, July 27, 1967.
12. TRW: AS-502 Cold Soak Attitude for March 1 to March 15, 1968. TRW IOC 3421.5-30, January 11, 1968.
13. Reed, Robert C., Jr.: Apollo Command Module (CM) Entry Air Radiation Heating Rates. MSC Memo ES5-1-9/6M, January 9, 1968.
14. TRW Systems: Operational Trajectory for Mission A-2/CSM 020 (Apollo 6), Reentry Phase. TRW Document 67-FMT-590, February 16, 1968.